

1993

## Beyond the Standard Model: New scalars and new leptons

Yao Yuan

*College of William & Mary - Arts & Sciences*

Follow this and additional works at: <https://scholarworks.wm.edu/etd>



Part of the [Physics Commons](#)

---

### Recommended Citation

Yuan, Yao, "Beyond the Standard Model: New scalars and new leptons" (1993). *Dissertations, Theses, and Masters Projects*. William & Mary. Paper 1539623845.

<https://dx.doi.org/doi:10.21220/s2-zcg2-az40>

This Dissertation is brought to you for free and open access by the Theses, Dissertations, & Master Projects at W&M ScholarWorks. It has been accepted for inclusion in Dissertations, Theses, and Masters Projects by an authorized administrator of W&M ScholarWorks. For more information, please contact [scholarworks@wm.edu](mailto:scholarworks@wm.edu).

## INFORMATION TO USERS

**This manuscript has been reproduced from the microfilm master. UMI films the text directly from the original or copy submitted. Thus, some thesis and dissertation copies are in typewriter face, while others may be from any type of computer printer.**

**The quality of this reproduction is dependent upon the quality of the copy submitted. Broken or indistinct print, colored or poor quality illustrations and photographs, print bleedthrough, substandard margins, and improper alignment can adversely affect reproduction.**

**In the unlikely event that the author did not send UMI a complete manuscript and there are missing pages, these will be noted. Also, if unauthorized copyright material had to be removed, a note will indicate the deletion.**

**Oversize materials (e.g., maps, drawings, charts) are reproduced by sectioning the original, beginning at the upper left-hand corner and continuing from left to right in equal sections with small overlaps. Each original is also photographed in one exposure and is included in reduced form at the back of the book.**

**Photographs included in the original manuscript have been reproduced xerographically in this copy. Higher quality 6" x 9" black and white photographic prints are available for any photographs or illustrations appearing in this copy for an additional charge. Contact UMI directly to order.**

# U·M·I

University Microfilms International  
A Bell & Howell Information Company  
300 North Zeeb Road, Ann Arbor, MI 48106-1346 USA  
313/761-4700 800/521-0600



**Order Number 9429682**

**Beyond the standard model: New scalars and new leptons**

**Yuan, Yao, Ph.D.**

**The College of William and Mary, 1993**

**U·M·I**  
300 N. Zeeb Rd.  
Ann Arbor, MI 48106



**BEYOND THE STANDARD MODEL:  
NEW SCALARS AND NEW LEPTONS**

---

Dissertation

Presented to

The faculty of the Department of Physics  
The College of William and Mary in Virginia

In Partial Fulfillment  
of the Requirements for the Degree of  
Doctor of Philosophy

---

by

Yao Yuan

1993

APPROVAL SHEET

This dissertation is submitted in partial fulfillment of  
the requirements for the degree of

Doctor of Philosophy

Yao Yuan

---

Author

Approved, November 1993



---

Marc Sher



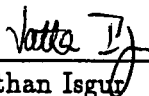
---

Carl Carlson



---

Franz Gross



---

Nathan Isgur



---

Gary DeFotis ( Professor, Department of Chemistry )

To my parents  
Hui Yuan and Ruiqian Di

# Contents

Acknowledgments	vi
List of Tables	vii
List of Figures	viii
Abstract	xi
1 Introduction	2
2 New Scalars	10
2.1 Introduction . . . . .	10
2.2 Flavor-Changing Neutral Currents . . . . .	13
2.3 Constraints from Rare $\tau$ Decays . . . . .	21
2.3.1 Three-body decays . . . . .	21
2.3.2 Radiative decays . . . . .	24
2.3.3 Other processes . . . . .	28
2.4 $B$ and $B_S$ Decays . . . . .	29
2.4.1 Three-body decays . . . . .	29
2.4.2 Two-body decays . . . . .	35
2.4.3 $K - \bar{K}$ and $B - \bar{B}$ mixing . . . . .	38
2.5 Results . . . . .	40
2.6 Conclusion . . . . .	44
3 Cosmological Bounds on the Lifetime of the New Leptons	46
4 New Leptons	64
4.1 Introduction . . . . .	64

4.3	Detection . . . . .	67
4.4	Production Cross Sections . . . . .	70
4.5	Results and Conclusions . . . . .	72
<b>5</b>	<b>Conclusion and Future Work</b>	<b>86</b>
<b>A</b>	<b>The Cross Sections for Chapter 2</b>	<b>90</b>
<b>B</b>	<b>Aspon Model</b>	<b>94</b>
<b>C</b>	<b>The Cross Sections for Chapter 3</b>	<b>98</b>
<b>D</b>	<b>Fortran Programm for Chapter 3</b>	<b>102</b>
<b>E</b>	<b>Approximating the Renormalization-Group Equations of Minimal Supersymmetry</b>	<b>108</b>
	<b>Bibliography</b>	<b>117</b>
	<b>Vita</b>	<b>121</b>

## Acknowledgments

The writer wishes to express her appreciation to Professor Marc Sher, under whose guidance this research was conducted, for his patient guidance and criticism throughout these years. Also the author would like to thank Professor Paul Frampton and Dr. Daniel Ng for a successful collaboration. The author is also indebted to Professors C. Carlson, F. Gross, N. Isgur and G. Defotis for their careful reading and criticism of the manuscript. The writer also wishes to thank her husband, Xiaoqiang Zhang, for his encouragement and support through the course of this work.

# List of Tables

1.1	The fields of the standard model. . . . .	3
2.1	Bounds on the flavor-changing couplings which arise from three-body leptonic decays. The numerical values should be understood as multiplied by $(m_s/m_W)^4[(m_p/m_W)^4]$ . The contribution is the same for scalar exchange and for pseudoscalar exchange, and so leads to identical bounds on the masses. . . . .	24
2.2	Bounds on flavor-changing couplings which arise from radiative decays of the $\tau$ and $\mu$ . The numerical values should be understood as multiplied by $(m_s/m_W)^4[(m_p/m_W)^4]$ . The bounds for the case of scalar exchange are slightly different from those for the case of pseudoscalar exchange; the number in parentheses gives the bound when the pseudoscalar mass is used. . . . .	27
2.3	Bounds on the flavor-changing couplings from three-body $B$ decays. Since only the scalar contributes, the bound only applies to the scalar mass, and not the pseudoscalar mass. The numerical values should be understood as multiplies by $(m_s/m_W)^4$ . . . . .	34
2.4	Bounds on flavor-changing couplings which arise from two-body decays of the $B$ and $B_s$ . Since only the pseudoscalar contributes, the only bounds apply to $m_p$ . The numerical values should be understood as multiplied by $(m_p/m_W)^4$ . . . . .	37
B.1	The fields of the aspon model. . . . .	95
E.1	For five representative values of the parameters. $M$ , $A$ , $m_4$ , and $h_t$ , we calculate the ratio of vacuum expectation values $\tan\beta = v_2/v_1$ , the top-quark mass, and the scalar quark mass using both the renormalization-group equations and the approximation. All masses are given in GeV. . . . .	116

## List of Figures

2.1	Lepton-number-violating $\tau$ decays can occur through exchange of an intermediate scalar. $l_1$ , $l_2$ , and $l_3$ are either electrons or muons. If two identical fermions are in the final state, an exchange diagram must be subtracted. In some cases, such as $\tau \rightarrow e^+e^-\mu^-$ , the process can occur with either $l_1 = \mu^-$ , $l_2 = e^-$ and $l_3 = e^+$ or $l_1 = e^-$ , $l_2 = \mu^-$ and $l_3 = e^+$ ; these two diagrams have different coupling constant dependences and are added. . .	22
2.2	Diagrams which lead to lepton-number-violating radiative decays. If $l_1$ and $l_3$ are identical, these diagrams give contributions to anomalous magnetic moment. . . . .	25
2.3	Contributions to three-body decays of the $B$ meson. The exchanged particle, in this case, must be a scalar. . . . .	30
2.4	Contributions to two-body decays of the $B$ (or the $B_s$ ) meson. The exchanged particle must be a pseudoscalar. . . . .	35
3.1	Diagrams contributing to the annihilation of long-lived charged leptons. Crossed diagrams have not been explicitly shown. . . .	49
3.2	Partial cross sections for $L^+L^-$ annihilation as a function of the $L$ mass in the non-relativistic limit. For t-channel annihilation into $W$ 's, a neutrino mass of twice the $L$ mass was used. . . . .	52
3.3	The total cross section for $L^+L^-$ annihilation as a function of the $L$ mass. When the cross section exceeds the unitarity bound, which occurs for $L$ masses above 1500 GeV, the unitarity bound has been used. . . . .	53
3.4	The value of $\Omega h^2$ is given as a function of the $L$ mass. Here, $\Omega$ is the ratio of the $L$ density to the critical density, and $h$ is the Hubble constant in units of 100 km/s/Mpc. . . . .	55

3.5	Final results for the limits on the mass and lifetime of charged leptons. The limits in the upper line arise from searches for heavy hydrogen in water and from plastic track detectors. The limit restricting the lifetime to be less than $10^{13}$ seconds arises from failure to directly detect the photons emitted in the decay in the diffuse photon background. The strongest bound, the lower line, comes from failure of the decay photons to appreciably distort the cosmic microwave background. The latter two limits would not eliminate the possibility of lifetimes much in excess of the age of the Universe ( $10^{17}$ seconds), but the bound from terrestrial searches does so. For masses in excess of $10^5$ GeV, the bounds will continue, until the $\Omega = 1$ line is reached; for masses in excess of $10^5$ GeV, this line is at $10^{32-3y}$ seconds for a mass of $10^y$ GeV. . . . .	61
4.1	Feynman diagram for the process (a) $gg \rightarrow L^+L^-$ and $NN$ , (b) $q\bar{q} \rightarrow L^+L^-$ , $NL^\pm$ and $NN$ , and (c) $q\bar{q} \rightarrow L^+L^-A$ , $NLA$ and $NNA$ . . . . .	71
4.2	Total cross sections for heavy lepton production $pp \rightarrow L^+L^-$ as a function of the charged lepton mass $m_L$ for model 1(solid lines), model 2 and 3(dashed lines) and model 4(dotted lines). The upper and lower sets are for the $E_{cm} = 40$ TeV and $E_{cm} = 17$ TeV. $m_H = 100$ GeV is assumed. . . . .	73
4.3	Total cross sections for the process $pp \rightarrow NN$ as a function of the heavy neutrino mass $m_N$ for model 1(solid lines), and model 2 and 3 (dashed lines). The upper and lower sets are for $E_{cm} = 40$ TeV and $E_{cm} = 17$ TeV. $m_H = 100$ GeV is assumed. . . . .	74
4.4	Total cross sections for the process $pp \rightarrow NL^\pm$ for model 1(solid lines), and model 2 and 3(dashed lines) for (a) $m_N/m_L = 0.5$ , (b) $m_N/m_L = 1$ , (c) $m_N/m_L = 2$ . The upper and lower sets are for $E_{cm} = 40$ TeV and $E_{cm} = 17$ TeV. $m_H = 100$ GeV is assumed. . . . .	77
4.5	Total cross sections for the process $pp \rightarrow L^+L^-A$ ( $A = aspon$ ) as a function of aspon mass $m_A$ for (a) model 3 and (b) model 4 with $m_L = 50$ GeV(solid lines) and $m_L = 150$ GeV(dashed lines). The upper and lower sets are for $E_{cm} = 40$ TeV and $E_{cm} = 17$ TeV. $m_H = 100$ GeV and the coupling of the aspon $\alpha_A = 0.1$ are assumed. . . . .	79

4.6	Total cross sections for the processes $pp \rightarrow NNA$ in model 3 for $m_L = m_N = 50$ GeV(solid lines) and $m_L = m_N = 150$ GeV(dashed lines). The upper and lower sets are for $E_{cm} = 40$ TeV and $E_{cm} = 17$ TeV. $m_H = 100$ GeV and the coupling of the aspon $\alpha_A = 0.1$ are assumed. . . . .	80
4.7	Total cross sections for the processes $pp \rightarrow NLA$ in model 3 for $m_L = m_N = 50$ GeV(solid lines) and $m_L = m_N = 150$ GeV(dashed lines). The upper and lower sets are for $E_{cm} = 40$ TeV and $E_{cm} = 17$ TeV. $m_H = 100$ GeV and the coupling of the aspon $\alpha_A = 0.1$ are assumed. . . . .	81
4.8	The velocity distributions $1/\sigma(d\sigma/d\beta)$ for the process $pp \rightarrow LL$ in model 2 and 3 at (a) $E_{cm} = 17$ TeV, and (b) $E_{cm} = 40$ TeV and for $m_L = 100$ GeV(solid line), 300 GeV(dashed line) and 500 GeV(dotted line) respectively. . . . .	83
E.1	Given the Yukawa coupling at $M_X$ , the Yukawa coupling at $M_W$ can be found in two ways: (1) using the renormalization-group equations and (2) using the approximation. The ratio of the results of the second method to the results of the first is plotted as a function of the Yukawa coupling at $M_W$ . . . . .	111
E.2	The splitting between the third-generation scalar quark mass and that of the other two is calculated in two ways: (1) using the renormalization-group equations and (2) using the approximation. The ratio of the results of the second method to the results of the first is plotted as a function of the Yukawa coupling at $M_W$ . Several choices of input parameters are used: for the upper line, $\xi = 2.5$ , $A = 0.5$ , and $m_4/m_0 = 1.4$ ; for the middle line, $\xi \equiv M/m_0 = 1.0$ , $A = 0.5$ , and $m_4/m_0 = 0.5$ ; for the lower line, $\xi = 1.0$ , $A = 1.0$ , and $m_4/m_0 = 1.4$ . . . . .	114

## Abstract

Physics that might lie beyond the standard model is discussed, with special emphasis on two possible extensions of the standard model: multi-Higgs extension and the fourth generation leptons.

In multi-Higgs-boson extensions of the standard model, tree-level flavor-changing neutral currents exist naturally, unless suppressed by some symmetry. For a given rate, the exchanged scalar or pseudoscalar mass is very sensitive to the flavor-changing coupling between the first two generations. Since the Yukawa couplings of the first two generations are unknown and certainly very small, bounds which rely on some assumed value of this flavor-changing couplings are quite dubious. One might expect the size (and reliability) of the Yukawa couplings involving the third generation to be greater. In this study, we consider processes involving  $\tau$ 's and  $B$ 's, and determine the bounds on the flavor-changing couplings which involve third-generation fields. The strongest bound in the quark sector comes from  $B - \bar{B}$  mixing and in the lepton sector, surprisingly, from  $\mu \rightarrow e\gamma$ . It is then noted that flavor-changing couplings in the quark sector are related to those in the lepton sector in many grand unified theories, and one can ask whether an analysis of rare  $\tau$  decays or rare  $B$  decays will provide the strongest constraints. We show that rare  $B$  decays provide the strongest bounds, and that *no* useful information can be obtained from rare  $\tau$  decays. It is also noted that the most promising decay modes are  $B \rightarrow K\mu\tau$  and  $B_s \rightarrow \mu\tau$ , and we urge experimenters to look for rare decay modes of the  $B$  in which a  $\tau$  is in the final state.

If a fourth generation of leptons exists, both the neutrino and the charged lepton must have masses in excess of 45 GeV. It is certainly possible that the neutrino will be the heavier of the two. In this case, the charged lepton can only decay through mixing with lighter generations, and might thus be extremely long-lived. First, we investigate the implications of very long-lived charged leptons for cosmology and astrophysics. We calculate the bounds on the mass and lifetime of long-lived charged particles which arise from terrestrial experiments, from astrophysical searches for the decay products and from cosmology. The strongest bounds come from the requirement that the decay products not unacceptably distort the cosmic microwave background. Phenomenological implications are also briefly discussed. Second, we study the production cross-sections and signatures for the SSC and LHC. Four models are considered which contain heavy leptons beyond the three families of the standard model. Two are fourth-generation extensions of the standard model in which the right-handed heavy leptons are either isosinglets or in an isodoublet; the other two are motivated by the aspon model of CP violation. In all these models, the heavy neutrino can either be heavier than, or comparable in mass to, the charged lepton leading to the possibility that the charged lepton is very long-lived. The detection methods for these heavy leptons are also discussed.

**BEYOND THE STANDARD MODEL:  
NEW SCALARS AND NEW LEPTONS**

# Chapter 1

## Introduction

The standard model of the electroweak interactions has been extremely successful phenomenologically, and yet the large number of free parameters, as well as the large number of unanswered questions, has led to a strong belief that the standard model is incomplete. For this reason, there have been many studies of possible extensions of the standard model. Before discussing the possibility of new scalars and new leptons, I will first review some of the concepts of the standard model[1].

The standard model is built from three types of particles: gauge bosons, fermions and Higgs. The best understood are the gauge bosons, whose couplings to matter fixed by the principle of gauge invariance. The standard-model gauge group is  $SU(3) \times SU(2)_L \times U(1)_Y$ , so we know that there must be a total of twelve gauge bosons: eight gluons, three weak vector bosons and one photon, as shown in Table 1. These particles have all been experimentally detected, and must form part of any extension to the standard model.

The next part of the standard model is the Higgs sector, in which the electroweak gauge group  $SU(2)_L \times U(1)_Y$  is broken to the  $U(1)_Q$  of electromagnetism. The Higgs sector contains a complex doublet  $\Phi$ , whose quantum numbers are shown in Table 1.

Table 1.1: The fields of the standard model.

Particle	$SU(3) \times SU(2) \times U(1)$
$G_\mu^\alpha$	(8, 1, 0)
$W_\mu^\alpha$	(1, 3, 0)
$B_\mu$	(1, 1, 0)
$q_L^i = \begin{pmatrix} u_L^i \\ d_L^i \end{pmatrix}$	(3, 2, 1/6)
$u_R^i$	(3, 1, 2/3)
$d_R^i$	(3, 1, -1/3)
$l_L^i = \begin{pmatrix} n_L^i \\ e_L^i \end{pmatrix}$	(1, 2, -1/2)
$e_R^i$	(1, 1, -1)
$\Phi = \begin{pmatrix} \phi^+ \\ \phi^0 \end{pmatrix}$	(1, 2, 1/2)

The complete gauge-invariant Lagrangian including the scalar fields is then

$$\mathcal{L} = \mathcal{L}_{Gauge} + \mathcal{L}_{Higgs} + \mathcal{L}_{Yukawa} . \quad (1.1)$$

The gauge-field Lagrangian is determined by the gauge symmetry,

$$\begin{aligned} \mathcal{L}_{Gauge} = & -\frac{1}{4}G_{\mu\nu}^\alpha G^{\alpha\mu\nu} - \frac{1}{4}W_{\mu\nu}^\alpha W^{\alpha\mu\nu} - \frac{1}{4}B_{\mu\nu}B^{\mu\nu} \\ & + i\bar{q}_L\gamma^\mu D_\mu q_L + i\bar{u}_R\gamma^\mu D_\mu u_R + i\bar{d}_R\gamma^\mu D_\mu d_R \\ & + i\bar{l}_L\gamma^\mu D_\mu l_L + i\bar{e}_R\gamma^\mu D_\mu e_R , \end{aligned} \quad (1.2)$$

where

$$\begin{aligned} G_{\mu\nu}^\alpha &= \partial_\mu G_\nu^\alpha - \partial_\nu G_\mu^\alpha + g_3 f^{abc} G_\mu^b G_\nu^c , \\ W_{\mu\nu}^\alpha &= \partial_\mu W_\nu^\alpha - \partial_\nu W_\mu^\alpha + g_2 \epsilon^{\alpha\beta\gamma} W_\mu^\beta W_\nu^\gamma , \\ B_{\mu\nu} &= \partial_\mu B_\nu - \partial_\nu B_\mu , \end{aligned} \quad (1.3)$$

and

$$D_\mu q_L^i = \partial_\mu q_L^i - g_3 \Lambda^a G_\mu^a q_L^i - ig_2 T^a W_\mu^a q_L^i - ig_1 \frac{Y}{2} B_\mu q_L^i ,$$

$$\begin{aligned}
D_\mu u_R^i &= \partial_\mu u_R^i + ig_3 T^\alpha G_\mu^\alpha u_R^i - ig_1 \frac{Y}{2} B_\mu u_R^i, \\
D_\mu d_R^i &= \partial_\mu d_R^i + ig_3 T^\alpha G_\mu^\alpha d_R^i - ig_1 \frac{Y}{2} B_\mu d_R^i, \\
D_\mu l_L^i &= \partial_\mu l_L^i - ig_2 T^\alpha W_\mu^\alpha l_L^i - ig_1 \frac{Y}{2} B_\mu l_L^i, \\
D_\mu e_R^i &= \partial_\mu e_R^i - ig_1 \frac{Y}{2} B_\mu e_R^i.
\end{aligned} \tag{1.4}$$

In these expressions, the  $f^{abc}$  and  $\Lambda$  are the structure constants and color operator of  $SU(3)$ , the  $\epsilon^{\alpha\beta\gamma}$  are the structure constants of  $SU(2)$ ,  $T$  is the weak isospin operator, and  $Y$  is the hypercharge generator. As we can see from Eqs. 1.3 and 1.4, the gauge-field Lagrangian depends only on the  $SU(3) \times SU(2)_L \times U(1)_Y$  coupling constants  $g_3$ ,  $g_2$  and  $g_1$ .

The Lagrangian for Higgs field is of the form

$$\mathcal{L}_{Higgs} = (D_\mu \Phi)^\dagger (D^\mu \Phi) - V(\Phi) \tag{1.5}$$

where

$$D_\mu \Phi = \partial_\mu \Phi - ig_2 T^\alpha W_\mu^\alpha \Phi - ig_1 \frac{Y}{2} B_\mu \Phi. \tag{1.6}$$

The Higgs Lagrangian is invariant under  $SU(2)_L \times U(1)_Y$  transformations. The potential is

$$V(\Phi) = -\mu^2 \Phi^\dagger \Phi + \lambda (\Phi^\dagger \Phi)^2. \tag{1.7}$$

The most general  $SU(2) \times U(1)$  Yukawa coupling between the scalar and fermions is given by

$$\mathcal{L}_{Yukawa} = f^{(e)} \bar{l}_L \Phi e_R + f^{(u)} \bar{q}_L \tilde{\Phi} u_R + f^{(d)} \bar{q}_L \Phi d_R + H.c. \tag{1.8}$$

with the isodoublet  $\tilde{\Phi} = i\tau_2 \Phi^*$ , having hypercharge  $Y(\tilde{\Phi}) = -1$ .

For positive values of  $\mu^2$  and  $\lambda$  in Eq. 1.7, we have spontaneous symmetry breakdown as the scalar develops a vacuum expectation values (VEV)

$$\langle \Phi \rangle_0 = \begin{pmatrix} 0 \\ \frac{v}{\sqrt{2}} \end{pmatrix} \quad \text{with } v = (\mu^2/\lambda)^{1/2}. \quad (1.9)$$

Using the polar variables for the scalar fields

$$\Phi = U^{-1}(\xi) \begin{pmatrix} 0 \\ \frac{v+H(x)}{\sqrt{2}} \end{pmatrix} \quad (1.10)$$

with  $U(\xi) = \exp[i\xi(x) \cdot \tau/v]$ . Thus the original two complex fields  $\phi^+(x)$  and  $\phi^0(x)$  in Tabel 1 are parametrized in terms of four real fields  $\xi_i(x)$  and  $H(x)$ .

Expanding around the VEV point, it is not hard to see that the Goldstone fields are massless, as required. The mass of the Higgs scalar is given by

$$M_H = \sqrt{2}\mu, \quad (1.11)$$

and the fermion masses are

$$m_e = f^{(e)}v/\sqrt{2}, \quad m_u = f^{(u)}v/\sqrt{2}, \quad m_d = f^{(d)}v/\sqrt{2} \quad (1.12)$$

The three 'would-be-Goldstone bosons'  $\xi(x)$  are 'eaten' by the gauge bosons to form three massive intermediate vector bosons. By substituting  $\langle \Phi \rangle_0$  into the Higgs kinetic energy, the mass terms for the electroweak gauge bosons can be found. The mass matrix is easily diagonalized; the physical mass eigenstates are the  $W^\pm$ , the  $Z$  and the photon  $A$ :

$$\begin{aligned} Z_\mu &= \cos \theta_w W_\mu^3 - \sin \theta_w B_\mu \\ A_\mu &= \sin \theta_w W_\mu^3 + \cos \theta_w B_\mu \\ W^\pm &= \frac{1}{\sqrt{2}}(W_\mu^1 \pm iW_\mu^2). \end{aligned} \quad (1.13)$$

As usual, the weak mixing angle is given by

$$\cos \theta_w = \frac{g_2}{\sqrt{g_1^2 + g_2^2}} . \quad (1.14)$$

The mass of the  $W$  is simply

$$M_W = \frac{1}{2} g_2 v , \quad (1.15)$$

while the mass of the  $Z$  is

$$M_Z = \frac{1}{\cos \theta_w} M_W . \quad (1.16)$$

The photon, of course, is massless.

The covariant derivatives tell us how the gauge fields couple to fermions. From Eqs. 1.2 and 1.4, we see that the  $W^\pm$  couples to the usual charged current,

$$\mathcal{L}_W = \frac{g_2}{\sqrt{2}} (\bar{u}_L \gamma^\mu d_L W_\mu^+ + \bar{n}_L \gamma^\mu e_L W_\mu^+) + H.c. . \quad (1.17)$$

The photon  $A$  couples to the electric charge  $Q$ , where  $Q = T^3 + \frac{1}{2}Y$ ,

$$\begin{aligned} \mathcal{L}_A = & e (\bar{q}_L \gamma^\mu Q q_L A_\mu - \bar{u}_R \gamma^\mu Q u_R A_\mu - \bar{d}_R \gamma^\mu Q d_R A_\mu \\ & + \bar{l}_L \gamma^\mu Q l_L A_\mu - \bar{e}_R \gamma^\mu Q e_R A_\mu) , \end{aligned} \quad (1.18)$$

where

$$e = \frac{g_1 g_2}{\sqrt{g_1^2 + g_2^2}} . \quad (1.19)$$

The  $Z$  couples to a second neutral current, specified by the weak charge  $Q_Z = T^3 - \sin^2 \theta_w Q$ ,

$$\begin{aligned} \mathcal{L}_Z = & \frac{g_2}{\cos \theta_w} (\bar{q}_L \gamma^\mu Q_Z q_L Z_\mu - \bar{u}_R \gamma^\mu Q_Z u_R Z_\mu - \bar{d}_R \gamma^\mu Q_Z d_R Z_\mu \\ & + \bar{l}_L \gamma^\mu Q_Z l_L Z_\mu - \bar{e}_R \gamma^\mu Q_Z e_R Z_\mu) . \end{aligned} \quad (1.20)$$

Although the experimental evidence in support of the gauge boson and the fermion sector of the standard model is very strong, experimental information concerning the scalar sector is very weak. The most important piece of evidence providing information about this sector is the  $\rho$ -parameter, defined as the ratio of the neutral current to charged current strength in the effective low-energy Lagrangian. In the standard model, at tree level,  $\rho = 1$ . If one introduces  $N$  scalar multiplets,  $\Phi_i$ , with vacuum expectation values  $v_i$ , which have isospin  $I_i$  and hypercharge  $Y_i$ , then

$$\rho = \frac{\sum_{i=1}^N [I_i(I_i + 1) - \frac{1}{4}Y_i^2]v_i}{\sum_{i=1}^N \frac{1}{2}Y_i^2v_i}. \quad (1.21)$$

The simplest method of satisfying experimental value of  $\rho \sim 1$  is to choose only representations such that  $I_i(I_i + 1) = \frac{3}{4}Y_i^2$ .  $SU(2) \times U(1)$  singlets obey this restriction, as do  $SU(2)$  doublets with  $Y = \pm 1$ . In chapter 2, we will consider the simplest extension of the scalar sector—a model with two scalar doublets of  $Y = \pm 1$ . It is often believed that the presence of tree-level flavor-changing neutral currents in this model is fatal, unless a discrete symmetry is added, since it requires the exchanged scalar to be extremely heavy. This follows, however, from the assumption that the flavor-changing coupling is quite large. Using a more natural value for the flavor-changing coupling, much smaller bounds were obtained. Unlike previous calculations, we calculate the bounds on the flavor-changing couplings of an additional scalar for the processes involving the third generation fields. We have also noted that in most grand unified theories, the  $\tau$  and bottom quark are in the same representation, thus the flavor-changing couplings in the quark sector are related to those in the lepton sector. Comparing flavor-changing  $B$  decays with rare  $\tau$  decays, we can answer which set of decays give better constraints.

The third sector of standard model fields is built from fermions, the quarks and leptons. Three families of quarks and leptons with quantum number in Table 1 have been observed, with the notable exception of the top quark. The family index runs from 1 to 3. From chapter 3, we will work on the possibility of a fourth generation heavy lepton. If a fourth generation exists, the lepton  $L$  and the neutrino  $N$  must both be heavier than 45 GeV. It is certainly possible that the neutrino can either be heavier than, or comparable in mass to, the charged lepton. In this case, the charged lepton can only decay through mixing with lighter generations, and might thus be extremely long-lived. In chapter 3, we investigate the implications of very long-lived charged leptons for cosmology and astrophysics. In the early universe, the relative abundance of a massive weakly interacted particle species “freezes out” when the annihilation rate becomes less than the expansion rate. We calculate the annihilation cross-sections. We also assume that the annihilation cross-section is subject to unitarity constraints and considered the mass range from 45 GeV to 100 TeV. Then we calculate the abundance today. If  $L$  decays, limits on the lifetime of a long-lived charged lepton can be found from several sources: direct detection of the  $L$  and direct detection of its decay products. We calculate the bounds on the mass and lifetime of long-lived charged particles which arise from terrestrial experiments, from astrophysical searches for the decay products and from cosmology which arise from the diffuse photon background (lifetime in excess of  $10^{13}$  sec.), and from the requirement that decay products not unacceptably distort the microwave background radiation (CMB).

In chapter 4, we study the production cross-sections and signatures for the SSC and LHC. We consider four models which contain heavy leptons for the

experimental detection at the Hadron Colliders. Two models are the fourth generation extensions of the standard model in which the right-handed heavy leptons are either isosinglets or in an isodoublet, the other two are motivated by the aspon model of CP violation (the Aspon model is described in appendix B), and contain also singlets or vector lepton doublets. We calculate the production cross-sections for all the processes into heavy leptons, neutrinos and aspon through quark fusion into a photon or  $Z$  (or  $W$ ), as well as through gluon fusion into a Higgs or a  $Z$ . In all these models, the heavy neutrino can either be heavier than, or comparable in mass to, the charged lepton leading to the possibility that the charged lepton can only decay through mixing, thus  $L$  could be very long-lived. We will also discuss the detection of these heavy leptons in Chapter 4.

At the time when I first started my research work, I also did some straightforward work about approximating the renormalization-group equations of minimal supersymmetry. I will include it in Appendix E.

## Chapter 2

### New Scalars

#### 2.1 Introduction

Despite the success of the standard model, there have been many studies of possible extensions of the standard model, ranging from simple extensions such as additional Higgs doublets to more complicated extensions such as supersymmetry and technicolor.

One feature that tends to occur in most extensions of the standard model is the presence of tree-level flavor-changing neutral currents (FCNC's). In fact, even in the simplest extension, with just the addition of a Higgs doublet, such currents will occur. When analyzing such models, virtually all theorists *require* that tree-level FCNC's, in both the quark and lepton sectors, are absent. This requirement is imposed in different ways; often a discrete symmetry is added to the model which eliminates these unwanted currents. In fact, many have examined the effects of virtual particles on one-loop FCNC's to constrain physics beyond the standard model, again *assuming* that this new physics does not give tree-level FCNC's.

The elimination of tree-level FCNC's often requires additional assumptions.

Why do model builders insist on it so frequently? Many point to the small value of the  $K_L - K_S$  mass difference, arguing that any tree-level contribution must be suppressed by making the exchanged particle very heavy; the small value of muon-electron transitions (either in  $\mu \rightarrow e\gamma$  or  $\mu N \rightarrow eN$ ) extends this argument to the lepton sector. Another reason is more psychological: the requirement that tree-level FCNC's be absent led to the prediction of the charmed quark and to the general acceptance of the standard model, and it is natural to suppose that it applies to the entire model.

We feel that the assumption of no tree-level FCNC's may not be as necessary as generally believed. In a model with an extra Higgs doublet, for example, it is often stated that the mass of the extra scalar must be greater than 100 TeV, to avoid too large a contribution to the  $K_L - K_S$  mass difference[2, 3]. This statement assumes, however, that the flavor-changing coupling is as large as the  $b$ -quark Yukawa coupling. A more natural value for the coupling would be[4] the geometric average of the  $d$ -quark and  $s$ -quark Yukawa couplings, which gives a bound on the exchanged particle mass of 1 TeV. Even that applies only to a pseudoscalar exchange; for a scalar, the bound is 300 GeV. Given the uncertainty in the Yukawa couplings of the first two generations, and the fact that Yukawa couplings in the standard model span six orders of magnitude, it is not implausible that the coupling would be somewhat smaller, thus making the bound even smaller. (In many grand unified theories, effective non-renormalizable interactions at the Planck scale[5] give  $\sim M_W M_X / M_{Pl} \sim 10$  MeV uncertainties in all masses, making reliance on the value of the down-quark Yukawa coupling quite dubious anyway.) In addition, the information one obtains from this result would apply only to mixing between the first

and second generations. Since Yukawa couplings in the standard model vary with mass, one might expect FCNC's couplings to also vary with mass, and thus FCNC's involving the third generation (flavor-changing  $B$  decays or  $\tau$  decays) could be considerably larger. Yet virtually all analyses of the effects of tree-level FCNC's in extended Higgs models have only addressed the first two generations[6].

In this chapter, we examine all the bounds that arise on flavor-changing couplings in extended Higgs models from an analysis of rare  $\tau$  and  $B$  decays. These bounds will all consist of an upper limit on the couplings (which are proportional to the exchanged scalar or pseudoscalar mass). The objective here will be to determine which of the many possible processes are most sensitive to these decays, and thus offer the greatest chance of success.

We will then note that in grand unified theories, the quarks and leptons are often in the same representation. This implies that their FCNC's couplings could be related. In other words, a  $\tau$  to  $\mu$  transition would be related to a  $b$ -quark to  $s$ -quark transition. Thus, one will be able to eliminate the  $b$ -quark flavor-changing couplings in favor of the  $\tau$  flavor-changing couplings. In the simplest grand unified theories, the couplings will be equal at the unification scale. The principle question we will address is: which set of decays ( $b$  or  $\tau$ ) will give stronger bounds? In other words, would one be more likely to detect them in  $\tau$  decays or in  $B$  decays? The relevance of this question to the current discussion over whether to build a  $\tau$  factory or a  $B$  factory is obvious. Furthermore, by examining the various bounds, we will be able to determine which processes are most important, and which (in the context of this model) are not.

In Sec. 2, we examine the model itself, and discuss the most reasonable value for the couplings; we also examine the relationship between the flavor-changing  $\tau$  and  $b$ -quark couplings. Sec. 3 contains an analysis of leptonic decays, including three-body decays, radiative decays, and  $\mu - e$  conversion in nuclei. In Sec. 4, we consider  $B$  and  $B_s$  decays, including three-body decays (which are sensitive to scalar exchange), two-body decays which are sensitive to pseudoscalar exchange), as well as  $B - \bar{B}$  mixing. In Sec. 5, our results are discussed and in Sec. 6, we give our conclusions.

## 2.2 Flavor-Changing Neutral Currents

We first consider the simplest possible extension of the standard model - the addition of a Higgs doublet. Since we are interested in neutral currents only, effects of the charged Higgs field will be ignored. The most general Yukawa couplings are given by

$$(\lambda_{ija} \bar{d}'_{iL} d'_{jR} \phi_a + \lambda_{ijb} \bar{d}'_{iL} d'_{jR} \phi_b) + H.c. , \quad (2.1)$$

where  $d'_i = (d', s', b')$ ,  $\phi_a$  and  $\phi_b$  are complex neutral fields and the  $\lambda_{ijk}$  are arbitrary. Similar terms can be written for the charge 2/3 quarks and for the charged leptons. In general, the real components of the Higgs fields will acquire vacuum expectation value  $v_a$  and  $v_b$ . We can then redefine two new scalar fields  $H$  and  $\phi$  as

$$H \equiv \cos \beta \phi_a + \sin \beta \phi_b, \quad \phi \equiv -\sin \beta \phi_a + \cos \beta \phi_b , \quad (2.2)$$

where  $\tan \beta \equiv v_b/v_a$ . The new fields  $H$  and  $\phi$  have real components with vacuum expectation values  $v = \sqrt{v_a^2 + v_b^2}$  and zero, respectively. Note that in

the standard model,  $v = 246$  GeV. The Yukawa couplings can be rewritten in terms of these new fields:

$$(f_{ij}\bar{d}'_{iL}d'_{jR}H + g_{ij}\bar{d}'_{iL}d'_{jR}\phi) + H.c. , \quad (2.3)$$

where the  $f_{ij}$  and  $g_{ij}$  are still arbitrary. The mass matrix is then given by

$$M_{ij} = f_{ij}v/\sqrt{2} . \quad (2.4)$$

When this matrix is diagonalized, we find, in terms of quark mass eigenstates,

$$\begin{aligned} & [m_d\bar{d}_Ld_R(\sqrt{2}H/v) + m_s\bar{s}_Ls_R(\sqrt{2}H/v) \\ & + m_b\bar{b}_Lb_R(\sqrt{2}H/v) + h_{ij}\bar{d}_{iL}d_{jR}\phi] + H.c. , \end{aligned} \quad (2.5)$$

where again, the  $h_{ij}$  are arbitrary. We see that the  $H$  field is the Higgs field of the standard model; the  $\phi$  field is simply an additional scalar which does not contribute to symmetry breaking or to quark and lepton masses; its couplings are, of course, completely arbitrary.

For simplicity, we will neglect mixing between the  $H$  fields and the  $\phi$  field. This will not affect our bounds significantly if the mixing is small. If they do mix, our results for the case of pseudoscalar exchange will be completely unchanged by any mixing. The reason is that the basis has been chosen so that  $H$  gets a vacuum expectation value, and  $\phi$  does not. In this basis, the imaginary part of  $H$  is the Goldstone boson which gives mass to the  $Z$ , and it does not mix with the imaginary part of the  $\phi$  field. All results we have given then still hold, since the  $Z$  couplings are flavor diagonal.

The scalars will mix, in general. If the mass eigenstates are  $H_1$  and  $H_2$ , then the couplings to  $H_1$  are given by

$$(g_{ud}\bar{d}d + g_{us}\bar{s}s + g_{ub}\bar{b}b)H_1 \cos \theta + (h_{ij}^{quark}\bar{d}_i d_j)H_1 \sin \theta , \quad (2.6)$$

and the couplings to  $H_2$  are the same with the obvious replacement of  $\cos \theta \rightarrow -\sin \theta$  and  $\sin \theta \rightarrow \cos \theta$ . Suppose we have a process in which both interactions are flavor changing (such as  $B \rightarrow K\mu\tau$ ). Then the bound on  $m_s$  will change to

$$\min \left[ \frac{m_{H_1}}{\sin \theta}, \frac{m_{H_2}}{\cos \theta} \right]^4 . \quad (2.7)$$

If one of the couplings is flavor diagonal, then the change is a bit more complicated, but straightforwardly calculated. Note that if the mixing is small, this gives the same results as before. Since all mixing angles known in the standard model have  $\cos \theta > 0.85$ , we do not expect mixing to give a significant effect, but one should certainly be aware of the possibility.

Neglecting the mixing, the  $H$  field is then identical to the standard-model Higgs field (with the imaginary component being the Goldstone boson absorbed by the  $Z$ ). The complex  $\phi$  field is composed of a scalar  $\phi_s$  and a pseudoscalar  $\phi_p$ . The couplings of the scalar are given by

$$\frac{h_{ij}}{\sqrt{2}} \bar{d}_i d_j \phi_s , \quad (2.8)$$

and those of the pseudoscalar by

$$\frac{h_{ij}}{\sqrt{2}} \bar{d}_i \gamma_5 d_j \phi_p , \quad (2.9)$$

with similar terms for the leptons. For simplicity, we will assume here that the Yukawa coupling matrices are Hermitian (or at least that the deviations from hermiticity are small).

These extra scalars will lead to tree-level flavor-changing neutral currents through scalar exchange. The rate for such processes will generally be proportional to  $h_{ij}^2 h_{kl}^2 / m_\phi^4$ . It is important to note that some processes, such as

two body  $B$  decays, will only occur through pseudoscalar exchange, and others, such as three body  $B$  decays, will only occur through scalar exchange. Some processes, such as  $\tau$  decays, occur through both. This has led to some misunderstandings in the literature. In the classic work of Shankar[2], many processes (again, involving only the first two generations) were listed in a table with the accompanying bound on the scalar mass (assuming the couplings were all equal to the  $b$  or  $\tau$  Yukawa coupling). In some cases, the bound refers to the scalar mass and in some, it refers to the pseudoscalar mass. In processes (such as  $\mu$  decays) with both, it was assumed that the masses were equal. Although this was stated early in the text, the table gave the impression that the various modes were competing with each other. This is not the case— the process  $K \rightarrow \mu e$  for example, only bounds the pseudoscalar mass, whereas the process  $K \rightarrow \pi \mu e$  only bounds the scalar mass. Since the masses are expected to be different, these two processes do not compete with each other. In this chapter, we will consider bounds on the scalar mass and bounds on the pseudoscalar mass to be completely separate, and give results for each. In experiments looking for rare decays, it is crucial to keep this distinction in mind when quoting bounds on scalar masses.

We now turn to the value of the coupling constants,  $h_{ij}^{quark}$  for the charged  $-1/3$  sector and the corresponding couplings  $h_{ij}^{lepton}$  for the lepton sector. Although they are in principle arbitrary, we do have some theoretical guidance. When citing bounds, experimenters calculate the bounds using couplings of the order of the gauge coupling; their bound is then cited in the form  $m_S h_{ij}/g$ . This makes the mass scale appearing in the bound quite large. However, not only is there no reason to expect these Yukawa couplings to be as large as

gauge couplings, but there is every reason to expect them to be much smaller. After all, fourteen of the fifteen Yukawa couplings in the standard model are orders of magnitude smaller than the gauge couplings, and those involving the first generation are five orders of magnitude smaller.

What is the most reasonable value for these couplings? Some early authors [2, 6] chose the following approach: since the most conservative approach is to take all couplings to be comparable, and since in some sense the heaviest fermion sets the scale for the whole matrix, we can assume that each element is given by the Yukawa coupling of the heaviest quark or lepton times some mixing angle. As we don't know these mixing angle factors, we set all of them to 1. Thus, all of the  $h_{ij}$  are given by the Yukawa coupling of the  $b$  or  $\tau$ . Many of the bounds cited in the literature for the mass scale of the exchanged scalar assume this coupling. This approach was strongly criticized in Ref. [4]. They argued that the assumption that all of the couplings are comparable was not reliable, since one of the most conspicuous features of the fermion mass spectrum is its hierarchical structure. They showed that if one assumes that there is no fine-tuning (in which large terms add together to make a small term), then there is a small set of phenomenologically sound Yukawa matrices, and that all of these possibilities lead to Yukawa couplings of the form

$$h_{ij}^{quark} = \sqrt{(g_Y)_i (g_Y)_j} , \quad (2.10)$$

where  $(g_Y)_i$  is the Yukawa coupling of  $d_i$ . A similar term arises for the leptons. In other words, the flavor-changing coupling of the additional scalar to, for example, the  $b$  and  $s$  quarks, should be of the order of the geometric mean of the Yukawa couplings of the  $b$  and  $s$  quarks. This assumption gives the observed Kobayashi Maskawa (KM) angles without fine-tuning.

Although we will keep our results general, we will consider the choice in Eq. 2.10 to be a “preferred” value, and will also express the results in terms of this value. To this end, we define

$$\eta_{ij}^{quark} \equiv \frac{h_{ij}^{quark}}{(g_Y)_b}, \quad \eta_{ij}^{lepton} \equiv \frac{h_{ij}^{lepton}}{(g_Y)_\tau}. \quad (2.11)$$

The early estimates will correspond to  $\eta_{ij} = 1$ . Substituting Eq. 2.10 into Eq. 2.11 gives the “most natural value” for the couplings. This value for  $\eta_{ij}^{quark}$  is  $\sqrt{m_i m_j / m_b}$  and that for  $\eta_{ij}^{lepton}$  is  $\sqrt{m_i m_j / m_\tau}$ .

Is there any connection between the flavor-changing neutral-current couplings in the quark sector and those in the lepton sector? In general, there is not, but one might expect a connection to exist in grand unified theories. In  $SU(5)$ , for example, the  $b$  and the  $\tau$  are in the same representation and have the same Yukawa couplings (at the unification scale  $M_X$ ). If one adds a Higgs 5-plet to the model, then the flavor-changing neutral-current couplings in the quark sector and in the lepton sector will be identical; i.e., the  $h_{b_s}$  coupling will be equal to the  $h_{\mu\tau}$  coupling, etc. How generic is this result? In models with a “grand desert”, the  $b$  to  $\tau$  mass ratio at  $M_X$  (obtained by extrapolating the observed low-energy value to high energies) is unity; i.e., the Yukawa couplings of the  $b$  and of the  $\tau$  are equal at  $M_X$ . If this occurs for group theoretic reasons [as it does in minimal  $SU(5)$  and  $SO(10)$ ], then FCNC’s couplings in simple extensions of the Higgs sector will be equal at  $M_X$ . Even in many intermediate scale models, as well as in supersymmetric models, the successful prediction of the low-energy  $b$  to  $\tau$  mass ratio is not significantly affected, thus the equality of the FCNC’s couplings also should not be. However, in models with family group symmetries, or in models with much more complicated Higgs structures [such as  $SU(5)$  with 5-plets and 45-plets], one would expect a different relation-

ship between the couplings, if any. Throughout this chapter, we will assume that the flavor-changing neutral-current couplings of the quarks equal those of the leptons at  $M_X$ , as expected in the simplest grand unified theories (GUTs).

If the couplings are equal at the GUT scale, we must renormalize them down to the electroweak scale. The renormalization-group equation for each coupling will be of the general form

$$\begin{aligned} \mu \frac{dh_{ij}}{d\mu} = & h_{ij}(C_Y \alpha_Y + C_s \alpha_s) \\ & + C_{w_{ij}} h_{kl} \alpha_w + C_{h_{ij}} h_{jk} h_{il} h_{kl} , \end{aligned} \quad (2.12)$$

where the  $\alpha$ 's are the gauge couplings and the  $C$ 's are easily calculable coefficients. In the cases of interest, the  $h_{ij}$  will always be smaller than the gauge couplings (especially smaller than the strong coupling), so the last term can be dropped. The  $\alpha_w$  term is identical for both quarks and leptons, so it will drop out of the ratio. The  $\alpha_s$  term, of course, only applies to  $h_{ij}^{quark}$ . The remaining equation is *identical* to the renormalization-group equation for the conventional Yukawa couplings in the standard model (under the same approximations). As a result, the ratio of  $h_{ij}^{quark}$  to  $h_{ij}^{lepton}$  should be the same as the ratio of the  $b$  to  $\tau$  Yukawa couplings, i.e., the ratio of the  $b$  mass to the  $\tau$  mass (see Ref. [7] for an explicit derivation):

$$\frac{h_{ij}^{quark}}{h_{ij}^{lepton}} = \frac{m_b}{m_\tau} . \quad (2.13)$$

Virtually all of the contribution to this ratio comes from the effects of the  $SU(3)$  coupling.

One minor caveat must be mentioned. In deriving the  $b$  to  $\tau$  mass ratio in grand unified theories, one runs the couplings down to  $Q^2 = 4m_b^2$ , since the  $b$  mass is "measured" by the threshold for  $b$ -pair production. Here, we only

need to run the coupling down to  $Q^2 = m_\phi^2$ . This introduces a correction to the right-hand side of Eq. 2.13 which is given by

$$\left[ \frac{\alpha_s(m_\phi^2)}{\alpha_s(4m_b^2)} \right]^{12/23} . \quad (2.14)$$

The factor of 12/23 is related to the anomalous dimension and  $\beta$  function of the QCD coupling, see Ref. [7] for details. For the range of  $m_\phi$  which is of interest (40 to 1000 GeV), this factor ranges from 82% to 92%. Since the uncertainty in matrix elements in  $b$  decays is typically a factor of 2, this correction will be smaller than the uncertainty in the results. We will, nonetheless, include a 10% correction in our final results (for each  $h_{ij}^{quark}$ ), although for simplicity, we will ignore it in the text.

We now can see the advantage of the notation used in Eq. 2.11. Plugging in Eq. 2.13, we find that

$$\eta_{ij}^{quark} = \eta_{ij}^{lepton} . \quad (2.15)$$

As in grand unified theories, this relation should be most reliable for second- and third-generation fields. We will use this relation (modulo the correction mentioned in the last paragraph) and express our results entirely in terms of  $\eta_{ij}^{lepton}$ . Note that the only assumption we have made is that the quark FCNC's and lepton FCNC's are identical at some grand unified scale—an assumption which is true in the simplest grand unified models. Our statement that the most natural value for  $\eta_{ij}^{lepton}$  is  $\sqrt{m_i m_j}/m_\tau$ , although plausible, is less reliable<sup>1</sup>, and is based on the “no fine-tuning” arguments of Ref.[4].

<sup>1</sup>Note that we have expressed our results in terms of  $\eta_{ij}^{lepton}$  instead of  $\eta_{ij}^{quark}$  since the “most natural value” for this will not be based on quark masses. The well-known problem of the  $SU(5)$  prediction  $m_d/m_s = m_e/m_\mu$ , which is presumably solved by the fact that nonrenormalizable Planck scale interactions (see Ref. [5]) give an uncertainty of  $\sim 10$  MeV in the masses, makes this value much more reliable for second- and third-generation fields than for first-generation fields, although even for these fields it should not be more than an order of magnitude off (in the square of coupling).

Let us summarize the results of this section. In the simplest extension of the standard model, the addition of another scalar multiplet, one generally has tree-level flavor-changing neutral currents. If the flavor-changing couplings are taken to be the same as the  $b$ -quark Yukawa coupling, then the resulting lower bound on the exchanged scalar mass is very large. However, it has been argued that a more natural value for these couplings is the geometric mean of the Yukawa couplings of the two quarks (or leptons), which leads to much lower couplings. We have noted that the Yukawa couplings of the first two generations are very small and uncertain, and have pointed out that bounds based on mixing with the third generation should be more reliable. We have also noted that in many grand unified theories the  $\tau$  and  $b$  flavor-changing couplings are identical at the unification scale. When they are renormalized, we find that  $\eta_{ij}^{quark} = \eta_{ij}^{lepton}$ , where  $\eta_{ij}^{quark(lepton)}$  is the ratio of the flavor-changing coupling between the  $i$ th quark and  $j$ th quark (lepton) to the Yukawa coupling of the  $b$  ( $\tau$ ). (This relation has a 10% correction which we include.) This relation will be used throughout, as we determine the bounds on the  $\eta_{ij}$  from various rare decays. The “most natural value” for the  $\eta_{ij}$  will not be explicitly used, but should be kept in mind in determining how strong the various constraints are.

## 2.3 Constraints from Rare $\tau$ Decays

### 2.3.1 Three-body decays

The flavor-changing interactions of the  $\phi$ , and  $\phi_p$  will lead to lepton-number-violating  $\tau$  decays, as shown in Fig. 2.1.

There are six rare  $\tau$  decays which will occur:

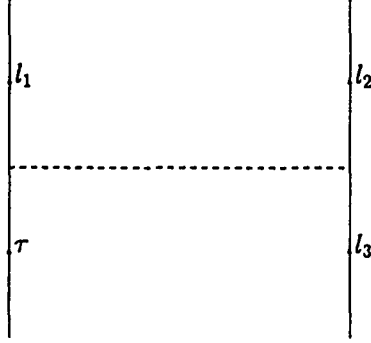


Figure 2.1: Lepton-number-violating  $\tau$  decays can occur through exchange of an intermediate scalar.  $l_1$ ,  $l_2$ , and  $l_3$  are either electrons or muons. If two identical fermions are in the final state, an exchange diagram must be subtracted. In some cases, such as  $\tau \rightarrow e^+ e^- \mu^-$ , the process can occur with either  $l_1 = \mu^-$ ,  $l_2 = e^-$  and  $l_3 = e^+$  or  $l_1 = e^-$ ,  $l_2 = \mu^-$  and  $l_3 = e^+$ ; these two diagrams have different coupling constant dependences and are added.

$$\begin{aligned} \tau \rightarrow e^- e^- e^+ , \tau \rightarrow \mu^- \mu^- \mu^+ , \tau \rightarrow e^- e^- \mu^+ , \\ \tau \rightarrow \mu^- \mu^- e^+ , \tau \rightarrow e^- \mu^- e^+ , \tau \rightarrow e^- \mu^- \mu^+ . \end{aligned} \quad (2.16)$$

The latter two can occur through two different processes; for example,  $\tau \rightarrow e^- \mu^- e^+$  can occur either through a  $h_{\mu\tau} h_{ee}$  term or through a  $h_{e\tau} h_{e\mu}$  term. For example, the matrix element can be written as

$$M = \frac{i}{m_s^2} (\bar{u}_\mu h_{e\mu} u_e \bar{u}_e h_{e\tau} u_\tau + \bar{u}_e h_{ee} u_e \bar{u}_\mu h_{\mu\tau} u_\tau) , \quad (2.17)$$

where we have ignored the momentum dependence of the propagator (since the scalar mass is so much larger than the momentum transfer). A similar term will exist from pseudoscalar exchange (with a  $\gamma_5$  in the vertices); as discussed in the preceding section, since only the lighter of the scalar and pseudoscalar will contribute much, we are considering the two cases separately. Note that if

the scalar and pseudoscalar masses were similar, then interference between the matrix elements would be important. However, the masses come from different terms in the Higgs potential, and will generally be different; we are assuming that they are sufficiently different that the interference term will not drastically change the results. The momentum dependence of the spinors has not been explicitly shown. Neglecting the mass of the muon, this gives a decay rate of

$$\omega = \frac{m_\tau^5}{3072\pi^3 m_s^4} (h_{e\tau}^2 h_{e\mu}^2 + h_{ee}^2 h_{\mu\tau}^2 + \frac{1}{2} h_{ee} h_{e\mu} h_{e\tau} h_{\mu\tau}). \quad (2.18)$$

The rate for pseudoscalar exchange is identical, with  $m_s \rightarrow m_p$ . The observed limit on the branching ratio is  $3.3 \times 10^{-5}$ . With this limit, we then find that

$$\eta_{e\tau}^2 \eta_{e\mu}^2 + \eta_{ee}^2 \eta_{\mu\tau}^2 + \frac{1}{2} \eta_{e\tau} \eta_{ee} \eta_{e\mu} \eta_{\mu\tau} < 1400 \left[ \frac{\min(m_s, m_p)}{m_W} \right]^4 \quad (2.19)$$

using the definition of  $\eta_{ij}$  given in the preceding section. Completing the square, and assuming maximal interference, gives

$$\eta_{e\tau}^2 \eta_{e\mu}^2 + \eta_{ee}^2 \eta_{\mu\tau}^2 < 1800 \left[ \frac{\min(m_s, m_p)}{m_W} \right]^4. \quad (2.20)$$

A similar calculation can be done for each of the above six processes. The results are given in Table 2.1, where we have also include the bound from the  $\mu \rightarrow 3e$  process. All experimental bounds in this chapter are from Ref. [8], unless explicitly stated otherwise.

Note how poor the bounds from  $\tau$  decays are. As discussed in the preceding section, the most natural values for the  $\eta_{ij}$  are much less than one, and thus these processes do not give any significant limits, even for a very light scalar or pseudoscalar. Improvement in the experimental bounds of at least three orders of magnitude (and generally four or five orders of magnitude) would be needed

Table 2.1: Bounds on the flavor-changing couplings which arise from three-body leptonic decays. The numerical values should be understood as multiplied by  $(m_s/m_W)^4[(m_p/m_W)^4]$ . The contribution is the same for scalar exchange and for pseudoscalar exchange, and so leads to identical bounds on the masses.

Decay process	Expt. limit	Bound
$\tau \rightarrow e^-e^-e^+$	$3.8 \times 10^{-5}$	$\eta_{ee}^2\eta_{e\tau}^2 < 2000$
$\tau \rightarrow \mu^-\mu^-\mu^+$	$2.9 \times 10^{-5}$	$\eta_{\mu\mu}^2\eta_{\mu\tau}^2 < 1600$
$\tau \rightarrow e^-e^-\mu^+$	$3.8 \times 10^{-5}$	$\eta_{e\tau}^2\eta_{e\mu}^2 < 2000$
$\tau \rightarrow \mu^-\mu^-e^+$	$3.8 \times 10^{-5}$	$\eta_{\mu\tau}^2\eta_{e\mu}^2 < 2000$
$\tau \rightarrow e^-\mu^-e^+$	$3.3 \times 10^{-5}$	$\eta_{e\tau}^2\eta_{e\mu}^2 + \eta_{ee}^2\eta_{\mu\tau}^2 < 1800$
$\tau \rightarrow e^-\mu^-\mu^+$	$3.3 \times 10^{-5}$	$\eta_{\mu\tau}^2\eta_{e\mu}^2 + \eta_{\mu\mu}^2\eta_{e\tau}^2 < 1800$
$\mu \rightarrow e^-e^-e^+$	$1.0 \times 10^{-12}$	$\eta_{ee}^2\eta_{e\mu}^2 < 10^{-5}$

to approach the interesting region <sup>2</sup>. We now turn to radiative decays.

### 2.3.2 Radiative decays

The flavor-violating couplings of the  $\phi_s$  and  $\phi_p$  will also lead to lepton-number-violating radiative decays of the  $\mu$  and  $\tau$ , through the one-loop diagrams shown in Fig. 2.2. One expects that these will give better bounds than flavor-changing radiative decays of the  $b$ , since the latter already occur at one-loop in the standard model. From electromagnetic gauge invariance the on-shell  $l_1 \rightarrow \gamma l_3$  amplitude is a magnetic transition

$$M = \epsilon^\mu \bar{u}_{l_3}(p') [iq^\nu \sigma_{\nu\mu} (A + B\gamma_5)] u_{l_1}(p). \quad (2.21)$$

<sup>2</sup>Even the original assumption of Shanker gave  $\eta_{ij} = 1$ , which will not be probed by  $\tau$  decays. Note, however, that the difference between our assumption regarding the most natural value of the  $\eta_{ij}$  and his does make a major difference in interpreting the  $\mu \rightarrow 3e$  bound. His assumption that the couplings (even for the first and second generations) are all equal to the  $\tau$  Yukawa coupling gives a lower bound on  $m_s$ , of about 1 TeV. Our assumption, discussed in Sec. 2.2, that  $\eta_{ij} = \sqrt{m_i m_j}/m_\tau$ , gives a lower bound on  $m_s$ , of only about 1 GeV, i.e., no significant bound at all.

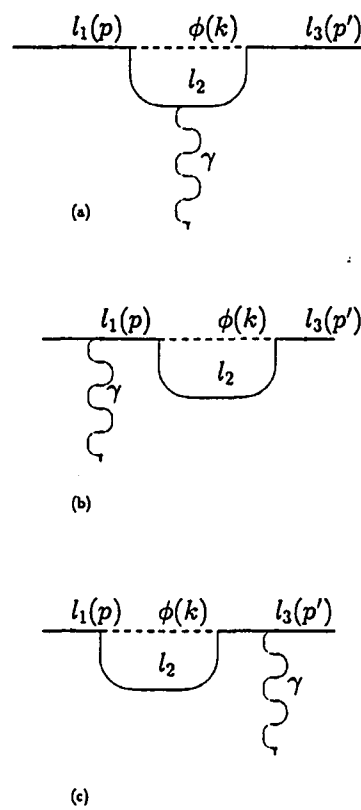


Figure 2.2: Diagrams which lead to lepton-number-violating radiative decays. If  $l_1$  and  $l_3$  are identical, these diagrams give contributions to anomalous magnetic moment.

This means that there is no need to calculate the diagrams in Fig. 2.2(b)-(c) since they are all proportional to  $\bar{u}_{l_3}\gamma^\mu u_{l_1}$  and will be cancelled by the terms of similar form comes from the diagram in Fig. 2.2(a). As we shall make the approximation  $m_s = 0$ , the two invariant amplitudes  $A$  and  $B$  are equal. We have

$$\begin{aligned} M &= A\bar{u}_{l_3}(p')iq^\nu\sigma_{\nu\mu}\epsilon^\mu(1+\gamma_5)u_{l_1}(p) \\ &= A\bar{u}_{l_3}(p')(2p\cdot\epsilon - m_2\gamma\cdot\epsilon)(1+\gamma_5)u_{l_1}(p) \end{aligned} \quad (2.22)$$

Thus in our calculation of  $A$  we need only to concentrate on the  $p\cdot\epsilon$  term. The invariant amplitude  $A$  is given by

$$A = -eh_{l_1l_2}h_{l_2l_3} \left[ -\int \frac{d^n k (\not{p}' - \not{k} + m_2)}{(2\pi)^n (p' - k)^2 - m_2^2} \frac{\gamma_\mu}{k^2 - m_s^2} \frac{(\not{p} - \not{k} + m_2)}{(p - k)^2 - m_2^2} \right]. \quad (2.23)$$

Here, we have only shown the result when the scalar is in the loop; if the pseudoscalar is in the loop, appropriate  $\gamma_5$ 's must be inserted.

First, consider  $\tau \rightarrow e\gamma$  decay. Performing all of the integrations and expanding in powers of  $m_\tau^2/m_s^2$ , we find that the leading term is  $O(m_\tau^2/m_s^2)$  and get

$$\begin{aligned} |M|^2 &= \frac{e^2 m_\tau^2}{256\pi^4 m_s^2} |\bar{u}_e(p') \left[ \not{\epsilon} - 2\frac{p\cdot\epsilon}{m_\tau} \right] u_\tau(p)|^2 \\ &\quad \times \left[ h_{\tau\tau}h_{e\tau} \left( -\frac{4}{3} - \ln \frac{m_\tau^2}{m_s^2} \right) + \frac{1}{6}(h_{e\tau}h_{ee} + h_{\mu\tau}h_{e\mu}) \right]^2. \end{aligned} \quad (2.24)$$

Unless there is fine-tuning, the interference terms will be negligible. Ignoring them, we get the overall decay rate

$$\omega = \frac{e^2 m_\tau^5}{2^{13} 9\pi^5 m_s^4} \left[ 4(4 + 3 \ln \frac{m_\tau^2}{m_s^2})^2 h_{\tau\tau}^2 h_{e\tau}^2 + h_{ee}^2 h_{e\tau}^2 + h_{\mu\tau}^2 h_{e\mu}^2 \right]. \quad (2.25)$$

Comparing with the standard  $\tau$  decay, we find that

$$4(4 + 3 \ln \frac{m_\tau^2}{m_s^2})^2 \frac{h_{\tau\tau}^2 h_{e\tau}^2}{g^4} + \left[ \frac{h_{ee}^2 h_{e\tau}^2 + h_{\mu\tau}^2 h_{e\mu}^2}{g^4} \right] < 1.4 \left[ \frac{m_s}{m_W} \right]^4. \quad (2.26)$$

Table 2.2: Bounds on flavor-changing couplings which arise from radiative decays of the  $\tau$  and  $\mu$ . The numerical values should be understood as multiplied by  $(m_s/m_W)^4[(m_p/m_W)^4]$ . The bounds for the case of scalar exchange are slightly different from those for the case of pseudoscalar exchange; the number in parentheses gives the bound when the pseudoscalar mass is used.

Decay process	Expt. limit	Bound
$\tau \rightarrow e\gamma$	$2.0 \times 10^{-4}$	$(4 + 3 \ln m_\tau^2/m_s^2)^2 \eta_{\tau\tau}^2 \eta_{e\tau}^2 < 5.5 \times 10^6 (2.2 \times 10^5)$
$\tau \rightarrow \mu\gamma$	$5.5 \times 10^{-4}$	$(4 + 3 \ln m_\tau^2/m_s^2)^2 \eta_{\tau\tau}^2 \eta_{\mu\tau}^2 < 1.7 \times 10^7 (6.8 \times 10^5)$
$\mu \rightarrow e\gamma$	$5.0 \times 10^{-11}$	$(3 + 2 \ln m_\tau^2/m_s^2)^2 \eta_{\mu\tau}^2 \eta_{e\tau}^2 < 3.6 \times 10^{-4} (3.6 \times 10^{-4})$

The terms in the square brackets are negligible, compared with the right-hand side, because of the bounds from three-body decays from Table 2.1. Dropping these and expressing the results in terms of the  $\eta_{ij}$  finally gives the results in Table 2.2. A similar calculation can be done for the process  $\tau \rightarrow \mu\gamma$ .

We can also calculate the process  $\mu \rightarrow e\gamma$ . Here, the dominant contribution (by many orders of magnitude) comes when the fermion line in the loop is a  $\tau$ . The calculation is similar; the matrix element is

$$|M|^2 = \frac{e^2}{256\pi^4} \frac{m_\tau^2 m_\mu^2}{m_s^4} h_{\mu\tau}^2 h_{e\tau}^2 \left( \frac{3}{2} + \ln \frac{m_\tau^2}{m_s^2} \right)^2 \times |\bar{u}_e(p') \left[ \not{\epsilon} - 2 \frac{p \cdot \epsilon}{m_\mu} \right] u_\mu(p)|^2. \quad (2.27)$$

which then gives the bound listed in Table 2.2:

$$(3 + 2 \ln \frac{m_\tau^2}{m_s^2})^2 \eta_{\mu\tau}^2 \eta_{e\tau}^2 < 3.6 \times 10^{-4} \left[ \frac{m_s(m_p)}{m_W} \right]^4, \quad (2.28)$$

Suppose we choose the “most natural” values for the  $\eta_{ij}$ , i.e.,  $\eta_{\mu\tau} = \sqrt{m_\mu/m_\tau}$ ,  $\eta_{e\tau} = \sqrt{m_e/m_\tau}$ . Then the bound on  $m_s$  and  $m_p$  is 4 GeV.

After this work was complete, Chang[9] estimated the two-loop contributions to  $\mu \rightarrow e\gamma$ . This is motivated by the work of Bjorken and Weinberg[10] who

showed that certain two-loop graphs may in fact dominate over the one-loop contribution. The bound is then given by

$$\eta_{\mu\tau}^2 \eta_{e\tau}^2 < 4.1 \times 10^{-7} \left[ \frac{m_s(m_p)}{m_W} \right]^4 . \quad (2.29)$$

Then the limit for  $m_s$  and  $m_p$  are above 200 GeV.

Let us restate this point. In the simplest extension of the standard model, with what we believe to be the most natural values for the additional flavor-changing couplings, one expects  $\mu \rightarrow e\gamma$  to occur at a rate not much below the current limit. If the extra scalars have masses about 200 GeV, as one might expect, then the decay will be observed within the next few years. Note that here, observation of  $\mu \rightarrow e\gamma$  *doesn't* indicate mixing between the muon and the electron, but rather between the muon and the tau, and between the electron and the tau. As we will see later, the bound from this process is the one of the most severe, and thus this decay may be the first signature of this simple extension.

Suppose the decay is seen. At that time, all theorists will come up with their particular models. Is there any way to distinguish between these models? The clearest way to determine which model is correct, of course, is to observe additional signatures. Although  $\mu \rightarrow e\gamma$  is the first signature likely to be observed, we will see in the next section that there are other signatures in rare  $B$  decays that may not be far behind. First, we consider other lepton-number-violating processes.

### 2.3.3 Other processes

It has been pointed out[11] that bounds from muon to electron conversion in nuclei are very often stronger than bounds from  $\mu \rightarrow e\gamma$ . The reason is that the

“exchanged particle” often couples coherently to the nucleus. Here, however, the bound from muon conversion will be weaker. The reason is that we are interested in bounds in couplings involving the third generation, i.e., it is still necessary to have a  $\tau$  in a loop; the relevant diagrams simply involve attaching the nucleus to the photon in the  $\mu \rightarrow e\gamma$  diagrams. The photon will couple coherently to the nucleus (the cross section will vary as  $Z^2$ ), but the loop is still necessary. We have calculated the rate for muon to electron conversion in titanium (which gives the strongest bound) and found the bound to be two orders of magnitude weaker than that from  $\mu \rightarrow e\gamma$ . We have not included QCD enhancements, finite-size effects, etc.; should these enhance the rate by a factor of 100, then muon to electron conversion would give bounds competitive with  $\mu \rightarrow e\gamma$  (at least until the latter is improved).

Bounds can also be calculated from the contribution of scalar exchange to the anomalous magnetic moments of the electron and muon. Nor surprisingly (since the standard electroweak contribution is too small to have been seen), these bounds are also much, much weaker than the other processes we have considered. Finally, one could also consider two-body  $\tau$  decays, such as  $\tau \rightarrow \mu K^0$ . These processes will all involve couplings involving the first generation fields, and are expected to be small; it turns out that the bounds are much weaker than those from  $B$  decays.

## 2.4 $B$ and $B_S$ Decays

### 2.4.1 Three-body decays

The flavor-changing neutral-current interaction will also lead to anomalous  $B$  decays. We will only consider semileptonic decays; nonleptonic decays are

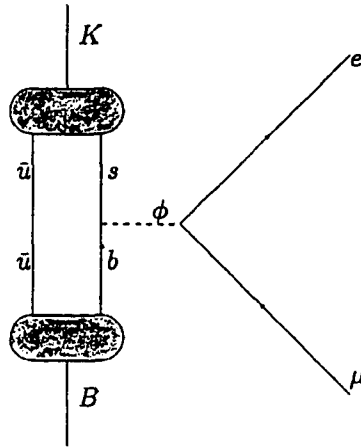


Figure 2.3: Contributions to three-body decays of the  $B$  meson. The exchanged particle, in this case, must be a scalar.

much more difficult to calculate and the experimental bounds are much, much worse. Of course, some processes, such as  $B \rightarrow K\mu^+\mu^-$  occur at the one-loop level in the standard model, but some, such as  $B \rightarrow K\mu^+\tau^-$ , do not. In all cases that we consider, the standard-model processes will occur at a rate far below the current experimental limit. For example, the process  $B \rightarrow K^-\mu^+e^-$  occurs through the diagram in Fig. 2.3. Unlike  $\tau$  decays, this process can not occur through either scalar or pseudoscalar exchange. The reason is simply that the parity of the  $B$  and the  $K$  are the same, and the interaction does not change the spin, thus only a scalar can be exchanged. (In two-body decays, only the pseudoscalar can be exchanged, as we will see.)

The matrix element is

$$M = i \frac{h_{e\mu} h_{sb}}{m_\phi^2} \bar{u}_e v_\mu f_+(q^2), \quad (2.30)$$

where  $f_+(q^2)$  is a Lorentz-invariant form factor which is only a function of  $q^2 = (p - p')^2$ . (Note that another possible form factor, often referred to as  $f_-$ , does not contribute because of conservation of the vector current; see Okun[12] for a discussion.) This form factor can be calculated with the nonrelativistic approximation of Isgur and Scora[13], which should cause an error somewhat less than a factor of 2. Their procedure can be outlined as follows.

We can write

$$f^+(q^2) = \langle K^-(p') | \bar{s} b | B^-(p) \rangle . \quad (2.31)$$

The nonrelativistic state vectors for the  $B^-$  and  $K^-$  bosons are given by

$$\begin{aligned} |B^-(p)\rangle &= \sqrt{2m_B} \int d^3k \phi_B(k) \sum \chi_{s\bar{s}} |b \left[ \frac{m_b}{m_B} p_B + k, s \right] \rangle \\ &\quad \times |\bar{u} \left[ \frac{m_u}{m_B} p_B - k, \bar{s} \right] \rangle , \\ |K^-(p')\rangle &= \sqrt{2m_K} \int d^3k' \phi_K(k') \sum \chi_{s's'} |s \left[ \frac{m_s}{m_K} p'_K + k', s' \right] \rangle \\ &\quad \times |\bar{u} \left[ \frac{m_u}{m_K} p'_K - k', \bar{s}' \right] \rangle , \end{aligned} \quad (2.32)$$

where  $\chi_{s\bar{s}}$  couples the spins  $s$  and  $\bar{s}$  to the total spin zero and  $\phi(k)$  is the relative momentum-space wave function. Isgur and Scora chose Schrödinger wave functions that are appropriate to a Coulomb plus linear potential and used variational solutions based on harmonic-oscillator wave function:

$$\phi^{1s}(r) = \frac{\beta_s^{3/2}}{\pi^{3/4}} \exp(-\beta_s^2 r^2 / 2) , \quad (2.33)$$

in which  $\beta_s$  is the variational parameter, whose value turns out to be  $\beta_s \sim 0.3$  GeV. We now compute the Fourier transform of these wave functions and substitute the result into Eqs. 2.31 and 2.32. Note that the form factor vanishes if a  $\gamma_{5s}$  is present, so that pseudoscalar exchange does not contribute. The

result for the form factor is

$$f_+(q^2) = 2\sqrt{m_B m_K} \frac{\beta_B^{3/2} \beta_K^{3/2}}{\beta_{BK}^3} \exp \left[ -\frac{m_u^2(t_m - t)}{4\beta_{BK}^2 m_B m_K} \right], \quad (2.34)$$

where  $\beta_{BK}^2 = (\beta_B^2 + \beta_K^2)/2$  and  $t_m = (m_B - m_K)^2$ . The decay rate is

$$\frac{h_{s^*}^2 h_{e\mu}^2 \beta_B^3 \beta_K^3 m_B^2 m_K^3}{16\pi^3 \beta_{BK}^4 m_s^4 m_u^2} \left( 1 - \frac{m_K \beta_{BK} \sqrt{2\pi}}{m_u m_B} \times \operatorname{erf} \left[ \frac{m_u m_B}{2\sqrt{2} m_K \beta_{BK}} \right] \right), \quad (2.35)$$

where  $\operatorname{erf}(x)$  is the error function [normalized so that  $\operatorname{erf}(\infty)=1$ ].

Since we know that the lifetime of the  $B^-$  is  $10^{-12}$  sec, we can compute the branching ratio for the process. The results are identical for all processes of the form  $B^- \rightarrow K^- l_1 l_2$  for any two leptons, with the obvious change in the couplings. If there is one  $\tau$  in the final state, there is a phase-space factor of 0.7; if there are two  $\tau$ 's, the phase-space factor is 0.4. The resulting bound on the  $\eta$ 's is given by (with inclusion of the factor of 20% in the conversion from  $\eta^{quark}$  to  $\eta^{lepton}$ )

$$\begin{aligned} \eta_{\mu\tau}^2 \eta_{l_1 l_2}^2 &< 7 \times 10^4 (\text{branching ratio}) \\ &\times \left[ \frac{m_s}{m_W} \right]^4 / (\text{phase - space factor}). \end{aligned} \quad (2.36)$$

All we need to do now is to put in the various branching ratios. Note that a similar calculation can be done for  $B^- \rightarrow \pi^- l_1 l_2$ , with an identical result (with  $m_K \rightarrow m_\pi$ ), although the nonrelativistic approximation is a bit more suspect in this case. Experimental bounds have been given for decays in which the two leptons are muons and/or electrons, but no bounds have been cited when one or both is a  $\tau$ . Nonetheless, one can make a rough estimate of the bounds from two processes which have been cited [14, 15]:

$$\begin{aligned} \frac{\Gamma(B \rightarrow e^+ e^- X) + \Gamma(B \rightarrow \mu^+ \mu^- X)}{\Gamma(B \rightarrow \text{all})} &< 2.4 \times 10^{-3}, \\ \frac{\Gamma(B \rightarrow \mu^+ \mu^- X)}{(\Gamma \rightarrow \text{all})} &< 5.3 \times 10^{-5}, \end{aligned} \quad (2.37)$$

where the charge of the  $B$  is undetermined. For example, if  $B \rightarrow K\mu\tau$  occurs, it will give a signal in the above process 17% of the time (the percentage of  $\tau$ 's which decay into muons). Consider the first of these bounds. We have made two modifications to it. First, in extracting their bound, the authors chose many different possible matrix elements to model the decay, and cited the one that gave the most conservative bound. Unfortunately, none of these matrix elements was a scalar. We have chosen to model the decay with a constant matrix element, resulting in a bound which is a factor of 2 smaller than the one they cite (virtually all of their choices gave a factor within 10% of this one). Second, they also searched for  $B \rightarrow e^+\mu^-X$ , *assumed* this was zero, and used that to check their background calculation. Since  $\tau$ 's decay into electrons and muons with equal enthusiasm, we will also get a signal here, so we have included these data in extracting the bound (they give the number of events seen). Regarding the second bound, we have not yet seen the detailed analysis, and will simply take the number at face value. Note that it gives no information on decays with an electron in the final state. From these values, we estimate that the limit on  $B \rightarrow \pi e\mu$  and  $B \rightarrow Ke\mu$  is  $10^{-3}$ ; the limit on  $B \rightarrow e\tau X$  is  $3 \times 10^{-3}$ ; the limit on  $B \rightarrow \mu\tau X$  is  $3.2 \times 10^{-4}$ , and the limit on  $B \rightarrow \tau\tau X$  is  $2 \times 10^{-3}$ . The other bounds are given in Ref. [8]. It is important to emphasize that these bounds involving final state  $\tau$ 's are only rough estimates, and should not be considered firm experimental limits. Experimental limits could be obtained from the above experiments if the appropriate Monte Carlo calculations were done, and we have not done so. The estimates have been done to give an idea of the bounds that can be obtained from such decays; we urge experimenters to determine limits on these branching ratios so that more

Table 2.3: Bounds on the flavor-changing couplings from three-body  $B$  decays. Since only the scalar contributes, the bound only applies to the scalar mass, and not the pseudoscalar mass. The numerical values should be understood as multiplies by  $(m_s/m_W)^4$ .

Decay process	Expt.limit	Bound
$B \rightarrow K\mu\mu$	$5 \times 10^{-5}$	$\eta_{\mu\tau}^2 \eta_{\mu\mu}^2 < 3$
$B \rightarrow \pi\mu\mu$	$5 \times 10^{-5}$	$\eta_{e\tau}^2 \eta_{\mu\mu}^2 < 330$
$B \rightarrow Kee$	$5 \times 10^{-5}$	$\eta_{\mu\tau}^2 \eta_{ee}^2 < 3.6$
$B \rightarrow \pi ee$	$5 \times 10^{-5}$	$\eta_{e\tau}^2 \eta_{ee}^2 < 360$
$B \rightarrow K\mu e$	$10^{-3}$	$\eta_{\mu\tau}^2 \eta_{e\mu}^2 < 70$
$B \rightarrow \pi\mu e$	$10^{-3}$	$\eta_{e\tau}^2 \eta_{e\mu}^2 < 7000$
$B \rightarrow K\mu\tau$	$(3 \times 10^{-4})$	$\eta_{\mu\tau}^4 < 30$
$B \rightarrow \pi\mu\tau$	$(3 \times 10^4)$	$\eta_{e\tau}^2 \eta_{\mu\tau}^2 < 3000$
$B \rightarrow Ke\tau$	$(3 \times 10^{-3})$	$\eta_{\mu\tau}^2 \eta_{e\tau}^2 < 300$
$B \rightarrow \pi e\tau$	$(3 \times 10^{-3})$	$\eta_{e\tau}^4 < 30000$
$B \rightarrow K\tau\tau$	$(2 \times 10^{-3})$	$\eta_{\mu\tau}^2 \eta_{\tau\tau}^2 < 350$
$B \rightarrow \pi\tau\tau$	$(2 \times 10^{-3})$	$\eta_{e\tau}^2 \eta_{\tau\tau}^2 < 35000$
$K \rightarrow \pi\mu\mu$	$2.3 \times 10^{-7}$	$\eta_{e\mu}^2 \eta_{\mu\mu}^2 < 200$
$K \rightarrow \pi\mu e$	$2.1 \times 10^{-10}$	$\eta_{e\mu}^4 < 0.18$
$K \rightarrow \pi ee$	$1.0 \times 10^{-8}$	$\eta_{ee}^2 \eta_{e\mu}^2 < 9$

precise bounds can be found.

The results are given in Table 2.3. Processes marked with parentheses are not from firm experimental bounds, but simply our estimate of the bound that could be obtained from the results in Eq. 2.37. Note that the bounds are much stronger than the corresponding bounds on  $\tau$  decays. Some of the processes, such as  $B \rightarrow Ke\tau$ , are proportional to the same couplings as in  $\mu \rightarrow e\gamma$ . The latter bound is so strong that these processes would be unobservable. Other processes depend on first-generation couplings and are expected to be small. Perhaps the most interesting process is  $B \rightarrow K\mu\tau$ . This decay depends only on  $\eta_{\mu\tau}$ , which is expected to be the largest flavor-changing coupling. The right-hand side will reach unity with an improvement of a factor of 30 in the rate.

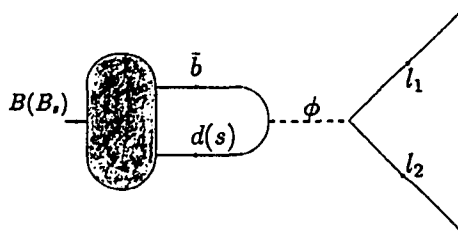


Figure 2.4: Contributions to two-body decays of the  $B$  (or the  $B_s$ ) meson. The exchanged particle must be a pseudoscalar.

This may seem extremely difficult, but the process has never been looked for. Such an improvement seems quite possible.

These processes all depend on scalar exchange. If the scalar were much heavier than the pseudoscalar, these decays would be negligible, while  $\tau$  decays would still occur. We now turn to two-body decays, which are not only sensitive to pseudoscalar exchange, but offer much more realistic prospects for experimental improvement in the bounds.

## 2.4.2 Two-body decays

Two-body decays of the  $B$  and  $B_s$  mesons occur through the diagram of Fig. 2.4. Since these mesons have negative parity, the decay can only occur through a pseudoscalar interaction. As an example, the matrix element for

the decay  $B_s \rightarrow e\mu$  can be written as

$$M = i \frac{h_{e\mu} h_{sb}}{m_p^2} \bar{u}_e v_\mu f_+(q^2), \quad (2.38)$$

where  $f_+(q^2) = \langle 0 | \bar{s} \gamma_5 b | B_s \rangle$ . The form factor can be evaluated by the method of the preceding subsection<sup>3</sup>, and is given by

$$f_+(q^2) = \sqrt{4m_B} \frac{\beta_B^{3/2}}{\pi^{3/4}}, \quad (2.39)$$

so that the decay rate is

$$\omega = \frac{h_{e\mu}^2 h_{sb}^2 \beta_B^3 m_B^2}{4\pi^{5/2} m_p^4}. \quad (2.40)$$

The same decay rate (with the obvious change in the subscripts on the coupling constants) applies to all other processes. With one  $\tau$  (two  $\tau$ 's) in the final state, a phase-space factor of 0.76(0.36) must be included. This will give a bound for  $B \rightarrow l_1 l_2$

$$\begin{aligned} \eta_{l_1 l_2}^2 \eta_{e\tau}^2 &< 3.0 \times 10^4 (\text{branching ratio}) \\ &\times \left[ \frac{m_p}{m_W} \right]^4 / (\text{phase - space factor}). \end{aligned} \quad (2.41)$$

For  $B_s$  decays, one obtains an identical result (the small mass difference between the  $B$  and  $B_s$  gives corrections much smaller than the factor-of-2 uncertainty in the form factor), with  $\eta_{e\tau}^2 \rightarrow \eta_{\mu\tau}^2$ .

To determine the branching ratio, we compare this rate with the observed  $B$  lifetime. For processes involving  $\tau$ 's, we use the results which followed Eq. 2.37. This does not work well for  $B_s$  decays, since the lifetime of the  $B_s$  has not been

---

<sup>3</sup>Of course, one could also evaluate the matrix element in terms of the  $B$  decay constant. Since the method of the preceding subsection gives the matrix element almost trivially (no integrals need to be done), we prefer that method. Comparing the two methods, one should be able to calculate the  $B$  decay constant. This has been done in Ref.[13], with the result that  $f_B = 130$  MeV.

Table 2.4: Bounds on flavor-changing couplings which arise from two-body decays of the  $B$  and  $B_s$ . Since only the pseudoscalar contributes, the only bounds apply to  $m_p$ . The numerical values should be understood as multiplied by  $(m_p/m_W)^4$ .

Decay process	Expt.limit	Bound
$B \rightarrow ee$	$3 \times 10^{-5}$	$\eta_{ee}^2 \eta_{e\tau}^2 < 1.0$
$B \rightarrow e\mu$	$4 \times 10^{-5}$	$\eta_{e\mu}^2 \eta_{e\tau}^2 < 1.4$
$B \rightarrow \mu\mu$	$9 \times 10^{-6}$	$\eta_{\mu\mu}^2 \eta_{e\tau}^2 < 0.3$
$B_s \rightarrow ee$	$X$	$\eta_{ee}^2 \eta_{\mu\tau}^2 < 3 \times 10^4 X$
$B_s \rightarrow e\mu$	$X$	$\eta_{e\mu}^2 \eta_{\mu\tau}^2 < 3 \times 10^4 X$
$B_s \rightarrow \mu\mu$	$4 \times 10^{-5}$	$\eta_{\mu\mu}^2 \eta_{\mu\tau}^2 < 1.2$
$B \rightarrow e\tau$	$(3 \times 10^{-3})$	$\eta_{e\tau}^4 < 140$
$B \rightarrow \mu\tau$	$(3 \times 10^{-4})$	$\eta_{e\tau}^2 \eta_{\mu\tau}^2 < 14$
$B \rightarrow \tau\tau$	$(2 \times 10^{-3})$	$\eta_{e\tau}^2 \eta_{\tau\tau}^2 < 190$
$B_s \rightarrow e\tau$	$X$	$\eta_{e\tau}^2 \eta_{\mu\tau}^2 < 4 \times 10^4 X$
$B_s \rightarrow \mu\tau$	$(1.2 \times 10^{-3})$	$\eta_{\mu\tau}^4 < 50$
$B_s \rightarrow \tau\tau$	$(8 \times 10^{-3})$	$\eta_{\mu\tau}^2 \eta_{\tau\tau}^2 < 640$
$K \rightarrow \mu\mu$	$6 \times 10^{-9}$	$\eta_{e\mu}^2 \eta_{\mu\mu}^2 < 0.02$
$K \rightarrow \mu e$	$2.2 \times 10^{-10}$	$\eta_{e\mu}^4 < 0.0008$
$K \rightarrow ee$	$3.2 \times 10^{-10}$	$\eta_{ee}^2 \eta_{e\mu}^2 < 0.0012$

measured. However, one expects the lifetime of the  $B_s$  to be the same as that of the  $B$ , since the standard-model decay proceeds through the weak decay of the  $b$  quark. Thus, we will take the lifetime of the two to be equal. In determining the branching ratio for the  $B_s$ , we note that the UA1 result[15] does not distinguish between  $B$ 's and  $B_s$ 's. We will assume that the relative production rate for  $B_s$ 's is a factor of 4 smaller than that for  $B$ 's (since the probability of popping an  $s$  pair out of the vacuum is about one-fourth that of  $d$  pairs[16]), and thus the bounds on the  $B_s$  branching ratio into  $\mu\mu$ ,  $\mu\tau$ , and  $\tau\tau$  is four times as large as that for  $B$ 's. Note that no bounds currently exist for  $B_s \rightarrow e\mu$  or  $B_s \rightarrow ee$ .

The results are given in Table 2.4. Processes marked with parentheses are

not firm experimental bounds, but simply our estimate of the bound that could be obtained from the results in Eq. 2.37. For the processes  $B_s \rightarrow ee$ ,  $B_s \rightarrow e\mu$  and  $B_s \rightarrow e\tau$ , there is currently no experimental limit; once a limit  $X$  is determined, the bound given in the third column follows. As in the three-body case, the bounds from two-body  $B$  decays are much stronger than the corresponding bounds from  $\tau$  decays.

### 2.4.3 $K - \bar{K}$ and $B - \bar{B}$ mixing

The strongest bounds on scalar- and/or pseudoscalar-mediated tree-level FCNC's quoted in the literature come from  $K - \bar{K}$  mixing. We now discuss the constraints from this and similar processes.

As discussed earlier, it has generally been recognized that the most stringent bounds on flavor-changing couplings (involving the first two generations) come from  $K - \bar{K}$  mixing. Here, this result is extended to include  $B - \bar{B}$  mixing.

A discussion of the calculation of  $K - \bar{K}$  mixing due to Higgs-scalar exchange can be found in Ref. [4], and references therein. The relevant matrix element discussed in these papers is  $\langle \bar{K} | (\bar{s}\gamma_5 d)(\bar{s}\gamma_5 d) | K \rangle$ , which has a value [3] of  $0.0085 \text{ GeV}^3$ . With a value for the coupling of  $\sqrt{(g_Y)_d(g_Y)_s}$ , a bound of 1.0 TeV on the mass of the exchanged particle is obtained.

The  $\gamma_5$  in the above matrix element shows that *pseudoscalar* exchange only was treated in these papers. If one considers scalar exchange, the matrix element will be different. It is easy to see why the matrix element with scalars will be smaller: If one uses the vacuum-insertion method, and inserts the vacuum state in the matrix element, then the fact that the kaon is a pseudoscalar implies that the matrix element for scalar exchange will vanish. The scalar

matrix element has been calculated[17] and is smaller by a factor of 12. This will lower the bound on the mass by a factor of  $\sqrt{12}$ . One thus finds that the bound on the pseudoscalar mass is 1000 GeV, and the bound on the scalar mass is only 300 GeV.

The weakness of these bounds may surprise those who have always felt that the bounds from  $K - \bar{K}$  mixing put very stringent constraints on the mass of flavor-changing scalars. Let us emphasize why this bound is so much smaller. The main difference is in the choice of coupling. The early authors chose a coupling equal to the  $b$ -quark Yukawa coupling; Cheng and Sher[4] then argued that choosing the geometric average of the  $d$ -quark and  $s$ -quark Yukawa couplings was much more natural and realistic. Finally, the scalar matrix element is much smaller than the pseudoscalar matrix element, leading to weaker bounds on the scalar mass. We wish to emphasize that this bound is highly uncertain, since it depends so heavily on mixing between the first two generations and on the light-quark Yukawa couplings.

Putting all of this together, we can extract the bound on the coupling:

$$\begin{aligned} \eta_{e\mu}^4 &< 9.0 \times 10^{-14} \left[ \frac{m_p}{m_W} \right]^4, \\ \eta_{e\mu}^4 &< 1.3 \times 10^{-11} \left[ \frac{m_s}{m_W} \right]^4. \end{aligned} \quad (2.42)$$

What about the bound on  $B - \bar{B}$  mixing? In the case of  $K - \bar{K}$  mixing, it was assumed that the contribution due to scalar exchange was not greater than the standard-model contribution, reflecting the factor-of-2 uncertainty in the standard-model contribution. The same uncertainty applies to  $B - \bar{B}$  mixing. The ratio of  $B - \bar{B}$  mixing to  $K - \bar{K}$  mixing is given by

$$\frac{\Delta m_B}{\Delta m_K} = \frac{h_{bd}^2 \langle \bar{B} | (\bar{b}\gamma_5 d)(\bar{b}\gamma_5 d) | B \rangle}{h_{sd}^2 \langle \bar{K} | (\bar{s}\gamma_5 d)(\bar{s}\gamma_5 d) | K \rangle}. \quad (2.43)$$

Estimating the matrix elements by the vacuum-insertion method, we find[4]

$$\frac{\langle \bar{B} | (\bar{b}\gamma_5 d)(\bar{b}\gamma_5 d) | B \rangle}{\langle \bar{K} | (\bar{s}\gamma_5 d)(\bar{s}\gamma_5 d) | K \rangle} = \frac{f_B^2 m_B^3}{f_K^2 m_K^3} \left[ \frac{m_s + m_d}{m_b + m_d} \right]^2. \quad (2.44)$$

Numerically, this ratio is 0.9. We will take the ratio of scalar matrix elements to be the same. We see that the ratio of  $\Delta m_B$  to  $\Delta m_K$  is almost entirely due to the difference in couplings. Taking the observed value of the mass splitting gives our bounds:

$$\begin{aligned} \eta_{er}^4 &< 2.0 \times 10^{-9} \left[ \frac{m_p}{m_W} \right]^4, \\ \eta_{er}^4 &< 3.0 \times 10^{-7} \left[ \frac{m_s}{m_W} \right]^4. \end{aligned} \quad (2.45)$$

It is interesting to note that our “most natural value” for  $\eta_{er}$  is  $\sqrt{m_e/m_\tau}$ , giving  $\eta_{er}^4 = 7.8 \times 10^{-8}$ , so that the bounds (in this case) on  $m_s$  and  $m_p$  are 60 and 200 GeV, respectively. These bounds should be more reliable than bounds from  $K - \bar{K}$  mixing (since they do not involve mixing between the first two generations), but less reliable than bounds involving mixing between the second and third generations.

Finally, what about  $B_s - \bar{B}_s$  bounds? In the standard model, this mixing is maximal, and adding extra contributions will make no difference. The only way in which scalar exchange could matter would be if it contributed with roughly the same magnitude and opposite sign to the standard model contribution. The uncertainties in both calculations would make any bounds found from this meaningless.

## 2.5 Results

Of all of the processes that have been considered, three stand out as giving very stringent bounds on flavor-changing neutral currents. Those three are

$\mu \rightarrow e\gamma$ ,  $K - \bar{K}$  mixing, and  $B - \bar{B}$  mixing. The bounds are given in Eqs. 2.29, 2.42, and 2.45. As discussed earlier, the bound on  $\mu \rightarrow e\gamma$  arises from a diagram in which a  $\tau$  is on an internal line, and is thus sensitive to the (more reliable) couplings which mix the third generation, and it is also at the edge of the most interesting region of parameter space. From the tables, one can see immediately that these three bounds eliminate the possibility of seeing many other processes. For example, the bound in Eq. 2.45 is much, much more stringent than that from  $B \rightarrow e\tau$  or  $B \rightarrow \pi e\tau$ ; the bound in Eq. 2.42 is much more stringent than that from  $K \rightarrow e\mu$  or  $K \rightarrow \pi e\mu$ ; and the bound in Eq. 2.29 is much more stringent than that from  $B \rightarrow \mu\tau$ ,  $B_s \rightarrow e\tau$ ,  $B \rightarrow \pi\mu\tau$ , or  $B \rightarrow Ke\tau$ .

The bounds from these three processes are so strong, in fact, that one can use perturbation theory to derive many additional constraints. In a grand unified theory, the validity of perturbation theory forces all of the  $\eta_{ij}$  to be small at all scales between the electroweak and unification scales. This gives an upper bound on the  $\eta_{ij}$  at the electroweak scale. A similar calculation for the top quark Yukawa coupling gives an upper bound on the top quark mass of 230 GeV, i.e., a bound on the coupling of 1.3. The same bound will apply here, and thus we have  $h_{ij} \leq 1.3$ , corresponding to  $\eta_{ij} \leq 45$ . Combining this with Eqs. 2.42 and 2.45, and noting that we are interested in cases in which the exchanged scalar is heavier than its current limit of 40 GeV, we find

$$\begin{aligned} \eta_{ij}^2 \eta_{e\tau}^2 &< 0.36 \left[ \frac{m_p}{m_W} \right]^4, \\ \eta_{ij}^2 \eta_{e\tau}^2 &< 4.4 \left[ \frac{m_s}{m_W} \right]^4, \\ \eta_{ij}^2 \eta_{e\mu}^2 &< 2.4 \times 10^{-3} \left[ \frac{m_p}{m_W} \right]^4, \end{aligned}$$

$$\eta_{ij}^2 \eta_{e\mu}^2 < 2.9 \times 10^{-2} \left[ \frac{m_s}{m_W} \right]^4 . \quad (2.46)$$

This bound must hold for *any*  $i$  and  $j$ , and is easily seen to be a more stringent bound than many of the processes in Tables 2.1, 2.2, and 2.3.

Let us now examine the various processes more explicitly to determine which offer the best possibilities in the future (as well as whether  $\tau$  or  $B$  decays are more likely to be productive). We first consider the case of scalar exchange.

Consider the various three-body  $\tau$  decays. It is easy to see that the bounds on the six  $\tau$  decays in Table 2.1 are much weaker than other processes. In the order given in Table 2.1, the processes which give better bounds are (i)  $B \rightarrow \pi ee$ , (ii)  $B \rightarrow K\mu\mu$ , (iii) Eq. 2.46, (iv)  $B \rightarrow K\mu e$ , (v) Eq. 2.46 and  $B \rightarrow Kee$ , and (vi)  $B \rightarrow \pi\mu\mu$  and  $B \rightarrow K\mu e$ . Now consider the two radiative  $\tau$  decays. The bound from  $\tau \rightarrow e\gamma$  is weaker than that from Eq. 2.46, and the bound from  $\tau \rightarrow \mu\gamma$  is weaker than that from  $B \rightarrow K\tau\tau$ . In all of these cases, the bound from  $\tau$  decays is so much weaker that even a slight improvement in the bound will not help. We conclude that there is no useful information which can be obtained from  $\tau$  decays in these models in which a scalar mediates flavor-changing neutral currents.

We have already noted that the most useful experiment in improving these bounds (or finding an effect) is  $\mu \rightarrow e\gamma$ . Which of the  $B$  decays is most likely to be productive? The decays which stand out here are  $B \rightarrow Kee$ ,  $B \rightarrow K\mu\mu$ ,  $B \rightarrow K\mu\tau$ , and  $B \rightarrow K\tau\tau$ . Using our "preferred" range of couplings, one can easily see that one needs to reach branching ratios of  $3 \times 10^{-10}$ ,  $3 \times 10^{-9}$ ,  $3 \times 10^{-8}$ , and  $3 \times 10^{-7}$ , respectively. In the case of  $B \rightarrow K\mu\mu$  and

$B \rightarrow K\tau\tau$ , these branching ratios are below (barely below for the latter) the standard model (one-loop) branching ratios. Keep in mind, however, that our “preferred range” is just a rough estimate, and the couplings could easily be somewhat higher (recall that a factor of 10 increase in a coupling corresponds to  $10^4$  in the rate). The process  $B \rightarrow K\mu\tau$ , however, vanishes in the standard model, and thus may offer the best (and least ambiguous) hope. Measuring its branching ratio to a level of a few times  $10^{-8}$  obviously is difficult, although at a  $B$  factory, it may not be impossible.

Next, we consider the case of pseudoscalar exchange. The bound from the decay  $\tau \rightarrow e^-e^-e^+$ ,  $\tau \rightarrow \mu^-\mu^-\mu^+$ , ( $\tau \rightarrow e^-e^-\mu^+$ ,  $\tau \rightarrow \mu^-\mu^-e^+$ ,  $\tau \rightarrow e^-\mu^-\mu^+$ ) is much weaker than that from the decay  $B \rightarrow ee$ ,  $B \rightarrow \mu\mu$  [all the others are weaker than the bound from Eq. 2.46]. The bound from  $\tau \rightarrow e^-\mu^-e^+$  is still better than other bounds, however, if one can measure  $B_s \rightarrow ee$  to have branching ratios less than 5%, then this process will set a better bound. It is hard to imagine that such a large branching ratio would have gone undetected (there would be many dramatic four electron events at UA1), and it is quite likely that this bound will be determined in the very near future. What about radiative decays? Again, the bound from  $B \rightarrow \tau\tau$  is much better than that from  $\tau \rightarrow e\gamma$ . Similarly, the bound from  $B_s \rightarrow \tau\tau$  is more stringent than that from  $\tau \rightarrow \mu\gamma$ . We thus conclude that improvement in rare  $\tau$  decays will not be useful in setting bounds, even in the case of pseudoscalar exchange.

Finally, which of these  $B$  decays will be most productive? The decays which stand out are those of the  $B_s$  meson into  $\tau\tau$ ,  $\mu\tau$ ,  $\mu\mu$ , and  $\mu e$ . The branching ratios needed to reach the preferred range of parameter space are  $7 \times 10^{-7}$ ,  $8 \times 10^{-8}$ ,  $6 \times 10^{-9}$ , and  $3 \times 10^{-11}$ , respectively. Here the rate for

$B_s \rightarrow \tau\tau$  is well below the standard-model prediction ( $\sim 10^{-6}$ ), and  $B_s \rightarrow \mu\mu$  is slightly below the standard-model prediction. Again, our preferred range is just an estimate, and the couplings could be somewhat larger. The most intriguing decay is  $B_s \rightarrow \mu\tau$ , which only depends on the single  $\eta_{\mu\tau}$  coupling. Measuring the branching ratio to get into the preferred range seems difficult, although the fact that it is a two-body decays with charged leptons may make it detectable at a  $B$  factory.

## 2.6 Conclusion

The simplest extension of standard model has an extra scalar field. This model will automatically have tree-level flavor-changing neutral currents, unless they are suppressed by some additional symmetry. It is often believed that the presence of tree-level flavor-changing neutral currents in this model is fatal, since it requires the exchanged scalar to be extremely heavy. This belief, however, is based on the assumption that the flavor-changing coupling is quite large. It has been pointed out that using a more natural value for the coupling (the geometric mean of the Yukawa couplings of the two fields) leads to much smaller bounds, closer to the range of several hundred GeV. Even this bound, however, is very sensitive to the precise value of the coupling. Given the uncertainty in assumptions involving the first generation Yukawa couplings (the couplings are five to six orders of magnitude smaller than gauge couplings, they are subject to uncalculable Planck mass corrections, etc.), even this bound of several hundred GeV certainly should not be considered particularly reliable.

With this in mind, we have calculated the bounds on the couplings of an additional scalar or pseudoscalar for processes involving the third generation

fields, which should be considerably more reliable. Since the masses of the scalar and the pseudoscalar are likely to be quite different, we have considered the bounds on each separately. The most stringent bound in the quark sector comes from  $B - \bar{B}$  mixing; using our “most natural” value of the couplings, one gets a bound of about a hundred GeV on the exchanged scalar mass. In the lepton sector, the strongest bound comes from  $\mu \rightarrow e\gamma$ , in which a  $\tau$  is on an internal line. This process is sensitive to mixing between the first and third generations as well as between the second and third generations (and is not as sensitive to mixing between the first and second generations, which is expected to be small). Using our most “natural” value, we get a bound of about 200 GeV on the exchanged scalar and pseudoscalar masses. Unlike the case of  $B - \bar{B}$  mixing, however, this process does not exist in the standard model, and thus the bound will be improved considerably as the experimental bound is lowered. We thus feel that  $\mu \rightarrow e\gamma$  is the best place to look for mixing involving the third generation.

In most grand unified theories, the  $\tau$  and  $b$  are in the same representation, and thus we expect flavor-changing couplings in the quark sector to be related to those in lepton sector. We have then asked the question: which processes,  $\tau$  or  $B$  decays, give the strongest bounds? The answer, from Tables 2.1– 2.4, is clear:  $B$  decays. We find no case in which  $\tau$  decays give better bounds, nor in which they are likely to in the near future. The most promising  $B$  decays are  $B \rightarrow K\mu\tau$  and  $B_s \rightarrow \mu\tau$ . In general, the interesting decays are those with  $\tau$ 's in the final state. A search for  $B \rightarrow \mu e X$  would have relatively little background and could be quite productive; a search for exclusive processes with a final state  $\tau$ , while more difficult, could also be quite useful.

## Chapter 3

# Cosmological Bounds on the Lifetime of the New Leptons

It is now known that the standard model has three generations of fermions with light or massless neutrinos. If a fourth generation exists, its neutrino, as well as the associated lepton, must be heavier than approximately 45 GeV [8]. This would mean that, unlike the other three generations, the neutrino and its associated charged lepton have masses of approximately the same order of magnitude. As a result, there is no particular reason to assume that this neutrino is lighter than the charged lepton.

The possibility that the fourth generation neutrino,  $N$ , could be heavier than the fourth generation charged lepton,  $L$ , has not been discussed in detail. One would expect the neutrino to decay rapidly into the  $L$  and a real or virtual  $W$ . The  $L$ , however, could not decay through normal weak interactions, *unless* there is mixing between the  $N$  and the three light neutrinos. In this case it would decay as a normal lepton (into a light neutrino and a  $W$ ), but with an anomalously long lifetime, longer by a factor of  $1/\sin^2 \theta$ , where  $\theta$  is the largest mixing angle between the  $N$  and the light neutrinos. In see-saw models, the

mixing angle is a ratio of masses; in this case, the ratio of the tau neutrino mass to the  $N$  mass is smaller than about  $10^{-11}$ , and it is thus plausible that the lifetime of the  $L$  is very long.

If the lifetime turned out to be less than  $10^{-13}$  seconds or so, detection would be identical to a conventional heavy lepton. If it is between  $10^{-13}$  and about  $10^{-8}$  seconds, it would decay (at least occasionally) inside the detectors at the SSC and would be easily detected. If it is longer than  $10^{-8}$  seconds, it would be effectively stable, and would look like a muon. However, since the cross section peaks at around the mass, many of the  $L$ 's would not be extremely relativistic. This would cause a time delay in the drift chambers at the SSC, which could also be detected, as long as a sufficient number of  $L$ 's is produced. The production cross section calculations for heavy leptons[18] indicate that effectively stable leptons up to about 200 GeV in mass could be detected. Detection at an electron-positron collider would be very straightforward. The details of the phenomenology are currently under investigation. In this chapter, we investigate the implications of very long-lived charged leptons for cosmology and astrophysics.

What are the cosmological and/or astrophysical implications? Much work has been done on the effects of very long-lived neutrinos. In this case, bounds on the mass and lifetime arise from two sources. First, the current density of neutrinos could be so large that it exceeds the critical density. Second, if the neutrino decays into a state with photons or (to a good approximation) charged particles, then the photons associated with the decay could either be directly detected, would affect the cosmic microwave background, or would

affect nucleosynthesis<sup>1</sup>. These bounds are all reviewed in detail in the book of Kolb and Turner (KT)[19].

In the case of a long lived charged lepton, similar effects can occur (and the decay will certainly involve charged particles). Another type of bound, not relevant for the case of long-lived neutrinos, is that the charged lepton (if sufficiently long-lived) may combine with electrons to form anomalously heavy isotopes of hydrogen, which can also be directly searched for. In addition, solid state and plastic track detectors could detect the lepton directly. We now consider these bounds in detail. Throughout, we will assume that there is no net asymmetry between positively charged and negatively charged leptons.

In the early universe, the  $L$ 's will be in thermal equilibrium with all other particles. As the universe cools, the temperature will drop below the mass of the  $L$ , and their number density will be suppressed by a Boltzmann factor. The number density continues to fall, until a temperature is reached at which electroweak interactions are too slow to keep them in thermal equilibrium (i.e. the expansion rate of the universe exceeds the annihilation rate), and then the number density "freezes out". For particles with masses above a few GeV, the freeze-out temperature is considerably smaller than the particle mass. The number density today is then easily determined, since the particle effectively no longer interacts. The calculation of the relic abundance, given the annihilation cross section, is a straightforward (if tedious) chore, outlined in KT. We first need to determine the annihilation cross section.

The possible annihilation diagrams are given in Fig. 3.1. As discussed by Enqvist et al.[20], for  $m_L > m_W$ , the dominant process will be  $W$  pair-

<sup>1</sup>Astrophysical bounds, such as constraints from supernovae, are irrelevant for neutrinos above a hundred MeV.

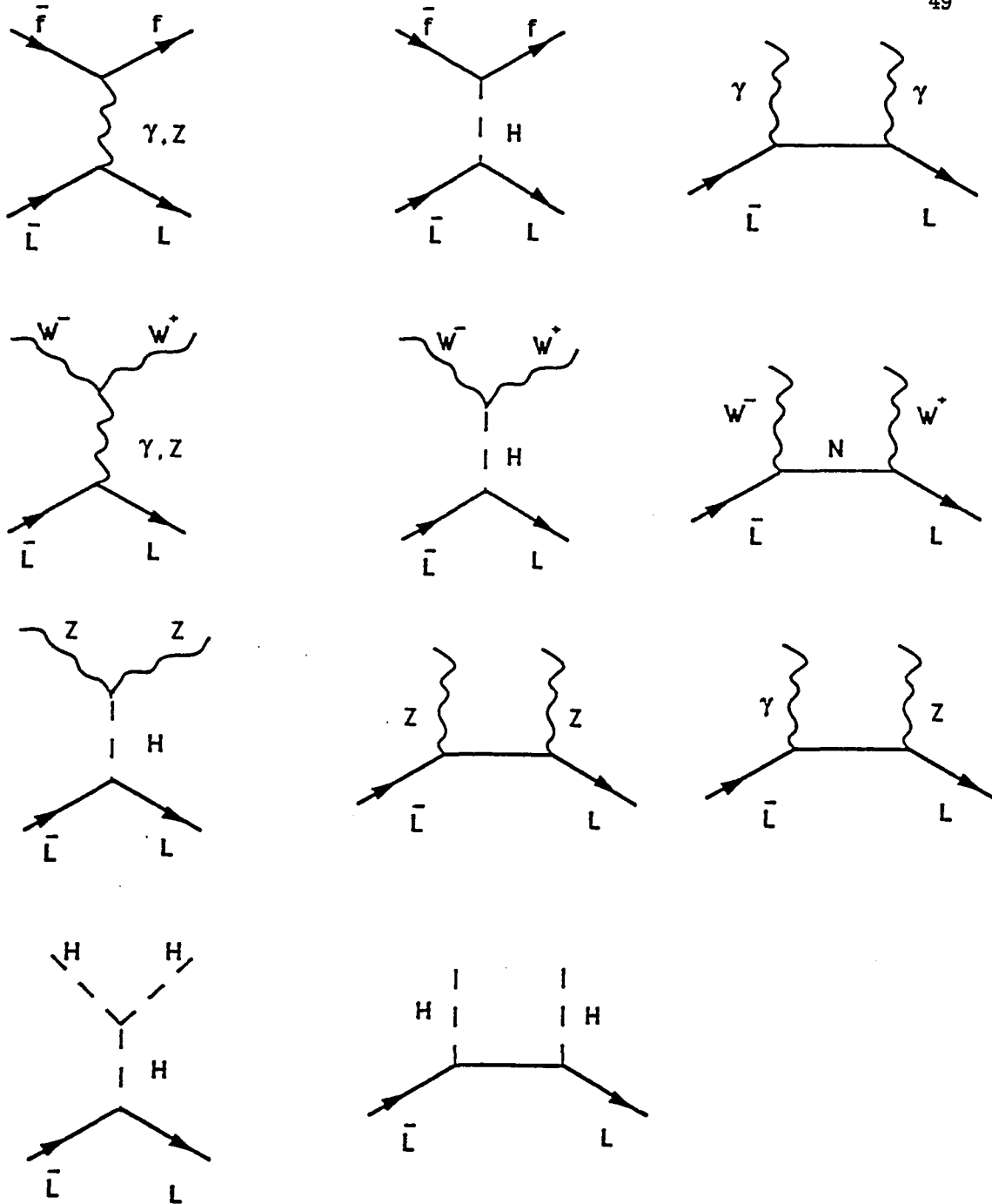


Figure 3.1: Diagrams contributing to the annihilation of long-lived charged leptons. Crossed diagrams have not been explicitly shown.

production. Enqvist et al. considered the annihilation of very heavy neutrinos. In this case, the diagrams are similar except that here we have s-channel annihilation through photons as well as  $Z$ 's, and the t-channel annihilation can go into  $\gamma\gamma$  and  $\gamma Z$  as well.

Since the annihilation rate is given by  $\Gamma = n_L \sigma v$ , where  $\sigma$  is the annihilation cross section and  $v$  is the relative velocity, one sees that if the cross section is proportional to  $s - 4m_L^2$ , the relative velocity is small and the contribution is small. As noted by Enqvist et al.[20], this means that the contribution from Higgs exchange is small, unless the Higgs mass is fairly close to twice the lepton mass (in which case the large resonant cross section overcomes the small relative velocity). Diagrams with s-channel Higgs exchange will thus generally give a small contribution, as will diagrams in which Higgs bosons are produced (these processes generally contribute much less than  $W$ -pair production). Even if the contribution were not small (due to resonance), these diagrams will increase the cross section. Increasing the cross section will decrease the abundance. Since we are interested in upper bounds on the abundance, the effect of Higgs bosons will be to strengthen our bounds <sup>2</sup>. We will thus not include diagrams with s-channel Higgs exchange and with Higgs pair production.

If the annihilation cross section decreases, the abundance (for a given lifetime) increases. If one requires that the annihilation cross section obey unitarity bounds, then it has an upper limit, and thus the abundance of a stable particle will have a lower limit. The further requirement that this abundance not overclose the universe has been used [21] to put an upper bound of  $O(200)$  TeV

---

<sup>2</sup>There could be destructive interference, but the graphs of Enqvist et al.[20] show that this is at most a factor of two or so in the current abundance, and this is smaller than the uncertainty in the Hubble constant.

on the mass of any elementary, stable particle. Throughout, we will assume that the annihilation cross section of the  $L$ 's is subject to unitarity constraints, and thus will not consider masses in excess of 100 TeV. Once the  $L$  mass exceeds 1 TeV, its coupling to the Higgs boson is nonperturbative—furthermore, above a TeV, the cross section calculated from the diagrams of Fig. 3.1 exceeds the unitarity bound. We will thus use the larger of the unitarity bound and the diagrams of Fig. 3.1 for the annihilation cross section<sup>3</sup>. One should be cautioned about our results for masses between 1 and 100 TeV ; above a TeV it isn't even clear that the  $L$  can be treated as an elementary particle.

Partial cross sections and the total cross section are shown in Fig. 3.2 and Fig. 3.3 respectively as a function of the lepton mass. Complete expressions for the cross section may be found in the Appendix A. The only arbitrary parameter is the heavy neutrino mass, which we have taken to be twice the lepton mass (its value has very little effect on the total annihilation cross section)<sup>4</sup>. As in the case of Enqvist et al.[20], the dominant process is into  $W$  pairs, if kinematically accessible. Unlike their work, however, the diagram with  $s$ -channel  $Z$  exchange is not very important. This is because in the limit of  $s \rightarrow 4m_L^2$ , only the vector coupling of the lepton to the  $Z$  enters. Since the vector coupling of charged leptons is very small, the diagram is suppressed relative to the same diagram for neutrino annihilation. The axial coupling does enter next order in  $v^2$ ; we have calculated this correction and found it to be

---

<sup>3</sup>For lepton masses near a TeV, the Yukawa coupling is large and diagrams involving  $s$ -channel Higgs exchange may not be negligible, even if the relative velocity is small. Nonetheless, these processes will still be much smaller than the  $W$ -pair production cross section, and as stated above, including them will slightly strengthen our bounds

<sup>4</sup>The top quark mass has a very small effect on the cross section; we have taken it to be 100 GeV.

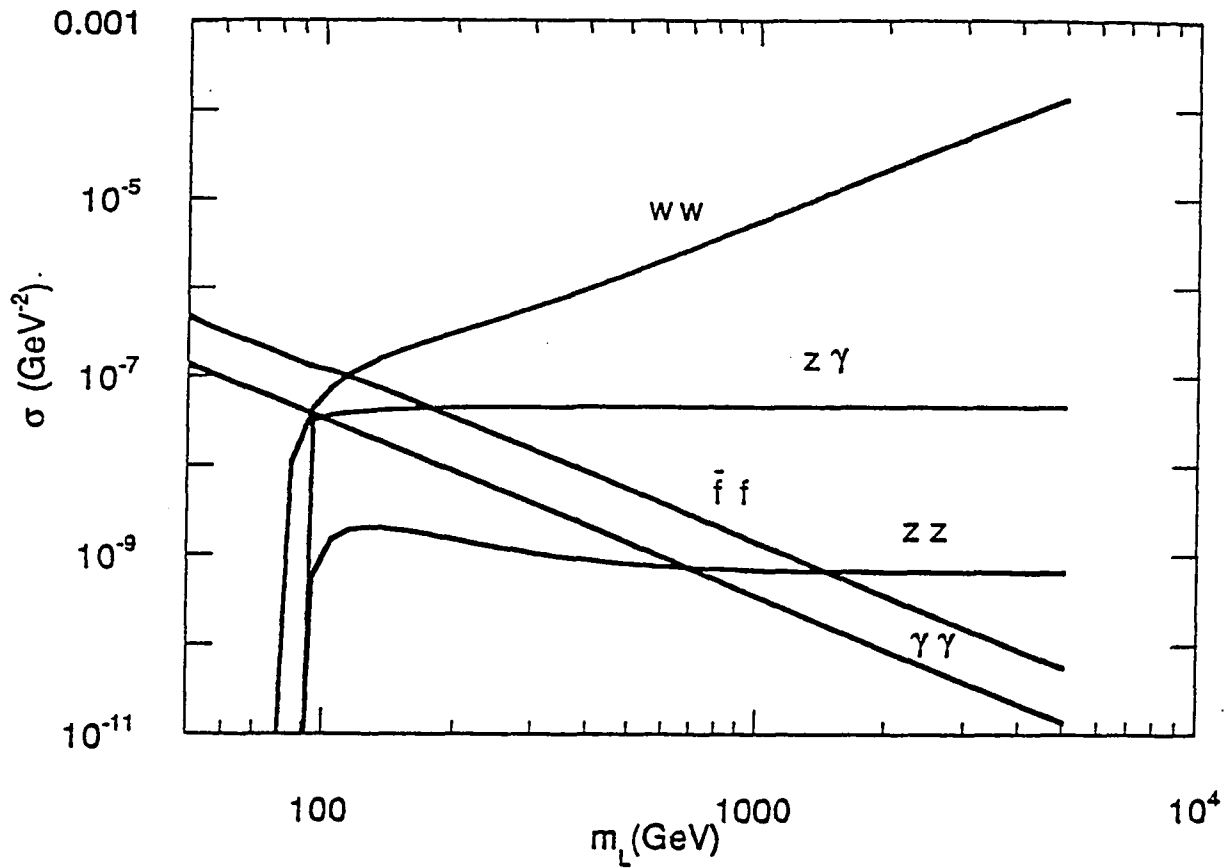


Figure 3.2: Partial cross sections for  $L^+L^-$  annihilation as a function of the  $L$  mass in the non-relativistic limit. For t-channel annihilation into  $W$ 's, a neutrino mass of twice the  $L$  mass was used.

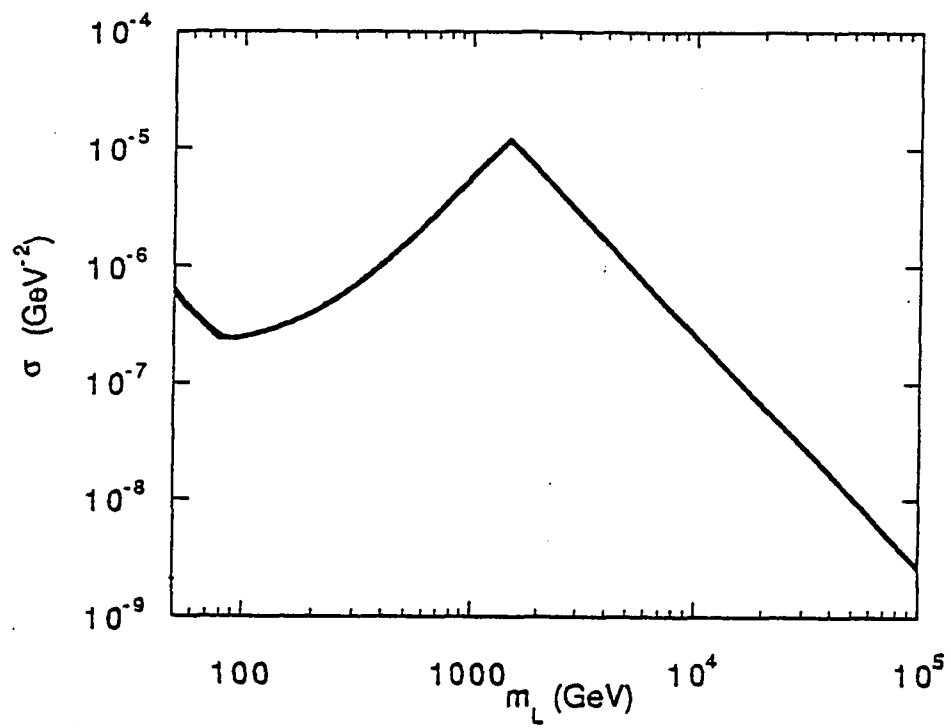


Figure 3.3: The total cross section for  $L^+L^-$  annihilation as a function of the  $L$  mass. When the cross section exceeds the unitarity bound, which occurs for  $L$  masses above 1500 GeV, the unitarity bound has been used.

negligible. However, also unlike the case of neutrino annihilation, we do have an  $s$ -channel photon exchange diagram, which dominates the annihilation. We thus still find annihilation into  $W$  pairs to be the dominant process, but find  $s$ -channel photon exchange to be the most important diagram.

Given the annihilation cross section, the abundance today (ignoring decays) can be calculated. Explicit formulae for the abundance in terms of the cross section can be found in KT[19]. In this case, since  $W$ -pair production through  $s$ -channel photon exchange dominates, the annihilation is predominantly  $s$ -wave, and the calculation of the relic abundance is very similar to that of Dirac neutrinos (the major difference is in the numerical value of the cross section). The result for the abundance today is given in Fig. 3.4. We see that if the lepton mass is below the threshold for  $W$  pair production, the abundance increases with mass (since the annihilation cross section decreases with mass). Above the threshold,  $W$ -pair production dominates rapidly, and the abundance decreases with mass, until the unitarity bound becomes important. These results are qualitatively similar to those of Enqvist et al.[20], who first noted the importance of considering  $W$ -pair production. The requirement that the abundance not overclose the universe only gives the very weak bound of 100 TeV on the lepton mass<sup>5</sup>. At this mass, as discussed earlier, it is unclear that  $L$  can be treated as an elementary particle.

If  $L$  decays, its abundance today is, of course, smaller by a factor of  $\exp(t_U/\tau)$ , where  $t_U$  is the current age of the Universe and  $\tau$  is the  $L$  lifetime. What about the decay products? Since we are interested in fairly long

---

<sup>5</sup>It was originally believed that the bound was closer to 1 TeV, but this ignored  $W$ -pair production. Enqvist et al. argued that  $W$ -pair production eliminates the bound altogether, then Griest and Kamionkowski noted that the unitarity limit gives a very weak bound of 100 TeV.

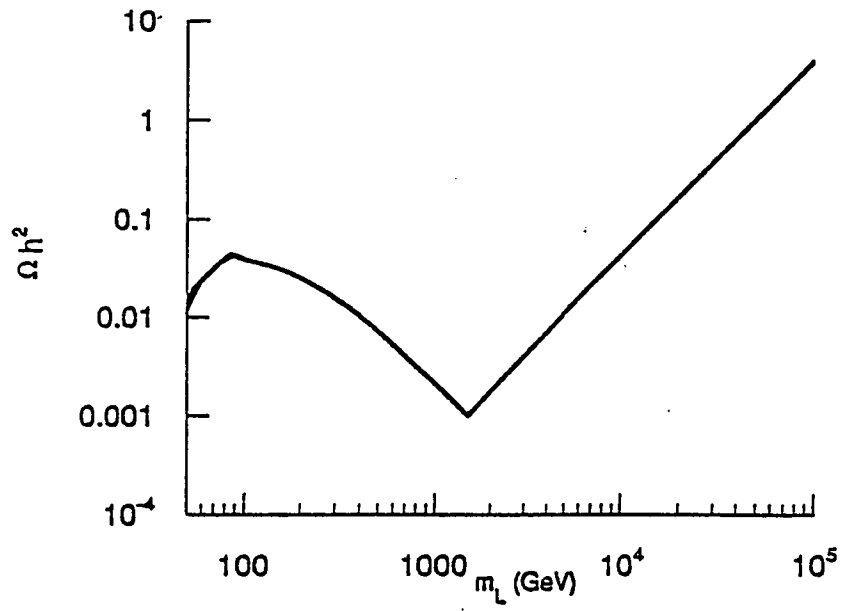


Figure 3.4: The value of  $\Omega h^2$  is given as a function of the  $L$  mass. Here,  $\Omega$  is the ratio of the  $L$  density to the critical density, and  $h$  is the Hubble constant in units of 100 km/s/Mpc.

lifetimes, all pions, muons, etc., will decay into relativistic electrons, neutrinos and photons. If the  $L$ 's do not overclose the universe (if stable), then neither will the decay products, since their energy density redshifts immediately after they are produced (thus the net energy density will decrease). Limits can be found from two sources: direct detection of the  $L$  and direct detection of its decay products. We first consider direct detection of the  $L$ .

In the work of Dimopoulos, Eichler, Esmailzadeh and Starkman (DEES) [22], they considered the possibility that the  $L$  could be the dark matter. As we have seen, this requires the mass of the  $L$  to be approximately 100 TeV. Still, the bounds of DEES can easily be carried over to the case in which the  $L$ 's do not dominate the mass density. They considered many different processes: (a) the failure to find  $(pL^-)$  or  $(eL^+)$  bound states in water, (b) the effects of the  $L$  on nucleosynthesis, (c) the effects on galaxies and stars, (d) the effects of  $L$  annihilation on the heating of gas giant planets, (e) detection in cosmic ray detectors, (f) radiation damage caused by  $L$  impacts on electronic components of satellites and (g) direct detection by plastic track detectors. Their results were generally given in terms of the mass of the charged lepton and its abundance; they were interested in the case in which the abundance gave closure density. In the mass range up to 10 TeV, the strongest bound comes from searches for heavy isotopes of hydrogen in water. The  $L^+$ 's will combine with electrons to form a substance chemically identical to heavy hydrogen; those arriving at the Earth will stop, primarily, in the ocean and will form an unusual water molecule (LHO). DEES show that the number density of LHO relative to  $H_2O$  is approximately  $8 \times 10^{-18} (\text{TeV}/m_L)(t_{acc}/\text{yr})\Omega_L$ , where  $t_{acc}$  is the time period over which LHO accumulates in the ocean and is not removed by geological or

chemical processes, and  $\Omega_L$  is the current density of  $L$ 's in units of the critical density. Smith[23] has searched for anomalously heavy hydrogen in water and finds, over the mass range up to 1200 GeV, that this ratio is less than  $10^{-28}$ . Over the mass range between 1200 GeV and 10 TeV, the limit is  $10^{-24}$ . From this, we find the bound

$$m_L > 10^{16} \text{ TeV } \Omega_L \quad (3.1)$$

for the mass range up to 1200 GeV, and

$$m_L > 10^{12} \text{ TeV } \Omega_L \quad (3.2)$$

for the range up to 10 TeV. Here, we have taken  $t_{acc}$  to be approximately  $10^5$  years, which is the typical time scale for geologic processes to completely mix the oceans. Above 10 TeV, the strongest bound comes from plastic track detectors, and is given by

$$m_L > 3.5 \times 10^{17} \beta (\rho/10^{-24} \text{ gcm}^{-3}) \text{ TeV} , \quad (3.3)$$

where  $\beta \sim 10^{-3}$  is the velocity of the  $L$ . They do note that the plastic track detectors have not yet been calibrated at this value of  $\beta$ , and this might weaken the bound by a few orders of magnitude. In our case, a few orders of magnitude in the bound will be irrelevant. We find the bound to be

$$m_L > 7 \times 10^9 \Omega_L . \quad (3.4)$$

The value of  $\Omega_L$  is given by the result in Fig. 3.4 multiplied by  $\exp(-t_U/\tau)$ ; thus for a given mass, we find an upper bound on the lifetime. Note that since the lifetime bound only varies logarithmically with the mass, and since we will be plotting the lifetime on a logarithmic scale, a change in these bounds by a couple of orders of magnitude will not significantly affect the results.

What about direct detection of the decay products? Since the  $L$  is charged, there will generally be photons associated with the decay. Following KT, we will assume that the decay produces a single photon with energy  $m_L/2$ . While this assumption is reasonable for radiative neutrino decays, it is not particularly good in this case. Instead, one expects a number of photons to be produced, each with an energy somewhat smaller. Nonetheless, bounds on fluxes and energies of diffuse photons are typically uncertain by an order of magnitude or two (see Fig. 5.5 of KT), and thus we will make the same assumption. Bounds arise from two sources. First, the photons could be detected directly in the diffuse photon background. These bounds will apply to photons produced after the cosmic microwave background (CMB), i.e. to lifetimes in excess of  $10^{13}$  seconds. Second, if the photons are produced before the CMB, then the energy density in the decays must not significantly distort the CMB and the entropy produced in the decays must not change the successful nucleosynthesis predictions.

Since terrestrial experiments preclude the possibility of a lifetime in excess of the age of the Universe for the  $L$ , we first consider the case in which the  $L$ 's decay after recombination (formation of the CMB at  $10^{13}$  s) and before the present era. The photons produced should appear in the diffuse photon background. The present flux of such photons[19] is

$$\frac{dF_\gamma}{d\Omega} = \frac{n_L c}{4\pi} , \quad (3.5)$$

where  $n_L = \Omega_L \rho_c / m_L$  is the number density that the  $L$ 's would have if they were stable. The observational limit on the flux is given by[19]

$$\frac{dF_\gamma}{d\Omega} \leq \left( \frac{1 \text{ MeV}}{E} \right) \text{ cm}^{-2} \text{ sr}^{-1} \text{ s}^{-1} . \quad (3.6)$$

Each photon is produced with an energy of  $m_L/2$  (see above discussion), which then redshifts by a factor of  $(1+z) \simeq (t_U/\tau)^{2/3}$ . Thus, using  $E = (m_L/2)(1+z)$  in Eq. 3.6, and Eq. 3.5 for the flux in Eq. 3.6, we find that

$$\tau < 8 \times 10^6 \text{ s} (\Omega_L h^2)^{-1.5} . \quad (3.7)$$

From the values of  $\Omega_L$  given in Fig. 3.4, we see that the right-hand side of Eq. 3.7 is always less than  $10^{13}$  seconds. Since the bound is only relevant for lifetimes in excess of  $10^{13}$  seconds (the photons would become part of the microwave background if they were produced earlier), we see that all lifetimes in excess of  $10^{13}$  seconds are ruled out. It should be noted that if the lifetime were much longer than the age of the Universe, then this bound, as well as the following bound from the CMB distortion, would not apply (since there are no decay photons), however terrestrial experiments preclude that possibility.

For lifetimes between  $10^6$  and  $10^{13}$  seconds, one must ensure that the photons produced do not unacceptably distort the microwave background radiation (CMB). If one requires that the electromagnetic energy density dumped into the vacuum not be greater than a fraction  $\delta$  of the CMB, then we must have

$$\frac{\rho_L}{\rho_\gamma} = \frac{\Omega_L \rho_c}{\rho_\gamma} < \delta , \quad (3.8)$$

which gives us the bound

$$\tau < \frac{9 \times 10^9 \text{ s}}{(\Omega_L h^2)^2} \delta^2 . \quad (3.9)$$

What value should one choose for  $\delta$ ? KT choose  $\delta = 1$  in determining bounds on radiative neutrino lifetimes, i.e. they simply required that the neutrino not dump more energy into the background than was already there. More recently, however, COBE has shown that the CMB is a pure black-body distribution to

unprecedented precision. The COBE results were used in Ref. [24] to place a limit on the fraction of electromagnetic energy that could be added to the microwave background as a function of the time of injection, which was taken to be between  $10^6$  and  $10^{13}$  seconds. Their results thus give us  $\delta$  as a function of  $\tau$ , which can be input into Eq. 3.9. To within a factor of two, their result for  $\delta$  is given by .01 for redshifts up to  $2.2 \times 10^6$  (corresponding to lifetimes above  $2 \times 10^6$  seconds) and it rises rapidly to unity by a redshift of  $5 \times 10^6$  (corresponding to a lifetime of  $4 \times 10^5$  seconds). This rise occurs because photons emitted at this early epoch are still able to thermalize and approach a Bose-Einstein distribution. We have thus taken  $\delta$  to be .01 for lifetimes above  $2 \times 10^6$  seconds, rising rapidly to unity for lifetimes of  $4 \times 10^5$  seconds. As can be seen from Ref. [24], the precise value for  $\delta$  may differ from this by up to a factor of two, however the uncertainty in the Hubble constant will overwhelm this discrepancy. For shorter lifetimes, it is easy to see that bound from nucleosynthesis will not significantly constrain leptons lighter than 100 TeV.

Our results are plotted in Fig. 3.5. We see that cosmological limits are much more stringent than terrestrial bounds, and that there is little hope for terrestrial experiments to approach the cosmological bounds. However, the cosmological bounds do not eliminate lifetimes much in excess of the age of the Universe, and the terrestrial limits are thus necessary to preclude that possibility. The COBE data provides the strongest bound, by far, on the lifetime. More precise data on the cosmic microwave background could improve the bound significantly; in Ref. [24], it is noted that more precise measurements at wavelengths greater than 1 cm will improve  $\delta$  by a factor of 10. In our case,

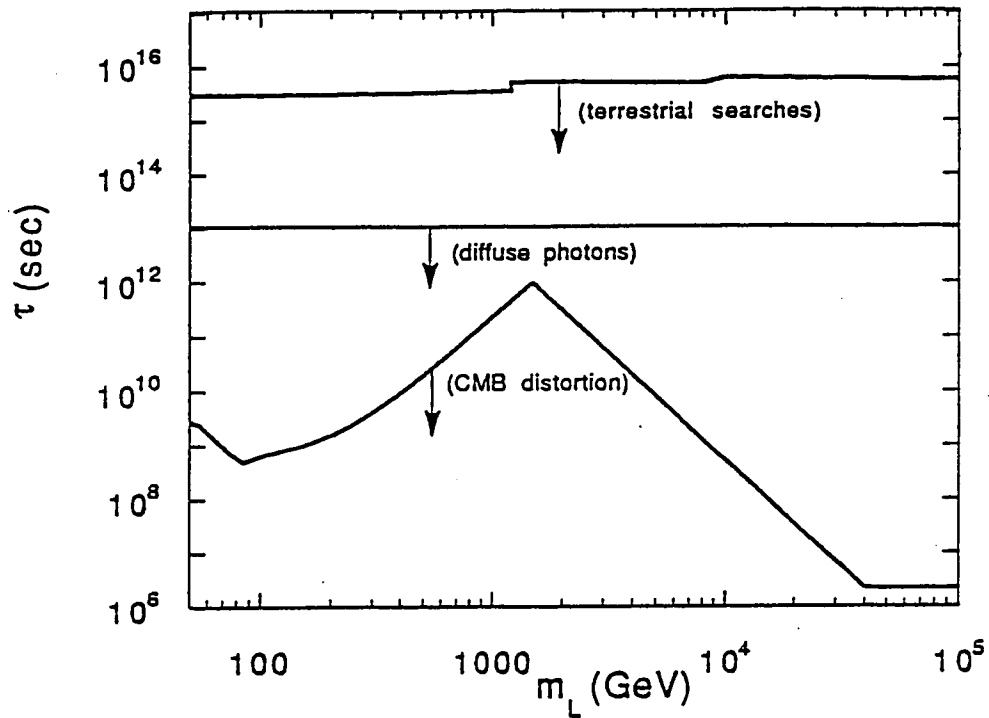


Figure 3.5: Final results for the limits on the mass and lifetime of charged leptons. The limits in the upper line arise from searches for heavy hydrogen in water and from plastic track detectors. The limit restricting the lifetime to be less than  $10^{13}$  seconds arises from failure to directly detect the photons emitted in the decay in the diffuse photon background. The strongest bound, the lower line, comes from failure of the decay photons to appreciably distort the cosmic microwave background. The latter two limits would not eliminate the possibility of lifetimes much in excess of the age of the Universe ( $10^{17}$  seconds), but the bound from terrestrial searches does so. For masses in excess of  $10^5$  GeV, the bounds will continue, until the  $\Omega = 1$  line is reached; for masses in excess of  $10^5$  GeV, this line is at  $10^{32-3\nu}$  seconds for a mass of  $10^\nu$  GeV.

this would lower the peak in the CMB distortion curve of Fig. 3.5 by two orders of magnitude; further improvements could bring the bound, across the entire mass region, down to approximately  $10^7$  seconds.

With these results, we can speculate as to plausible values for the  $L$  lifetime. As discussed above, the lifetime is a typical weak interaction lifetime divided by  $\sin^2 \theta$ , where  $\theta$  is the mixing angle between the fourth generation neutrino,  $N$ , and the lighter neutrinos. What are reasonable values for this mixing angle? If the mixing is confined to the neutrino mass matrices, then one might be guided by see-saw models for neutrino masses and mixings. In this case,  $\sin^2 \theta$  is given by the ratio of the tau neutrino mass to the  $N$  mass. For  $\nu_\tau$  masses between  $10^{-4}$  eV and 10 eV, this gives an  $L$  lifetime of approximately  $10^{-10} - 10^{-5}$  seconds, which is an extremely interesting value for detection at the SSC. It is not an interesting value for cosmological purposes, however. One could modify the see-saw mechanism to generate smaller values of  $\sin^2 \theta$  (which vary, say, as the square of the mass ratio); these would give lifetimes approaching our bounds. More natural, however, might be to assume that there is no mixing at all in the mass matrices. In this case, the only source of mixing would come from grand unified and/or Planck mass effects. This might give a typical mixing angle of  $M_W/M_{Pl}$ , leading to lifetimes in the cosmologically interesting range. Thus, the long lifetimes considered in this chapter are not completely implausible.

Should the lifetime exceed a few years, one can also think about the possible uses of these leptons. Since only a few hundred thousand can be produced annually (at best) at the SSC, they could not be used as an explosive device. They also could not be used to catalyze fusion reactions; even at one catalysis

per picosecond, a million  $L$ 's could only generate about 100 kilowatts. Since these objects would have the mass of a large nucleus, and would orbit deeply inside the nucleus, they could teach us a good deal about nuclear structure. Obviously, the first step is to find them at the supercollider; studies of the signatures are discussed in next chapter.

## Chapter 4

### New Leptons

#### 4.1 Introduction

Since the accurate measurement of the parameters of  $Z^0$  decay[25], it has been known that there exist only three light neutrinos,  $\nu_e$ ,  $\nu_\mu$  and  $\nu_\tau$ , coupling to the  $Z^0$  in the manner prescribed by the standard model. The simplest supposition is then that the lepton sector comprises these three light neutrinos and their charged counterparts,  $e$ ,  $\mu$  and  $\tau$ . However, it is quite possible that heavy leptons exist. Such heavy leptons, which shall be designated as  $L$  and  $N$ , for the charged and neutral varieties respectively, will be a target of investigation at the next generation of particle colliders, most notably the Superconducting Super Collider (SSC) and the Large Hadron Collider (LHC). In this chapter we specify four simple models which contain such heavy leptons and calculate their production cross sections at the SSC and LHC. The first two models are fourth-generation models where the right-handed  $L$  and  $N$  are doublets and singlets respectively under electroweak  $SU(2)$ . The third and fourth models are inspired by the aspon model[26] of CP violation.

Many analyses of heavy lepton production have previously been done[18].

Our work differs from Ref. [18] in two respects. First, it is now known[25] that the masses of any additional neutrinos must be greater than 45 GeV. It is thus possible that the mass of the heavy charged lepton is degenerate with or smaller than that of its neutral counterpart. In particular, the charged lepton is mass degenerate with the heavy neutrino at lowest order in models with vector-like leptons; it can be lighter in models with right-handed singlet leptons. These considerations lead to the possibility that the  $L$  could be very long-lived, perhaps not decaying inside a detector. To our knowledge, no discussion of this possibility has appeared. Second, if the right-handed  $L$  and  $N$  are in an  $SU(2)$  doublet, the GIM mechanism breaks down, leading to the flavor changing decay  $L \rightarrow \tau Z$ . Discovery of such heavy leptons would revolutionize our understanding of the fundamental fermion spectrum. If they exist, it would be natural, by consideration of quark-lepton symmetry, to expect further quarks, beyond the top quark, to occur also, but in the present thesis we shall not consider this possibility.

The layout of this chapter is as follows: Sec. 2 discusses the four models containing heavy leptons; in Sec. 3 are remarks on how detection of the heavy leptons depends crucially on their lifetime which could lie within a wide range, depending on the details of the mass spectrum; the production cross section formulae are presented in Sec. 4; finally, the results are provided in Sec. 5.

## 4.2 The Models

In the standard model, each of the three generations of quarks and leptons mimics the first generation in which the leptons transform under  $SU(2) \times U(1)$  as one doublet  $(\nu_e, e^-)$  with  $Y = -1$  ( $Q = T_3 + \frac{1}{2}Y$ ) and a singlet  $e^+$  with

$Y = +2$ .

It is still unclear whether the  $\nu_i$  ( $i = e, \mu, \tau$ ) are strictly massless or if there exist nonzero neutrino masses. Evidence for the latter comes from at least two sources: the solar neutrino measurements which suggest a solar neutrino flux below that predicted by the standard solar model[27]; the recent gallium experiment results from SAGE[28] and GALLEX[29] lend some support to the deficit established at the Davis chlorine experiment[30] and at the Kamiokande water detector[31], suggesting neutrino oscillations between massive neutrinos. A popular oscillation mechanism is that of MSW[32] where the electron neutrinos partially convert to muon neutrinos within the interior of the Sun. Another evidence for a massive neutrino is the 17 keV neutrino claimed in the Simpson experiment and later experiments, but not reproduced in other efforts[33]. All in all, none of these claims clearly disproves that the first three neutrinos are massless. On the other hand, we know from  $Z^0$  decay measurements[25] that any fourth neutrino coupling normally to  $Z^0$  must be heavier than  $M_Z/2 \sim 45$  GeV.

In our first model (model 1), we shall suppose that the fourth generation leptons fall into the following representations

$$\left( \begin{array}{c} N \\ L \end{array} \right)_L, L_R, N_R, \quad (4.1)$$

similar to the three light families except for the inclusion of the right handed neutrino  $N_R$  which allows a Dirac neutrino mass.

The second model (model 2) will instead assume representations

$$\left( \begin{array}{c} N \\ L \end{array} \right)_L, \left( \begin{array}{c} N \\ L \end{array} \right)_R. \quad (4.2)$$

They are called *vector leptons* because both the left- and right-handed components transform identically under  $SU(2)_L$ .

Our third and fourth models are inspired by the aspon model[26] of CP violation. To solve the strong CP problem, the aspon model incorporates *vector quarks* at a scale of a few hundred GeV. Only colored states contribute to the relevant anomaly so that leptons are not required in solving the strong CP problem but by quark-lepton symmetry we may expect that such a model possesses also vector leptons. The vector quarks may be in  $SU(2)$  doublets or singlets. So there is a corresponding choice for the heavy leptons. Our third model (model 3) will therefore contain vector lepton doublets as in Eq. 4.2 above, appended to the aspon model of Ref. [26]. Finally, the fourth model (model 4) will contain singlets

$$L_L, N_L, L_R, N_R, \quad (4.3)$$

added to the aspon model with  $SU(2)$ -singlet vector quarks.

### 4.3 Detection

In this section, we first note that  $L$  could be very long-lived. If it is lighter than the  $N$ , and if both  $N$  and  $L$  do not mix with the standard model leptons, then  $L$  would be absolutely stable. This would be a cosmological disaster; cosmological and astrophysical arguments from last chapter limit the lifetime to under 100 years. In the models we are considering in this chapter, it is quite natural to have mixings, and thus the lifetime of  $L$  is model dependent. Knowing the lifetime is crucial for experimental detection: if it is under  $10^{-13}$  seconds, the  $L$  will decay at the vertex; if it is between  $10^{-13}$  and  $10^{-8}$  seconds,

it will decay in the middle of the detector; if it is greater than  $10^{-8}$  seconds, it will pass through the detector, and will look like a muon.

Let us first consider model 1. If the  $N$  is heavier than the  $L$ , and if it does mix with a lighter neutrino (taken to be  $\nu_\tau$ ), the  $L$  lifetime will be increased by a factor of  $\sin^2 \theta$  (where  $\theta$  is the mixing angle) over the lifetime it would have if the  $N$  were massless. For a 100 GeV  $L$ , this gives a lifetime of  $O(10^{-20} \text{ s})/\sin^2 \theta$ . What are plausible values of  $\sin^2 \theta$ ? In see-saw type models,  $\sin^2 \theta$  is given by either  $m_\tau/m_L$  or by  $m_{\nu_\tau}/m_N$ , depending on whether the mixing can occur in the charged lepton sector or whether it is confined to the neutrino sector. In the former case, the lifetime is  $O(10^{-18})$  seconds; i.e.  $L$  will decay at the vertex. However, in the latter case, the lifetime is  $O(10^{-9})$  seconds, and could easily be long enough that the  $L$  would pass through any detector.

In the case in which the  $L_R$  and  $N_R$  form a doublet (model 2 and model 3), the masses are degenerate at tree level. The  $L$  and  $N$  will acquire a mass splitting from radiative corrections. This gives a splitting of  $O(200)$  MeV; the precise splitting depends on masses and on the particle content of the model. This splitting gives a lifetime between  $10^{-9}$  seconds and  $10^{-7}$  seconds,  $L$  will decay inside the detector.

One can thus see that all three lifetimes: (a) decay at the vertex, (b) decay in the detector and (c) decay outside the detector are all plausible, and each possibility must be considered.

If  $L$  decays before leaving the vertex, the analysis of the detection will be the same as that for a conventional heavy lepton, with one crucial exception. The heavy  $L$ 's transform differently from the standard model charged leptons in models 2, 3 and 4, and the GIM mechanism will break down, leading to

flavor changing decays such as  $L \rightarrow \tau Z$ .

By neglecting the mass of  $\tau$ , one finds the ratio (for  $m_L > m_Z$ ):

$$\frac{\Gamma(L \rightarrow \tau Z)}{\Gamma(L \rightarrow \nu_\tau W)} = \frac{16|U_{L\tau}|^2}{\cos^2\theta_W|U_{L\nu_\tau}|^2} \frac{(m_L^2 - 2m_Z^2 + m_L^4/m_Z^2)(m_L^2 - m_Z^2)}{(m_L^2 - 2m_W^2 + m_L^4/m_W^2)(m_L^2 - m_W^2)}. \quad (4.4)$$

An estimate of the value of  $U_{L\tau}$  can be made by analogy with similar GIM violation in the aspon model[26] which gives  $U_{L\tau} = (m_\tau/m_L)x_\tau$ , where  $x_\tau$  gives the ratio of  $M_{34}$  to  $M_{44}$  in the lepton mass matrix.  $U_{L\nu_\tau}$  is expected to be of order of  $\sqrt{m_\tau/m_L}$  or  $\sqrt{m_{\nu_\tau}/m_N}$ . In the former case, one finds the branching ratio to be of the order of a few percent; in the latter it is nearly one hundred percent. Even if we take a small branching ratio, the background for a particle decaying into  $Z\tau$  would be extremely small (especially if a vertex detector could pick up the tau). A major problem with the conventional heavy lepton detection has been backgrounds; the  $L \rightarrow \tau Z$  signal, even with a branching ratio as low as 1%, may be easy to pick up.

If the decay is in the middle of the detector, but away from the vertex, it should be easy to detect. An apparent muon will suddenly decay into missing energy and a real or virtual  $W$ . The backgrounds should be negligible.

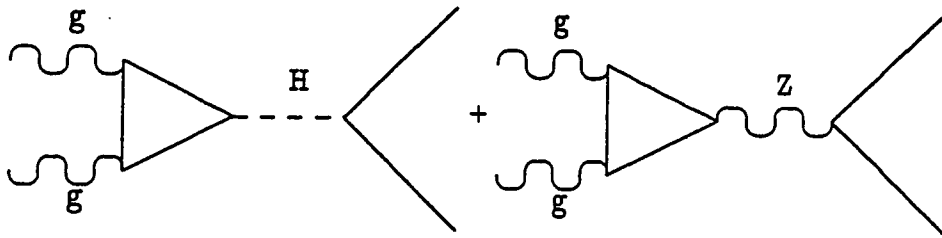
If the decay is outside the detector, the  $L$  will be indistinguishable from a muon. The production cross section, as will be shown in the next section, is large enough that thousands of  $L$ 's could be produced annually at the SSC, but it is small compared with muon pair production, so the "extra" muons would not be noticed. One possible method of detection would be time-of-flight. Many of the  $L$ 's will have  $\beta < 1$  ( see Sec. 5 for  $d\sigma/d\beta$ ), and if timing is installed in the detectors, the  $L$ 's could be seen. It is interesting that 1000's of  $L$ 's could be produced, but that they could be missed if timing is not present.

## 4.4 Production Cross Sections

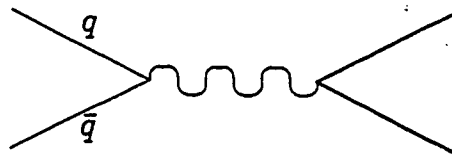
In this chapter, we consider the production processes for  $pp \rightarrow L^+L^-$ ,  $NN$ ,  $NL^\pm$ , as well as  $pp \rightarrow L^+L^-A$ ,  $NNA$  and  $NLA$  where  $A$  is the aspon in models 3 and 4. The cross sections and Feynman graphs for all relevant subprocesses are given in Appendix C and Fig. 4.1 respectively. The Fortran program for the process  $pp \rightarrow LL$  is given in Appendix D as an example. The total cross sections for all the above processes are computed by using EHLQ[34] parton structure functions (set 1). Previous calculations of heavy neutrino production have been done (see Ref. [18]); we include these cross sections for completeness and because, if the  $N$  is heavier than the  $L$ , each  $N$  will immediately decay into an  $L$  and a virtual  $W$ . This will increase the production rate of  $L$ 's. As noted in Ref. [18], if the  $N$ 's are Majorana particles, some of the  $L$ -pairs produced will be like-sign.

For model 1, gluon fusion production (see Fig. 4.1(a)), by  $Z$  and  $H$  exchange, is more important because the cross sections are proportional to the square of the lepton mass. For the vector lepton models (models 2, 3 and 4), gluon fusion will not contribute, since vector leptons do not couple to  $H$  and a vectorlike coupling to the  $Z$  gives no contribution due to Furry's theorem. Thus, the only contributions for the pair production of leptons in these models are by quark fusion (see Fig. 4.1(b)) in which the cross sections fall off faster.

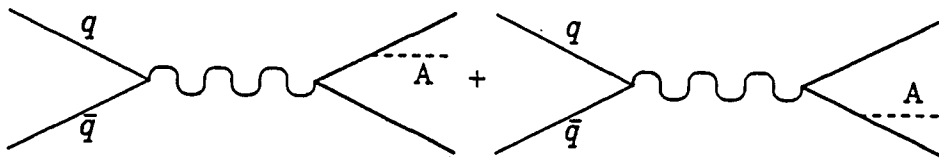
In addition, an aspon  $A$  can be produced through the bremsstrahlung effect from the heavy leptons (see Fig. 4.1(c)). For completeness, we include also the production cross sections for  $pp \rightarrow L^+L^-A$ ,  $NNA$  and  $NLA$  at the SSC and LHC.



(a)



(b)



(c)

Figure 4.1: Feynman diagram for the process (a)  $gg \rightarrow L^+L^-$  and  $NN$ , (b)  $q\bar{q} \rightarrow L^+L^-$ ,  $NL^\pm$  and  $NN$ , and (c)  $q\bar{q} \rightarrow L^+L^-A$ ,  $NLA$  and  $NNA$

As we discussed in the previous sections, a long-lived charged lepton can only be discovered if there are timing facilities in detectors. A long-lived charged lepton is more likely to appear in the vector lepton doublet models such as models 2 and 3. The velocity distribution,  $d\sigma/d\beta$ , where  $\beta$  is defined as the ratio of the momentum to the energy of  $L$  in lab-frame, has been calculated at the LHC and SSC energies for  $m_L = 100, 300$  and  $500$  GeV; the results are reported at the end of the following section.

## 4.5 Results and Conclusions

The results for the production cross sections at the SSC ( $\sqrt{s} = 40$  TeV) and the LHC ( $\sqrt{s} = 17$  TeV) are displayed for the different final states of  $pp$  collisions in Figs. 4.2-4.6. From these figures one can estimate easily the number of events per collider-year using the projected luminosities of the two machines (SSC:  $10^{33}$   $\text{cm}^{-2}\text{s}^{-1}$ ; LHC:  $10^{34}$   $\text{cm}^{-2}\text{s}^{-1}$ ) and the corresponding annual integrated luminosities  $10 \text{ fb}^{-1} \text{ y}^{-1}$  and  $100 \text{ fb}^{-1}\text{y}^{-1}$  respectively.

For heavy  $L$  or  $N$ , the cross sections for  $pp \rightarrow L^+L^-$ ,  $NN$  are largest for model 1 because of the dominant gluon fusion contribution (with  $Z$  and  $H$  exchange) in which cross sections are proportional to the square of the masses; there is no such contribution for vector leptons (models 2, 3 and 4) because both the  $Z$  and  $H$  diagrams (Fig. 4.1(a)) vanish, as discussed earlier. In particular, for  $pp \rightarrow L^+L^-$  (Fig. 4.2) and  $M_L = 400$  GeV there are predicted to be 10,000 events for model 1 per year at the SSC and the LHC. For models 2, 3 and 4 (where the gluon fusion contributions vanish), there are 1,000 or 2,000 events for model 2 and 3; and 500 or 1,000 events for model 4 at the SSC or the LHC respectively. Similar rates are predicted for  $pp \rightarrow NN$  (which is not allowed in

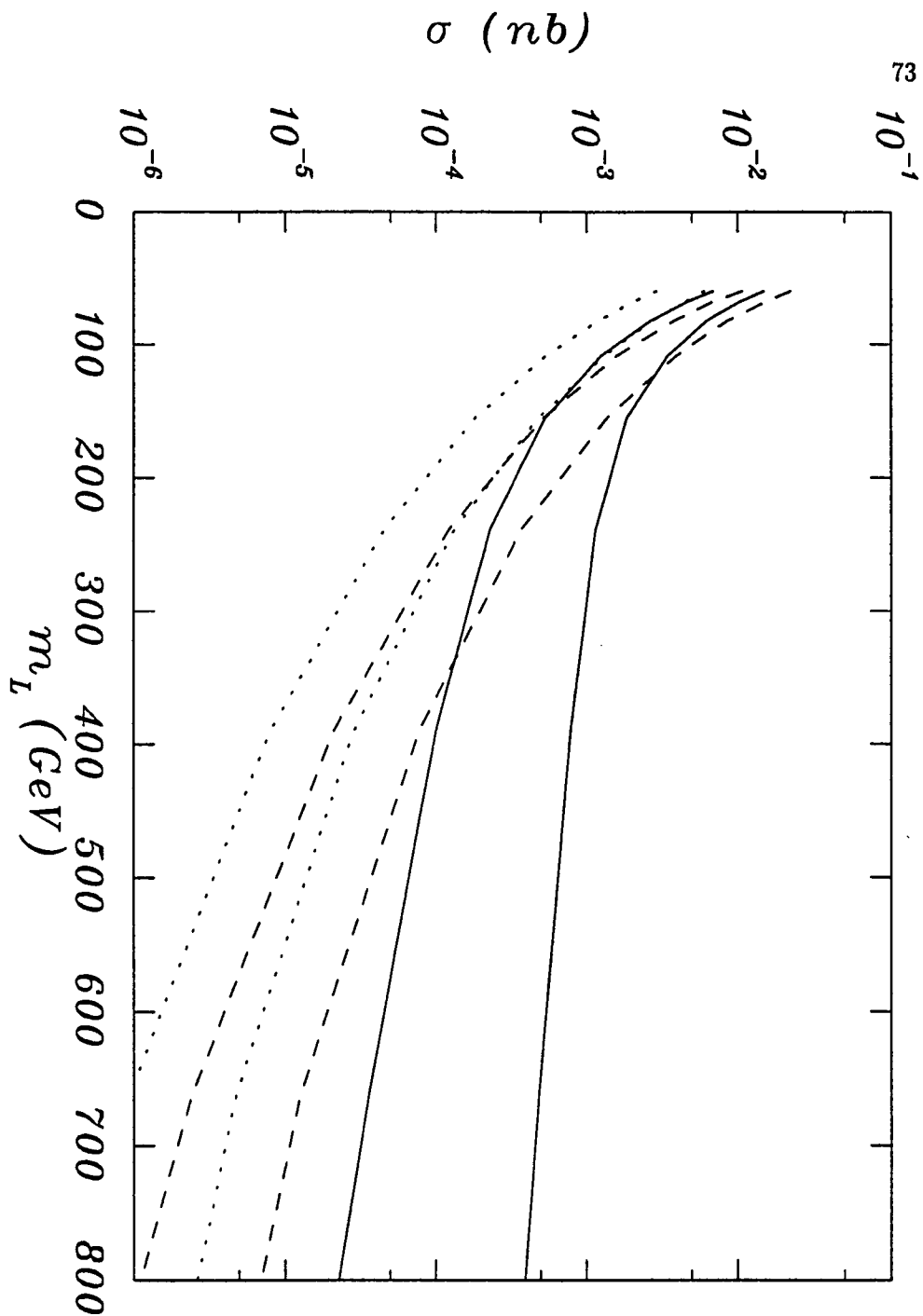


Figure 4.2: Total cross sections for heavy lepton production  $pp \rightarrow L^+L^-$  as a function of the charged lepton mass  $m_L$  for model 1(solid lines), model 2 and 3(dashed lines) and model 4(dotted lines). The upper and lower sets are for the  $E_{cm} = 40$  TeV and  $E_{cm} = 17$  TeV.  $m_H = 100$  GeV is assumed.

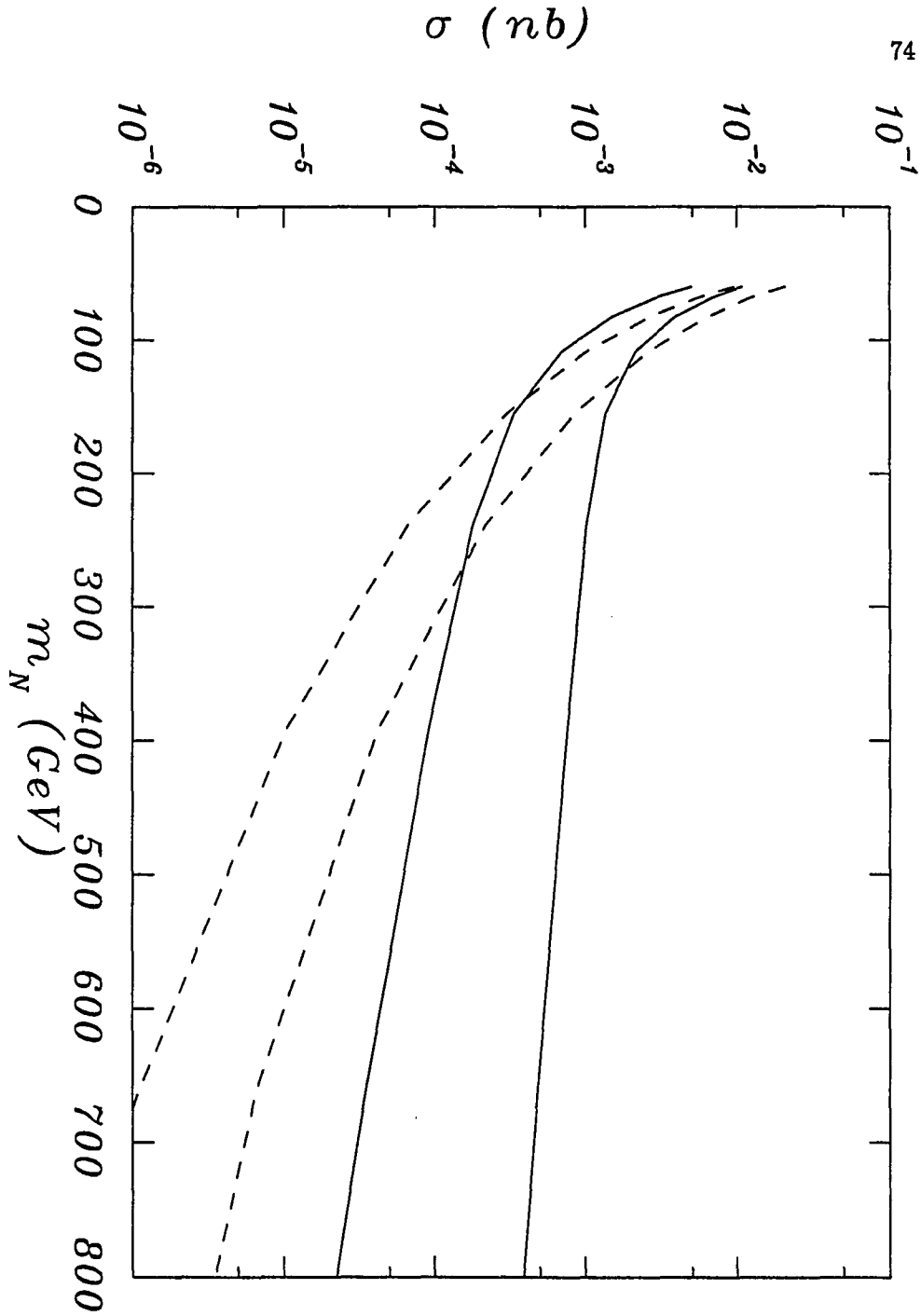
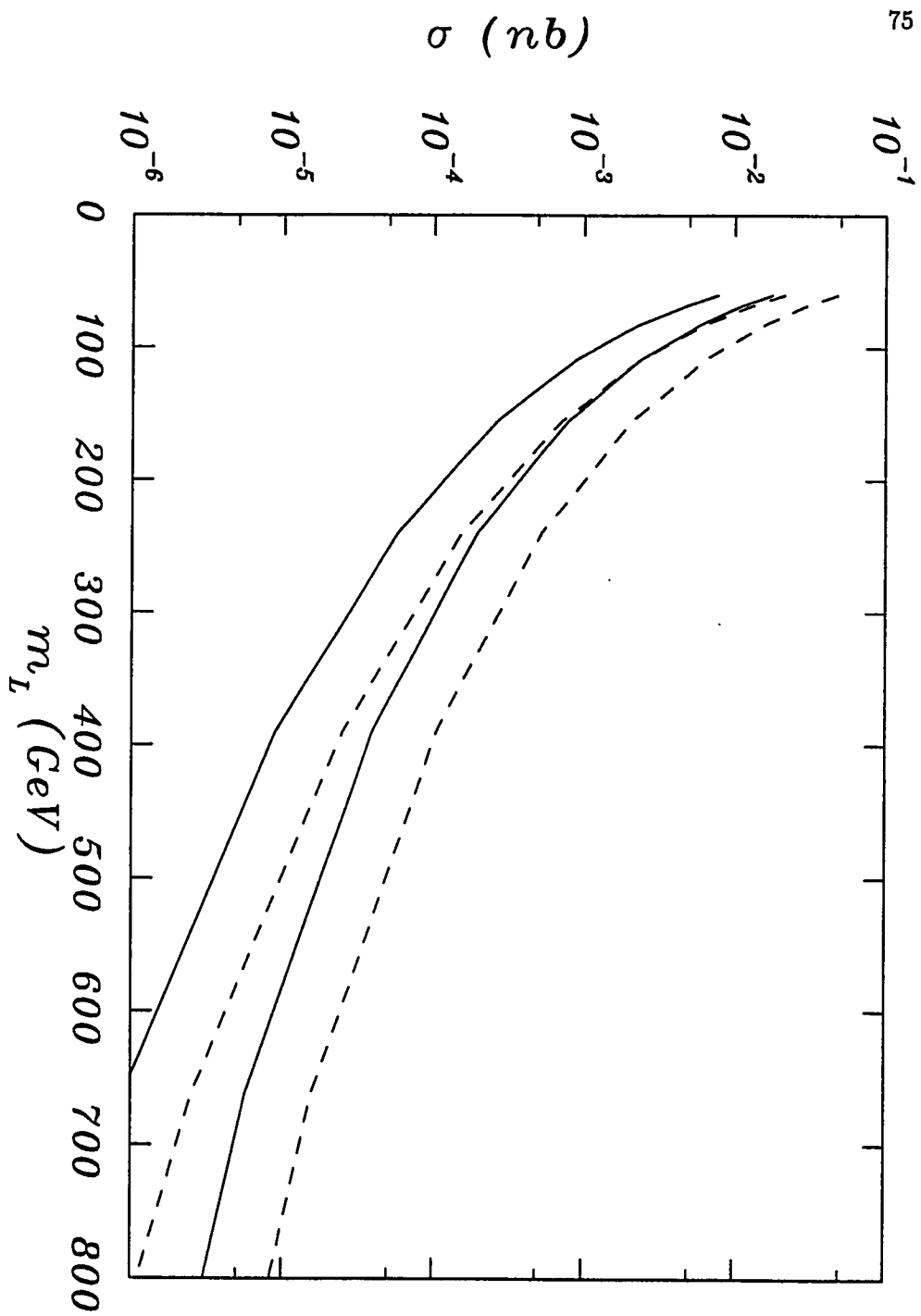
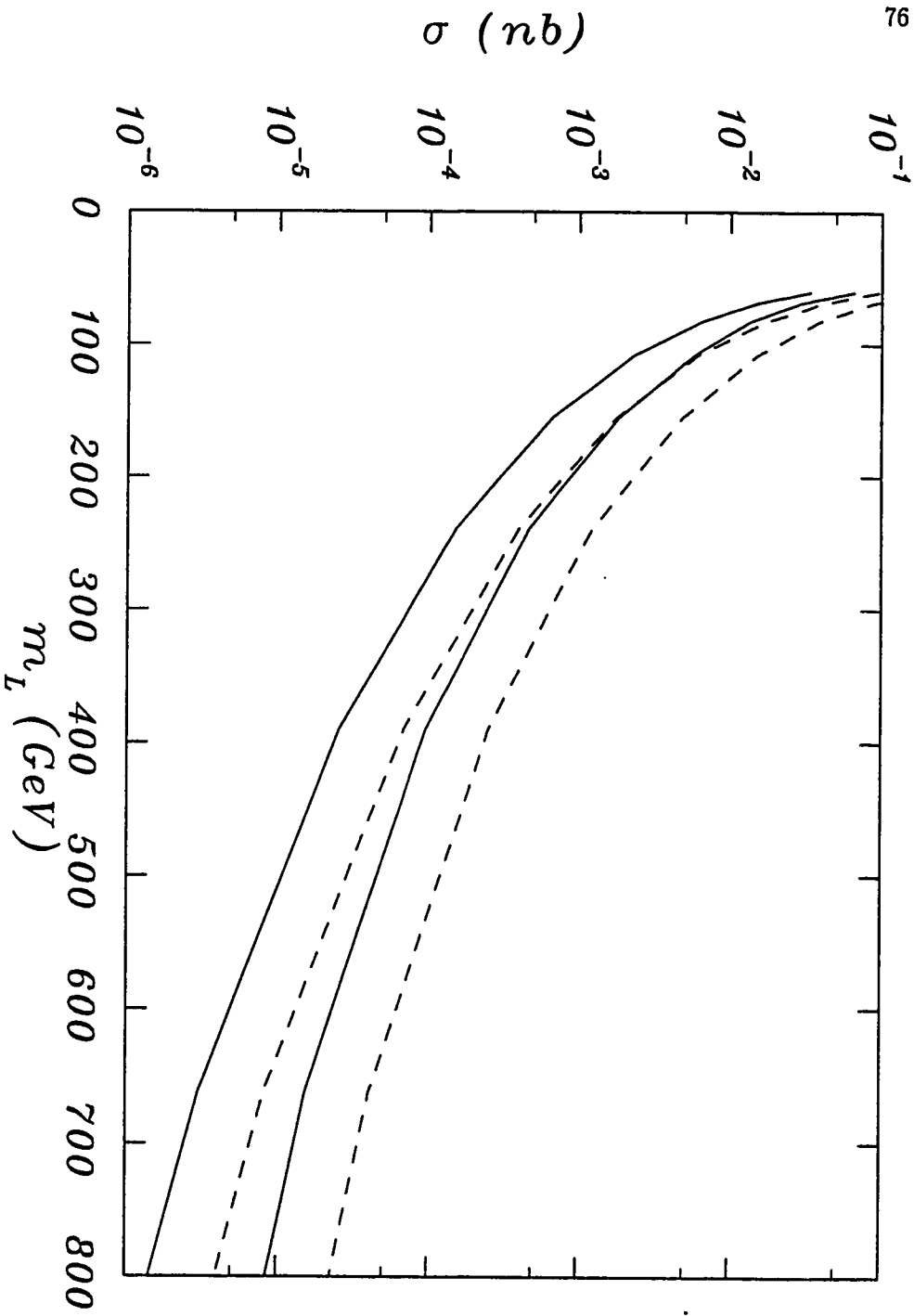


Figure 4.3: Total cross sections for the process  $pp \rightarrow NN$  as a function of the heavy neutrino mass  $m_N$  for model 1 (solid lines), and model 2 and 3 (dashed lines). The upper and lower sets are for  $E_{cm} = 40$  TeV and  $E_{cm} = 17$  TeV.  $m_H = 100$  GeV is assumed.



(a)



(b)

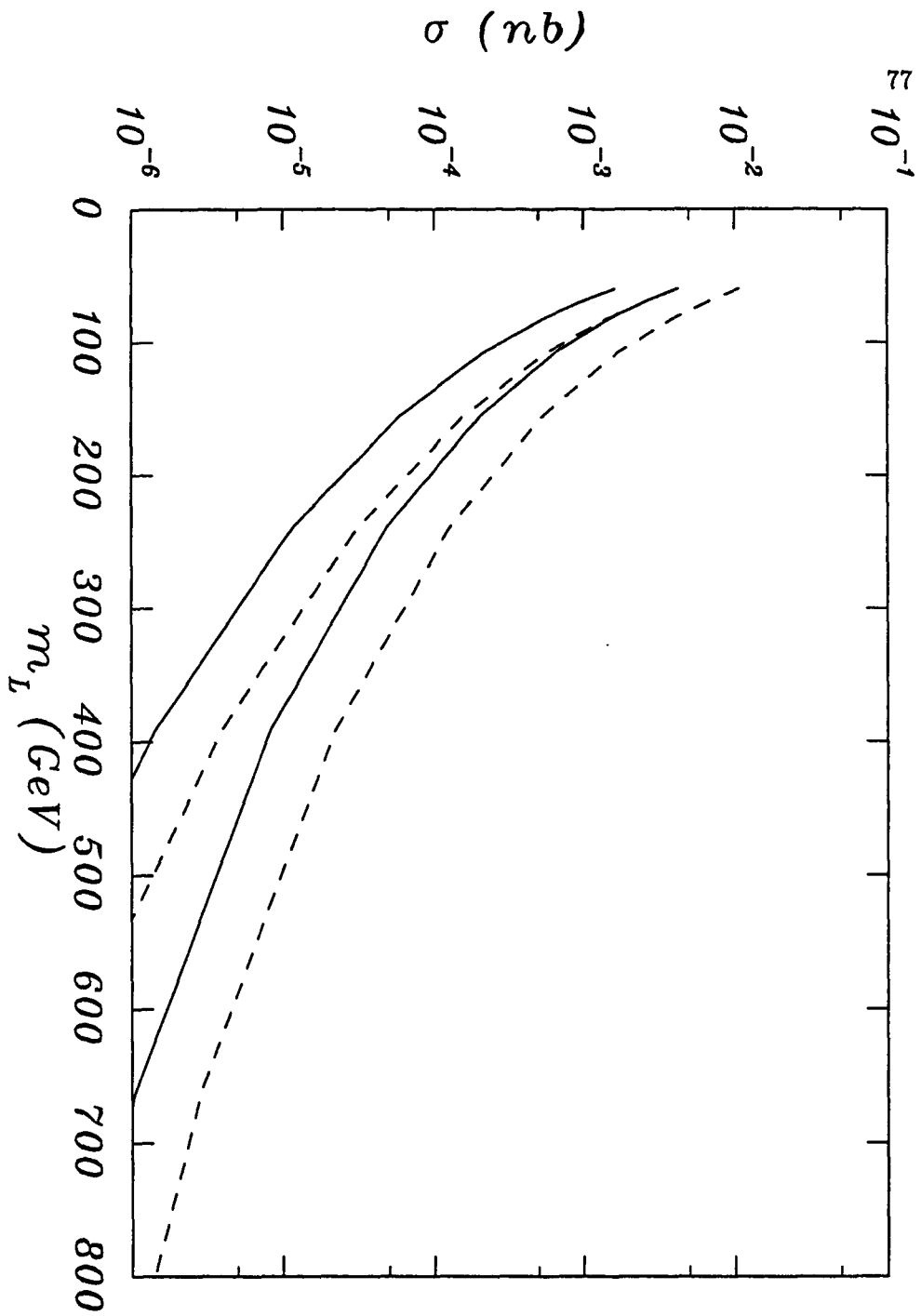
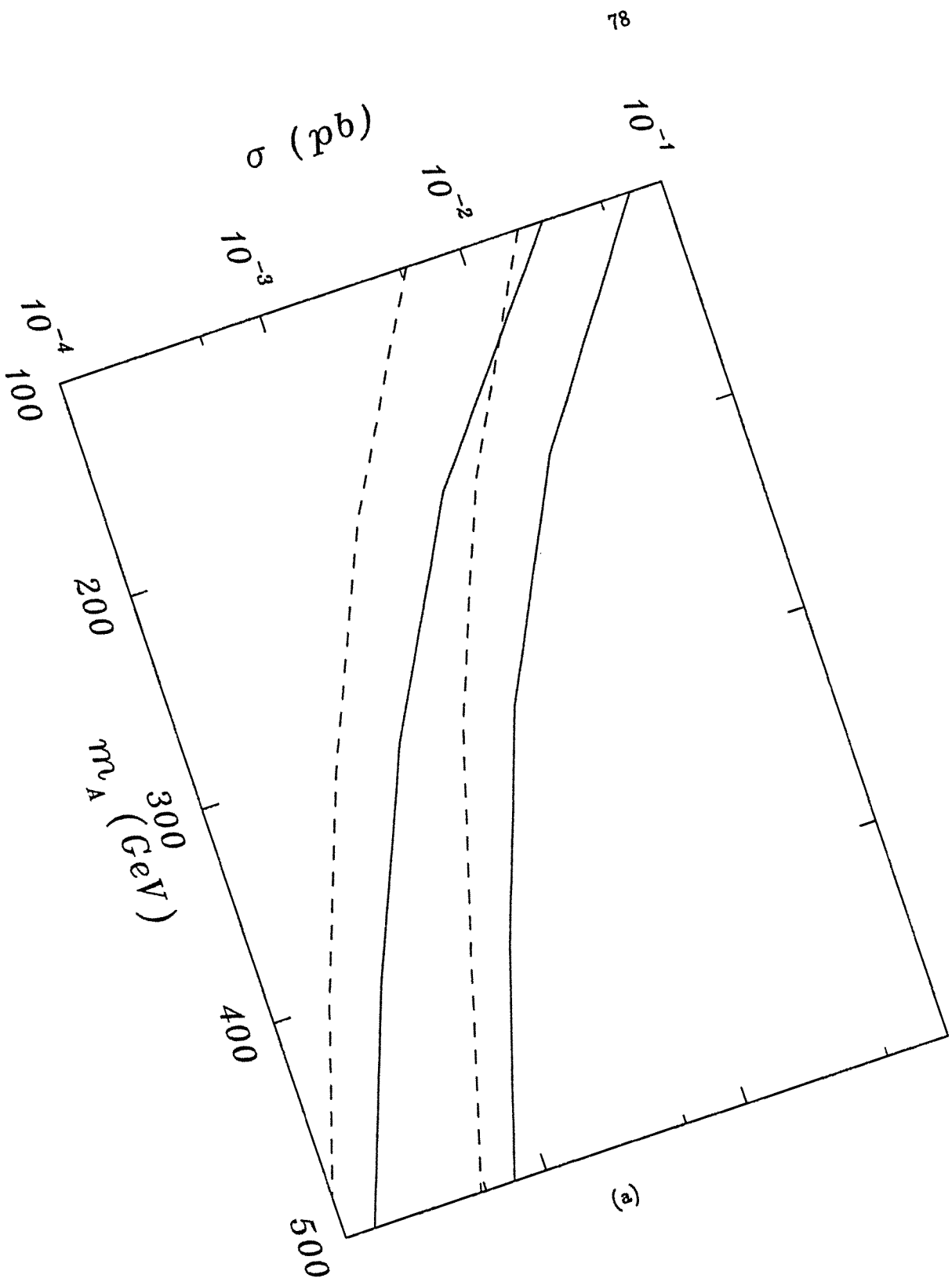


Figure 4.4: Total cross sections for the process  $pp \rightarrow NL^\pm$  for model 1(solid lines), and model 2 and 3(dashed lines) for (a)  $m_N/m_L = 0.5$ , (b)  $m_N/m_L = 1$ , (c)  $m_N/m_L = 2$ . The upper and lower sets are for  $E_{cm} = 40$  TeV and  $E_{cm} = 17$  TeV.  $m_H = 100$  GeV is assumed.



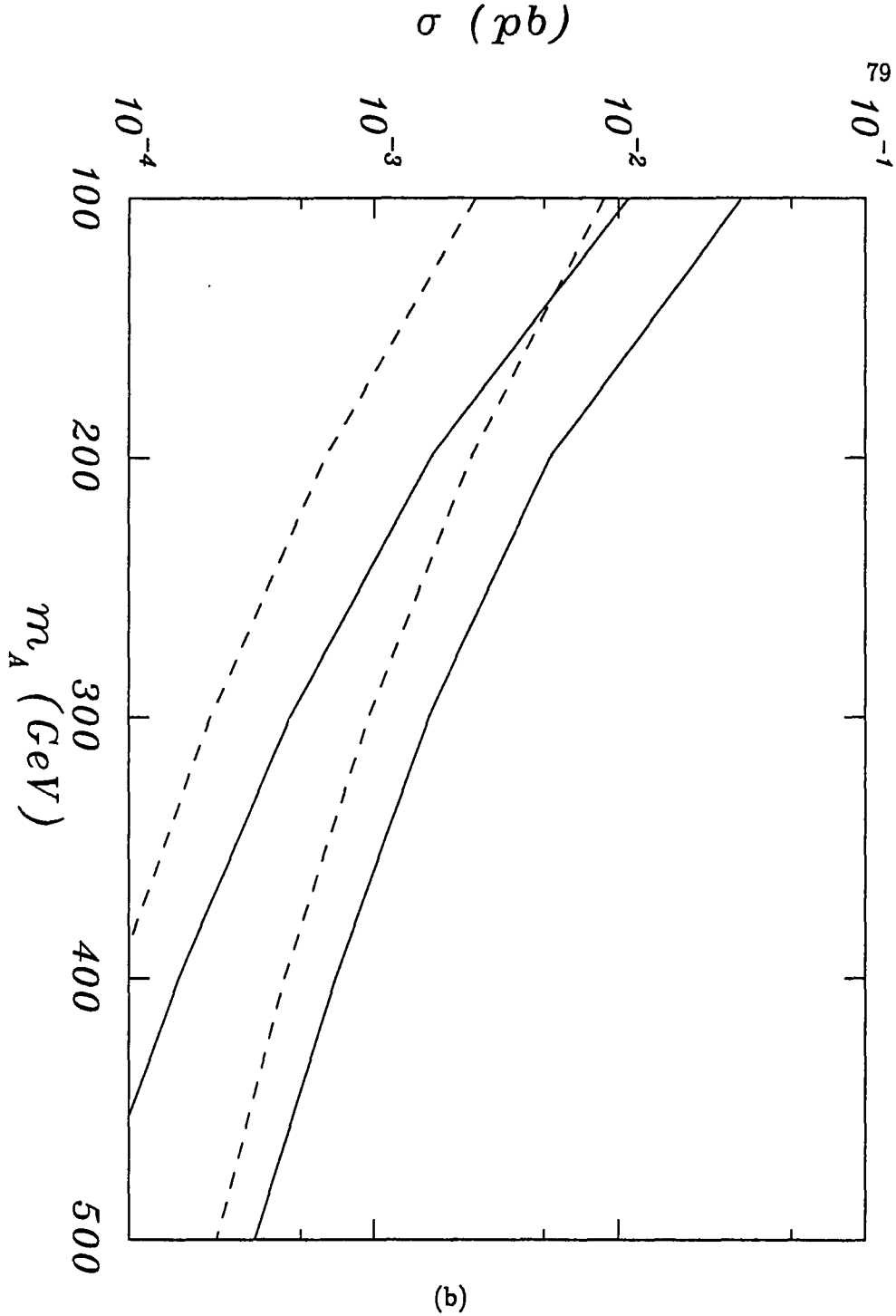


Figure 4.5: Total cross sections for the process  $pp \rightarrow L^+L^-A$  ( $A = aspon$ ) as a function of aspon mass  $m_A$  for (a) model 3 and (b) model 4 with  $m_L = 50$  GeV (solid lines) and  $m_L = 150$  GeV (dashed lines). The upper and lower sets are for  $E_{cm} = 40$  TeV and  $E_{cm} = 17$  TeV.  $m_H = 100$  GeV and the coupling of the aspon  $\alpha_A = 0.1$  are assumed.

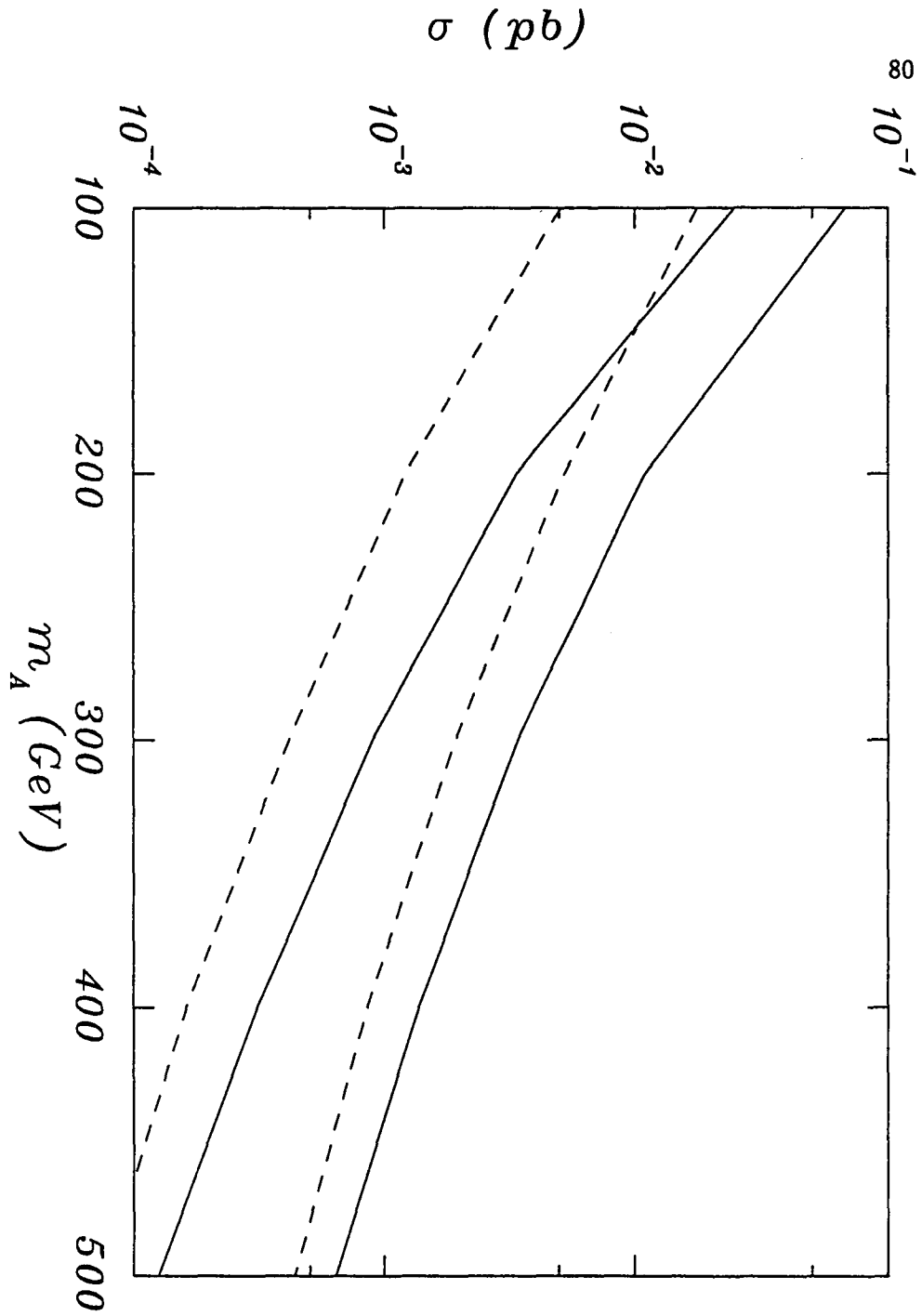


Figure 4.6: Total cross sections for the processes  $pp \rightarrow NNA$  in model 3 for  $m_L = m_N = 50$  GeV (solid lines) and  $m_L = m_N = 150$  GeV (dashed lines). The upper and lower sets are for  $E_{cm} = 40$  TeV and  $E_{cm} = 17$  TeV.  $m_H = 100$  GeV and the coupling of the aspon  $\alpha_A = 0.1$  are assumed.

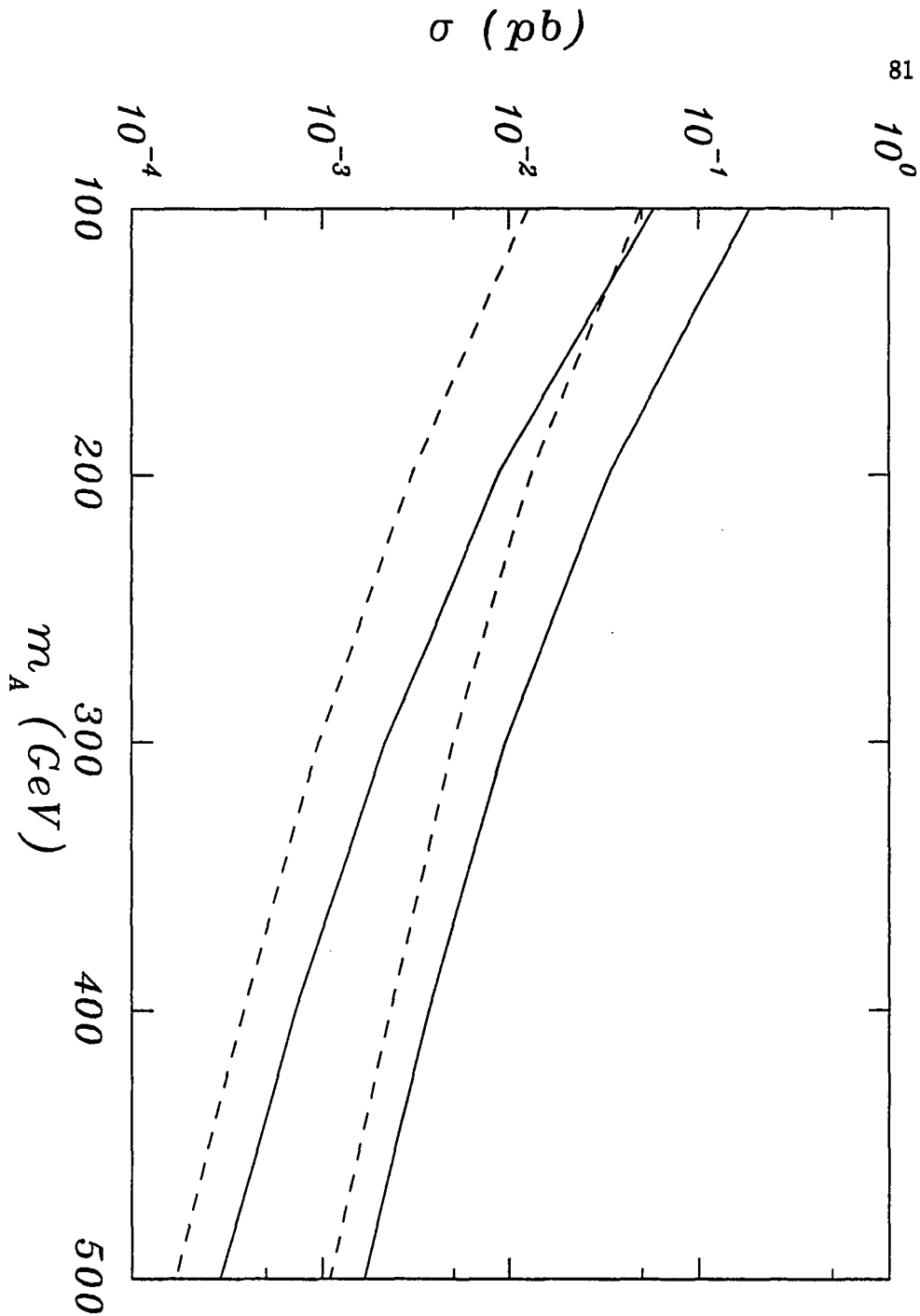
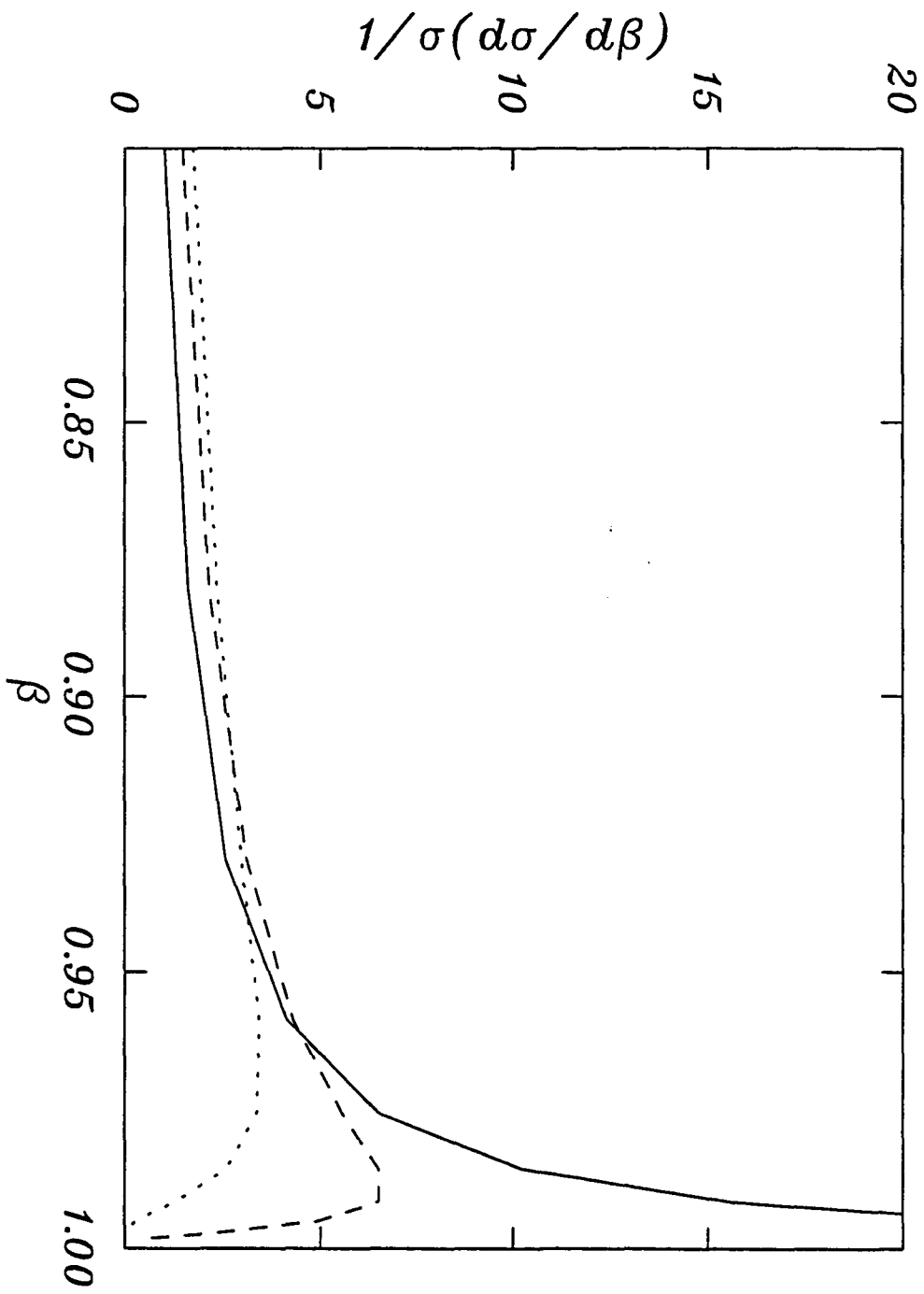


Figure 4.7: Total cross sections for the processes  $pp \rightarrow NLA$  in model 3 for  $m_L = m_N = 50$  GeV (solid lines) and  $m_L = m_N = 150$  GeV (dashed lines). The upper and lower sets are for  $E_{cm} = 40$  TeV and  $E_{cm} = 17$  TeV.  $m_H = 100$  GeV and the coupling of the aspon  $\alpha_A = 0.1$  are assumed.



(a)

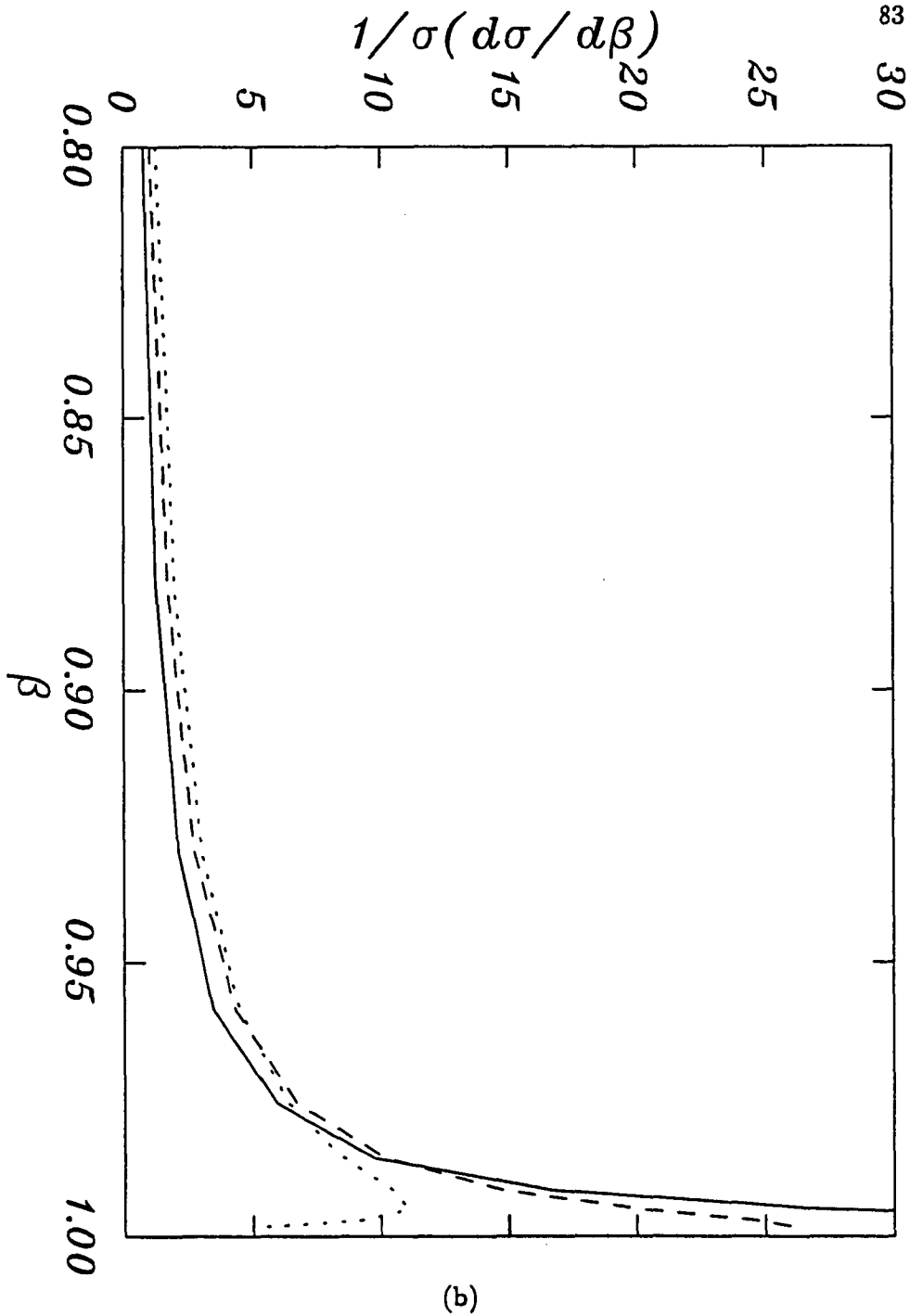


Figure 4.8: The velocity distributions  $1/\sigma(d\sigma/d\beta)$  for the process  $pp \rightarrow LL$  in model 2 and 3 at (a)  $E_{cm} = 17$  TeV, and (b)  $E_{cm} = 40$  TeV and for  $m_L = 100$  GeV(solid line), 300 GeV(dashed line) and 500 GeV(dotted line) respectively.

model 4) although the photon contribution vanishes. Finally, the cross sections for  $pp \rightarrow NL^\pm$ , which are allowed by  $W$  exchange, can be read off from Fig. 4.4. Although the luminosity is ten times higher at the LHC, the number of heavy leptons produced in general is just two times that at the SSC.

Note that although the cross sections for models 2, 3 and 4 are considerably smaller, these models do have an  $L \rightarrow \tau Z$  decay mode, and thus possibly a much cleaner signature, if it decays in the detector. For  $pp \rightarrow NL^\pm$  in which only the  $W$  exchange is allowed, models 1, 2 and 3 give similar cross sections.

For  $pp \rightarrow L^+L^-A$ ,  $NNA$  and  $NLA$  with an aspon in the final state, the cross sections, which are shown in Figs. 4.5-4.7, are about 100 times smaller than without an aspon, but are still within the range of detectability of SSC and LHC. Model 3 (heavy lepton doublets) gives a slightly larger cross section than model 4 (heavy lepton singlets) because the former allows certain  $W$  and  $Z$  couplings.

If timing facilities are installed in detectors, the  $\beta$  distribution functions  $1/\sigma(d\sigma/d\beta)$  would be relevant. In Fig. 4.8, we plot the  $\beta$  distributions for  $pp \rightarrow L^+L^-$  in the vector doublet models (models 2 and 3) for  $m_L = 100, 300$  and  $500$  GeV at the LHC (Fig. 4.8(a)) and the SSC (Fig. 4.8(b)). For a muon, the distribution is, of course, a delta function at  $\beta = 1$ ; whereas the  $\beta$  distribution spreads out to  $\beta < 1$  for a heavy lepton with an enhancement near  $\beta = 1$ . From Fig. 4.8, we conclude that in searching for a long-lived charged lepton, time-of-flight is a valuable method because of the characteristic spreading to  $\beta < 1$ ; at SSC this is viable up to at least  $m_L = 500$  GeV. Thus timing in the SSC detector would be particularly useful. Actually, the designers of the detector at the LHC have been using our results. They are aware of the

of the possibility of missing these leptons and will arrange the hardware and software to have the capability of looking for them.

## Chapter 5

### Conclusion and Future Work

Two extensions beyond the standard model were discussed.

The first extension of standard model involved an additional Higgs-boson. This model will automatically have tree-level flavor-changing neutral currents, unless they are suppressed by some additional symmetry. It is often believed that the presence of tree-level flavor-changing neutral currents in this model is fatal, unless a discrete symmetry is added, since it requires the exchanged scalar to be extremely heavy. This follows, however, from the assumption that the flavor-changing coupling is quite large. Using a more natural value for the flavor-changing coupling, much smaller bounds were obtained. Unlike previous calculations, we calculated the bounds on the flavor-changing couplings of an additional scalar for the processes involving the third generation fields which should be considerably more reliable. Since the masses of the scalar and the pseudoscalar are likely to be quite different, we have considered the bounds on each separately. From the processes  $\tau$  three-body and radiative decays, muon-electron conversion in nuclei,  $B$  and  $B_s$  three-body decays,  $B$  and  $B_s$  two-body decays and  $B - \bar{B}$  mixing, we found that in the quark sector the strongest

bound comes from  $B - \bar{B}$  mixing and in the lepton sector the strongest bound on the flavor-changing coupling involving the  $\tau$  comes from the radiative decay of the muon. We have also noted that in most grand unified theories, the  $\tau$  and bottom quark are in the same representation, thus the flavor-changing couplings in the quark sector are related to those in the lepton sector. Comparing flavor-changing  $B$  decays with rare  $\tau$  decays, we found that rare  $B$  decays provide the strongest bounds and that the most promising decay modes are  $B \rightarrow K\mu\tau$  and  $B_s \rightarrow \mu\tau$  with  $\tau$ 's in the final state.

The second extension of the standard model we considered is about the fourth generation heavy leptons. If a fourth generation exists, the lepton  $L$  and the neutrino  $N$  must both be heavier than 45 GeV. It is certainly possible that the neutrino will be the heavier of the two. In this case, the charged lepton can only decay through mixing with lighter generations, and might thus be extremely long-lived. First, we investigated the implications of very long-lived charged leptons for cosmology and astrophysics. In the early universe, the relative abundance of a massive weakly interacted particle species "freezes out" when the annihilation rate becomes less than the expansion rate. We calculated the annihilation cross-sections and found that the dominant process will be  $W$  pair-production with the s-channel photon exchange. We also assume that the annihilation cross-section is subject to unitarity constraints and considered the mass range from 45 GeV to 100 TeV. Then we calculated the abundance today and obtained the bounds on the mass. If  $L$  decays, limits on the lifetime of a long-lived charged lepton can be found from several sources: direct detection of the  $L$  and direct detection of its decay products. From terrestrial experiments, the strongest one comes from searches for the heavy

isotopes of hydrogen in water for the mass range up to 10 TeV, and above 10 TeV, the strongest bounds comes from plastic track detectors. From astrophysical searches for the decay products and from cosmology, we checked the the bounds from the diffuse photon background (lifetime in excess of  $10^{13}$  sec.) and from the requirement that the decay products not unacceptably distort the microwave background radiation (CMB). We found the strongest cosmological bounds on the lifetime come from very recent COBE data. Then we studied the production cross-sections and signatures for the SSC and LHC. We considered four models which contain heavy leptons for the experimental detection at the Hadron Colliders. Two models are the fourth generation extensions of the standard model in which the right-handed heavy leptons are either isosinglets or in an isodoublet, the other two are motivated by the aspon model of CP violation, and contain also singlets or vector lepton doublets. We calculated the production cross-sections for all the processes into heavy leptons, neutrinos and aspon through quark fusion into a photon or  $Z$ (or  $W$ ), as well as through gluon fusion into a Higgs or a  $Z$ . For the first model, gluon fusion production is more important, and for the vector lepton models, only quark fusion contributes, in which case the cross-sections fall off faster. And the production cross-section for the processes with an aspon in the final state will be even smaller. In all these models, the heavy neutrino can either be heavier than, or comparable in mass to, the charged lepton leading to the possibility that the charged lepton can only decay through mixing, thus  $L$  could be very long-lived. If the lifetime of  $L$  is under  $10^{-13}$  seconds, it will decay in the middle of the vertex; the analysis of the detection will be the same as that for a conventional heavy lepton, with one crucial exception. For the vector lepton models, the

GIM mechanism will break down, leading to flavor-changing decays such as  $L \rightarrow \tau Z$ . For this decay the background would be extremely small and the signal may be easy to pick up. If the lifetime is between  $10^{-13}$  and  $10^{-8}$  seconds, the  $L$  will decay in the middle of the detector. If the lifetime is greater than  $10^{-8}$ , it will pass through the detector like a muon. The only possible method of detection would then be time-of-flight. Since 1000's of  $L$ 's could be produced at the SSC and LHC, timing in these detector would be very useful for finding these heavy leptons.

There are several related projects that I hope to pursue in the next few months. One involves the phenomenology of production of these heavy leptons in electron colliders; especially in the vector-like models, which naturally have long-lived heavy leptons. In the aspon model, one has a diagram which could lead to *resonant* production of an aspon. Another project, also related to the aspijon model, concerns CP violation in the lepton sector. The aspon model was desired to eliminate strong CP problem. The CP-violating couplings are thus constrained by the observations of  $K$  decay. Such constraints are much weaker in the lepton sector, which could then have large CP violation effects.

## Appendix A

### The Cross Sections for Chapter 2

Here we shall give explicit expressions for all the cross sections in Chapter 2.

1) Annihilation  $\bar{L}L \rightarrow \bar{f}f$

$$\begin{aligned}
 \sigma\beta_{\text{rel}} = & N_c\beta_f\pi\alpha^2 \left\{ \left( \frac{8Q^2}{3s} + \frac{4Qg_V^f g_A^L (s - m_Z^2) |D_Z|^2}{3x_W(1 - x_W)} \right) \right. \\
 & \times \left( 1 + \frac{2(m_L^2 + m_f^2)}{s} + \frac{4m_L^2 m_f^2}{s^2} \right) \\
 & + \frac{s|D_Z|^2}{8x_W^2(1 - x_W)^2} \left[ (g_V^{L^2} + g_A^{L^2})(g_V^{f^2} + g_A^{f^2}) \left( 1 + \frac{1}{3}\beta_f^2\beta_L^2 \right) \right. \\
 & + (g_V^{L^2} + g_A^{L^2})(g_V^{f^2} - g_A^{f^2}) \frac{4m_f^2}{s} + (g_V^{L^2} - g_A^{L^2})(g_V^{f^2} + g_A^{f^2}) \frac{4m_L^2}{s} \\
 & \left. \left. - (g_A^{L^2} g_V^{f^2} + g_A^{f^2} g_V^{L^2} - 2g_A^{L^2} g_A^{f^2}) \frac{16m_L^2 m_f^2}{s^2} \right] \right\} , \quad (\text{A.1})
 \end{aligned}$$

where  $x_W = \sin^2\theta_W$ , and  $g_V$  and  $g_A$  are the standard neutral vector and axial current couplings, respectively.  $N_c$  is a color factor,  $s$  is the center of mass energy squared, and  $\beta_f$  is the velocity of  $f$ :  $\beta_f = (1 - 4m_f^2/s)^{1/2}$ . Finally,  $|D_Z|^2$  is the propagator factor of the  $Z$ -boson;

$$|D_Z|^2 = [(s - m_Z^2)^2 + \Gamma_Z^2 m_Z^2]^{-1} .$$

2) Annihilation  $\bar{L}L \rightarrow W^+W^-$

$$\sigma_{(LL \rightarrow W+W^-)} = \sigma_{\gamma\gamma} + \sigma_{\gamma Z} + \sigma_{ZZ} + \sigma_{LL} + \sigma_{LZ} + \sigma_{L\gamma}, \quad (\text{A.2})$$

$$\begin{aligned} \sigma_{\gamma\gamma+\gamma Z+ZZ}\beta_{\text{rel}} &= m_W^4 \beta_W \pi \alpha^2 \left( \frac{\bar{s}^3}{6} + \frac{8\bar{s}^2}{3} - \frac{34\bar{s}}{3} - 8 \right) (\bar{s} + 2\tilde{m}_L^2) \\ &\times \left[ \frac{1}{s^3} - \frac{g_V^L(s - m_Z^2)|D_Z|^2}{x_W s^2} + \frac{|D_Z|^2}{4x_W^2 s} \left( g_V^{L^2} + \frac{g_A^{L^2}(\bar{s} - 4\tilde{m}_L^2)}{(\bar{s} + 2\tilde{m}_L^2)} \right) \right], \end{aligned} \quad (\text{A.3})$$

$$\begin{aligned} \sigma_{LL}\beta_{\text{rel}} &= \frac{\beta_W \pi \alpha^2}{4x_W^2 s} \left[ \frac{1}{12}(\bar{s}^2 + 20\bar{s} - 24) + \left( \frac{1}{6}\bar{s} - \frac{5}{3} \right) \tilde{m}_L^2 - \frac{3}{2} \tilde{m}_L^4 \right. \\ &+ P_1 L_1 - \frac{1}{2}(2 - \tilde{m}_L^2 - \tilde{m}_L^4)^2 R_1 \\ &- \tilde{m}_N^2 \left( \frac{1}{2}\bar{s} - 1 - 3\tilde{m}_L^2 + 2P_2 L_1 + \frac{1}{2}P_1 R_1 \right) \\ &- \tilde{m}_N^4 \left( \frac{3}{2} - 3(\bar{s} - 2 - 4\tilde{m}_L^2)L_1 - \frac{1}{2}P_2 R_1 \right) \\ &\left. + \tilde{m}_N^6 \left( 4L_1 - \left( \frac{1}{2}\bar{s} - 1 - 2\tilde{m}_L^2 \right) R_1 \right) - \frac{1}{2} \tilde{m}_N^8 R_1 \right], \end{aligned} \quad (\text{A.4})$$

$$\begin{aligned} \sigma_{LZ}\beta_{\text{rel}} &= \frac{\beta_W \pi \alpha^2 m_W^2 (s - m_Z^2) |D_Z|^2}{8x_W^2 s} \left\{ (g_V^L + g_A^L) \left[ -\frac{1}{3}[\bar{s}^3 + 18\bar{s}^2 - 28\bar{s} - 24 \right. \right. \\ &- (\bar{s}^2 + 6\bar{s} + 8)\tilde{m}_L^2 - 6(\bar{s} - 2)\tilde{m}_L^4] + 4L_1[8\bar{s} + 4 - (10\bar{s} + 4)\tilde{m}_L^2 \\ &+ (\bar{s} + 2)\tilde{m}_L^4 + (\bar{s} - 2)\tilde{m}_L^6] + \tilde{m}_N^2[\bar{s}^2 - 4\bar{s} - 4 - (4\bar{s} - 8)\tilde{m}_L^2 \\ &+ 4L_1(4\bar{s}^2 - 5\bar{s} - 6 + (\bar{s}^2 - 5\bar{s} - 2)\tilde{m}_L^2 - 3(\bar{s} - 2)\tilde{m}_L^4)] \\ &\left. + \tilde{m}_N^4[2(\bar{s} - 2) - 4L_1(\bar{s}(\bar{s} - 4) - 3(\bar{s} - 2)\tilde{m}_L^2)] - \tilde{m}_N^6 L_1(4\bar{s} - 8) \right] \\ &\left. - (g_V^L - g_A^L)\tilde{m}_L^2(12 + 10\bar{s})[1 + 2L_1(\tilde{m}_L^2 - \tilde{m}_N^2 - 1)] \right\}, \end{aligned} \quad (\text{A.5})$$

$$\begin{aligned} \sigma_{L\gamma}\beta_{\text{rel}} &= \frac{\beta_W \pi \alpha^2 m_W^2 g_V^L}{4x_W s^2} \left\{ \frac{1}{3}[\bar{s}^3 + 18\bar{s}^2 - 28\bar{s} - 24 - (\bar{s}^2 - 24\bar{s} - 28)\tilde{m}_L^2 - 6 \right. \\ &\times (\bar{s} - 2)\tilde{m}_L^4] - 4L_1[8\bar{s} + 4 + (2 - 5\bar{s})\tilde{m}_L^2 - (4\bar{s} + 4)\tilde{m}_L^4 + (\bar{s} - 2)\tilde{m}_L^6] \\ &- \tilde{m}_N^2[\bar{s}^2 - 4\bar{s} - 4 - (4\bar{s} - 8)\tilde{m}_L^2 + 4L_1(4\bar{s}^2 - 5\bar{s} - 6 + (\bar{s}^2 + 4)\tilde{m}_L^2 \\ &\left. - 3(\bar{s} - 2)\tilde{m}_L^4)] - \tilde{m}_N^4[2(\bar{s} - 2) - 4L_1(\bar{s}(\bar{s} - 4) - 3(\bar{s} - 2)\tilde{m}_L^2)] \right\} \end{aligned}$$

$$+\tilde{m}_N^6(4\bar{s}-8)L_1\} , \quad (\text{A.6})$$

where  $P_1, P_2, L_1$  and  $R_1$  are defined as

$$\begin{aligned} \bar{s} &= s/m_W^2, \quad \tilde{m}_L^2 = m_L^2/m_W^2, \\ P_1 &= 4(\bar{s}-2) + 4\bar{s}\tilde{m}_L^2 + (\bar{s}-6)\tilde{m}_L^4 - 4\tilde{m}_L^6, \\ P_2 &= 4\bar{s}-5 + (2\bar{s}-6)\tilde{m}_L^2 - 6\tilde{m}_L^4, \\ L_1 &= -\frac{1}{2\bar{s}\beta_L\beta_W} \ln \left( \frac{2-\bar{s}+2\tilde{m}_L^2-2\tilde{m}_N^2+\bar{s}\beta_L\beta_W}{2-\bar{s}+2\tilde{m}_L^2-2\tilde{m}_N^2-\bar{s}\beta_L\beta_W} \right), \\ R_1 &= [(1-\tilde{m}_L^2)^2 - \tilde{m}_N^2(2-\bar{s}+2\tilde{m}_L^2) + \tilde{m}_L^4]^{-1}. \end{aligned} \quad (\text{A.7})$$

3) Annihilation  $\bar{L}L \rightarrow ZZ$

$$\begin{aligned} \sigma_{\text{rel}} &= \frac{\beta_Z \pi \alpha^2}{4x_W^2(1-x_W)^2s} \left\{ [(g_V^{L^2} + g_A^{L^2})^2 + 4g_V^{L^2}g_A^{L^2}] \left[ -2 - 2\tilde{m}_L^2 + \frac{\tilde{m}_L^2\bar{s}}{2} \right. \right. \\ &+ L_2 \left( \frac{\bar{s}^3}{8} + \frac{5\bar{s}^2}{4} + \bar{s} - 8 + \tilde{m}_L^2(6 - \bar{s}^2) \right) - R_2(2 + 2\tilde{m}_L^2(\bar{s} - 3) + \tilde{m}_L^4) \\ &+ B \left( \frac{\bar{s}^4}{8} + \bar{s}^3 - \frac{11\bar{s}^2}{2} - 10\bar{s} + \tilde{m}_L^2(-\bar{s}^3 - 2\bar{s}^2 + 30\bar{s} + 20) \right. \\ &\left. \left. + \tilde{m}_L^4(2\bar{s}^2 - 8\bar{s} - 12) \right) \right] + (g_V^{L^4} - g_A^{L^4}) [\tilde{m}_L^2(8 - 2\bar{s}) \\ &+ 12R_2\tilde{m}_L^2(\tilde{m}_L^2 - 1) + L_2\tilde{m}_L^2(2\bar{s}^2 - 6\bar{s} - 8) \\ &+ B(\tilde{m}_L^2(2\bar{s}^3 - 2\bar{s}^2 - 28\bar{s}) - \tilde{m}_L^4(8\bar{s}^2 - 32\bar{s} - 16))] \\ &\times (g_V^{L^2} - g_A^{L^2})^2 \left[ \tilde{m}_L^2 \left( \frac{3\bar{s}}{2} - 6 \right) - L_2\tilde{m}_L^2(\bar{s}^2 - 10\bar{s} - 2) \right. \\ &+ R_2\tilde{m}_L^2(2\bar{s} - 2 - 19\tilde{m}_L^2) + B(\tilde{m}_L^2(-\bar{s}^3 + 8\bar{s}^2 - 26\bar{s} + 12) \\ &\left. \left. + \tilde{m}_L^4(6\bar{s}^2 - 24\bar{s} + 28) \right) \right] \} , \end{aligned} \quad (\text{A.8})$$

where  $\tilde{s} = s/m_Z^2$ , and  $\tilde{m}_L^2 = m_L^2/m_Z^2$ ,

$$\begin{aligned} L_2 &= -\frac{1}{2\tilde{s}\beta_L\beta_Z} \ln \left( \frac{2 - \tilde{s} + \tilde{s}\beta_L\beta_Z}{2 - \tilde{s} - \tilde{s}\beta_L\beta_Z} \right) , \\ R_2 &= (1 - 4\tilde{m}_L^2 + \tilde{m}_L^2\tilde{s})^{-1} , \\ B &= \frac{L_2}{(2 - \tilde{s})} . \end{aligned} \quad (\text{A.9})$$

4) Annihilation  $\bar{L}L \rightarrow \gamma Z$

$$\begin{aligned} \sigma\beta_{\text{rel}} &= -\frac{\pi\alpha^2}{2x_W(1-x_W)s} \left\{ (g_V^{L^2} - g_A^{L^2})6m_L^2(L_3 + 4R_3m_L^2) \right. \\ &\quad - (g_V^{L^2} + g_A^{L^2}) \left[ 8R_3m_L^4 + L_3(-2m_L^2 - 2s + m_L^2\tilde{s}(1 - \beta_Z)) \right. \\ &\quad \left. \left. \frac{2}{s} \left( -8m_L^2 + 2m_L^2\tilde{s} - 3s + \frac{s\tilde{s}}{2}(1 + \beta_Z) \right) \right] \right\} , \end{aligned} \quad (\text{A.10})$$

where  $L_3$  and  $R_3$  are defined as

$$\begin{aligned} R_3 &= (sm_L^2)^{-1} , \\ L_3 &= \frac{2}{s\beta_L} \ln \left( \frac{1 - \beta_L}{1 + \beta_L} \right) . \end{aligned} \quad (\text{A.11})$$

5) Annihilation  $\bar{L}L \rightarrow \gamma\gamma$

$$\sigma\beta_{\text{rel}} = \frac{\pi\alpha^2}{s^2} \left[ -8s + L_3(32m_L^4 - 16m_L^2s - 4s^2) - 32R_3m_L^4s \right] . \quad (\text{A.12})$$

## Appendix B

### Aspon Model

Frampton and Kephart proposed a simple model , the aspon model[26], in which the gauge group is  $SU(3)_C \times SU(2)_L \times U(1)_Y \times U(1)_{new}$  with an additional vectorlike quark (lepton) doublet and two singlet Higgs scalars transforming nontrivially under the global  $U(1)_{new}$ . Vacuum expectation values of the Higgs singlet are responsible for  $U(1)_{new}$  and CP breaking. Mass matrix elements are complex but their determinants are real at the tree level. Therefore,  $\bar{\theta}$  picks up a nonzero value only through radiative corrections. Since  $U(1)_{new}$  is anomaly-free, it makes this solution of strong CP problem seem more appealing than solutions which involve the necessarily global anomalous  $U(1)_{PQ}$ . The particle assignments are showed in Table B. The particle content is not unique;  $U$ ,  $D$ ,  $N$ , and  $L$  can be *alternatively* assigned to be  $SU(2)$  singlets.

The Yukawa interactions are given by

$$\begin{aligned}
 -\mathcal{L}_Y = & \bar{q}_L \mathbf{m}_d d_R \left[ \frac{\sqrt{2}}{v} \Phi \right] + \bar{q}_L \mathbf{m}_u u_R \left[ \frac{\sqrt{2}}{v} \bar{\Phi} \right] \\
 & + \bar{l}_L \mathbf{m}_e e_R \left[ \frac{\sqrt{2}}{v} \bar{\Phi} \right] + h^\alpha \bar{q}_L Q_R \chi_\alpha + H.c. , \quad (B.1)
 \end{aligned}$$

where  $v/\sqrt{2}$  is defined as the VEV of  $\phi^0$  and  $\bar{\Phi}$  as  $(\bar{\phi}^0, -\phi^-)^T$ .  $\alpha = 1, 2$ . The generation indices are implicit. Usual quarks and leptons acquire their masses

Table B.1: The fields of the aspon model.

Particle	$SU(3)_C \times SU(2)_L \times U(1)_Y \times U(1)_{new}$
$q_L = \begin{pmatrix} u \\ d \end{pmatrix}_L$	(3, 2, 1/6, 0)
$u_R$	(3, 1, 2/3, 0)
$d_R$	(3, 1, -1/3, 0)
$l_L = \begin{pmatrix} \nu \\ e \end{pmatrix}_L$	(1, 2, -1/2, 0)
$e_R$	(1, 1, -1, 0)
$\Phi_L = \begin{pmatrix} \phi^+ \\ \phi^0 \end{pmatrix}$	(1, 2, 1/2, 0)
$Q_L = \begin{pmatrix} U \\ D \end{pmatrix}_L$	(3, 2, 1/6, -1)
$Q_R = \begin{pmatrix} U \\ D \end{pmatrix}_R$	(3, 2, 1/6, -1)
$L_L = \begin{pmatrix} N \\ L \end{pmatrix}_L$	(1, 2, -1/2, -1)
$L_R = \begin{pmatrix} N \\ L \end{pmatrix}_R$	(1, 2, -1/2, -1)
$\chi_1, \chi_2$	(1, 1, 0, 1)

through spontaneous symmetry breaking induced by the VEV of the double Higgs scalar. The new quarks and leptons acquire their mass through a gauge-invariant mass of the form  $M\bar{Q}_L Q_R$ . Hence,  $U(N)$  and  $D(E)$  quarks (leptons) are degenerate in mass.  $m_u, m_d, m_e, \nu, h^{1,2}$ , and  $M$  are real by the assumption of CP invariance. The VEV's of  $\chi_1$  and  $\chi_2$  are chosen to be

$$\langle \chi_1 \rangle = \frac{1}{\sqrt{2}} \kappa_1 e^{i\theta} \text{ and } \langle \chi_2 \rangle = \frac{1}{\sqrt{2}} \kappa_2 . \quad (\text{B.2})$$

Hence CP is broken spontaneously.

Take the lepton mass matrix as an example, it is in the form

$$\mathcal{M}_l = \begin{bmatrix} \mathbf{m}_1 & \mathbf{F} \\ 0 & \mathbf{M} \end{bmatrix} , \quad (\text{B.3})$$

where  $\mathbf{F} = h^1 \langle \chi_1 \rangle + h^2 \langle \chi_2 \rangle$ .

After introducing the new vectorlike lepton doublet, we find that there are FCNC's induced by  $Z$  coupling because of the mismatch of the new and usual leptons in the right-handed sector. Therefore, the flavor-changing  $Z$  couplings are induced by the terms

$$\mathcal{L}_Z^{FCNC} = \left(-\frac{1}{2}\right) \frac{g_2}{\cos \theta_W} \bar{L}_R \gamma_\mu L_R Z^\mu + (N_R \text{ contribution}) , \quad (\text{B.4})$$

where the factor  $-\frac{1}{2}$  is the isospin of  $L_R$  and  $g_2$  is the  $SU(2)$  gauge coupling constant. Without losing any generality, we assume the lepton mass matrix is diagonalized form

$$\mathcal{M}_l = \begin{bmatrix} m_e & 0 & 0 & F_1 \\ 0 & m_\mu & 0 & F_2 \\ 0 & 0 & m_\tau & F_3 \\ 0 & 0 & 0 & M \end{bmatrix} . \quad (\text{B.5})$$

Thus Eq B.4 can be rewritten in terms of mass eigenstates  $l^i$  as

$$\mathcal{L}_Z^{FCNC} = \beta_{ij} \bar{l}_R^i \gamma_\mu l_R^j Z^\mu \text{ for } i \neq j , \quad (\text{B.6})$$

and

$$\beta_{ij} = \left(-\frac{1}{2}\right) \frac{g_2}{\cos \theta_W} \frac{m_i m_j}{MM} x_i x_j^* . \quad (\text{B.7})$$

where  $x_i = F_i/M$ . Therefore, the FCNC induced by  $Z$  coupling is highly suppressed by the small ratio of usual to new leptons.

FCNC's can also be induced by aspon( $A$ ) couplings, which are given by

$$\mathcal{L}_A^{FCNC} = -g_A x_i x_j^* \bar{l}_L^i \gamma_\mu l_L^j A^\mu \quad \text{for } i \neq j . \quad (\text{B.8})$$

Therefore, FCNC's induced by  $A$  will be important if  $A$  is not too heavy compared to  $Z$ .

## Appendix C

### The Cross Sections for Chapter 3

The cross sections for the various subprocesses in chapter 3 are listed below.

$gg \rightarrow L^+L^-$  and  $gg \rightarrow NN$

This production mechanism, by Z and H exchange, is allowed in model 1 only. The cross sections by Z and H exchange are given respectively by

$$\begin{aligned}\hat{\sigma}_Z(gg \rightarrow L^+L^-) &= \frac{\beta\alpha^2\alpha_s^2m_L^2}{2048\pi\sin^4m_W^4}|I|^2, \\ \hat{\sigma}_H(gg \rightarrow L^+L^-) &= \frac{\beta^3\alpha^2\alpha_s^2m_L^2}{4608\pi\sin^4m_W^4}\frac{\hat{s}^2}{((\hat{s}-m_H^2)^2+\Gamma_H^2m_H^2)}|J|^2, \quad (\text{C.1})\end{aligned}$$

where  $\sqrt{\hat{s}}$  is the center of mass energy available for the subprocess and  $\beta$  defined as  $\beta = \sqrt{1-4m_L^2/\hat{s}}$  is the velocity of  $L$ .  $I$  and  $J$  are given by

$$\begin{aligned}I &= 2\sum_q(\pm)\int_0^1dx\int_0^{1-x}dy\frac{xy}{xy-m_q^2/\hat{s}}, \\ J &= 3\sum_q\int_0^1dx\int_0^{1-x}dy\frac{1-4xy}{1-xy\hat{s}/m_q^2}.\end{aligned}\quad (\text{C.2})$$

The sum runs over all known quarks and top-quark ( $m_t = 100$  GeV is assumed). The  $+(-)$  sign in the above equation applies to the quarks with isospins  $T_3 = 1/2$  ( $-1/2$ ).

$\hat{\sigma}_Z(gg \rightarrow NN)$  and  $\hat{\sigma}_H(gg \rightarrow NN)$  are the same as Eq. C.1 respectively with  $m_L$  replaced by  $m_N$ .

$q\bar{q} \rightarrow L^+L^-$  and  $q\bar{q} \rightarrow NN$

The cross section for  $q\bar{q} \rightarrow L^+L^-$  (and  $q\bar{q} \rightarrow NN$ , see below) is given by

$$\begin{aligned} \hat{\sigma}(q\bar{q} \rightarrow L^+L^-) = & \frac{2\pi\alpha^2\beta B}{9\hat{s}} \left( q_i^2 - \frac{q_i\hat{s}(\hat{s} - m_Z^2)(g_L^q + g_R^q)(g_L^l + g_R^l)}{2\sin^2\theta_W \cos^2\theta_W((\hat{s} - m_Z^2)^2 + \Gamma_Z^2 m_Z^2)} \right) \\ & + \frac{\pi\alpha^2\beta\hat{s}(g_L^l{}^2 + g_R^l{}^2)(B(g_L^q + g_R^q)^2 + 2\beta^2(g_L^q - g_R^q)^2)}{36\sin^4\theta_W \cos^4\theta_W((\hat{s} - m_Z^2)^2 + \Gamma_Z^2 m_Z^2)} \end{aligned} \quad (\text{C.3})$$

where  $B = 3 - \beta^2$  with  $\beta = \sqrt{1 - 4m_{L,N}^2/\hat{s}}$ , and  $q_i e$  is the charge of the quark of type  $i$ .  $g_L^q = T_3 - q_i \sin^2\theta_W$  and  $g_R^q = -q_i \sin^2\theta_W$  are the quark and  $Z$  boson neutral coupling coefficients. For leptons, the coefficients  $g_L^l$  and  $g_R^l$  for various models are given by

$$g_L^l = \begin{cases} T_3 - Q_l \sin^2\theta_W, & \text{model 1, 2 and 3} \\ -Q_l \sin^2\theta_W, & \text{model 4} \end{cases}, \quad (\text{C.4})$$

and

$$g_R^l = \begin{cases} T_3 - Q_l \sin^2\theta_W, & \text{model 2 and 3} \\ -Q_l \sin^2\theta_W, & \text{model 1 and 4} \end{cases}, \quad (\text{C.5})$$

where  $T_3 = 1/2$  ( $-1/2$ ) and  $Q_l = 0$  ( $-1$ ) for  $l = N$  ( $L$ ). For the process  $q\bar{q} \rightarrow NN$ ,  $q_i = 0$  is used in Eq. C.3 because the photon does not contribute.

$q\bar{q}' \rightarrow NL^\pm$

The cross section of this sub-process is

$$\hat{\sigma}(q\bar{q}' \rightarrow NL^\pm) = \frac{\pi\alpha^2|U_{qq'}|^2\beta\hat{s}F}{24\sin^4\theta_W((\hat{s} - m_W^2)^2 + \Gamma_W^2 m_W^2)}, \quad (\text{C.6})$$

where

$$F = \begin{cases} 0.5 \left[ 1 + \beta^2/3 - ((m_L^2 - m_N^2)/\hat{s})^2 \right] , & \text{model 1} \\ \left[ 1 + \beta^2/3 - ((m_L^2 - m_N^2)/\hat{s})^2 + 3m_L m_N/\hat{s} \right] , & \text{models 2 and 3} \\ 0, & \text{model 4} \end{cases} , \quad (\text{C.7})$$

with  $\beta = [1 - 2(m_L^2 + m_N^2)/\hat{s} + ((m_L^2 - m_N^2)/\hat{s})^2]^{1/2}$  is again the speed of the charged lepton  $L$  in the  $q\bar{q}'$  center-of-mass.

$$\underline{q\bar{q} \rightarrow L^+ L^- A, q\bar{q} \rightarrow NNA \text{ and } q\bar{q}' \rightarrow NLA}$$

The amplitude squared of these sub-processes (in model 3 and 4 only), with the momenta  $p_1 + p_2 \rightarrow p_3 + p_4 + p_5$  respectively, are given by

$$32(G_L^2 + G_R^2)(A_1 + A_2 + A_{12}) , \quad (\text{C.8})$$

with

$$\begin{aligned} A_1 = & \frac{1}{((p_3 + p_5)^2 - m_3^2)^2} \\ & \times \left[ (2p_3 \cdot p_5 - 2m_3^2)(p_1 \cdot p_4 p_2 \cdot p_5 + p_1 \cdot p_5 p_2 \cdot p_4) \right. \\ & - (2m_3^2 + m_A^2)(p_1 \cdot p_3 p_2 \cdot p_4 + p_1 \cdot p_4 p_2 \cdot p_3) \\ & \left. - 2m_3 m_4 p_1 \cdot p_2 (m_3^2 + m_A^2 + p_5 \cdot p_3) \right] , \end{aligned} \quad (\text{C.9})$$

$$A_2 = A_1(p_3 \leftrightarrow p_4, m_3 \leftrightarrow m_4) , \quad (\text{C.10})$$

$$\begin{aligned} A_{12} = & \frac{1}{((p_3 + p_5)^2 - m_3^2)((p_4 + p_5)^2 - m_4^2)} \\ & \times \left[ -4p_4 \cdot p_5 p_1 \cdot p_3 p_2 \cdot p_3 - 4 p_3 \cdot p_5 p_1 \cdot p_4 p_2 \cdot p_4 \right. \\ & + 2p_3 \cdot p_4 (p_1 \cdot p_4 p_2 \cdot p_5 + p_1 \cdot p_5 p_2 \cdot p_4 + p_1 \cdot p_3 p_2 \cdot p_5 + p_1 \cdot p_5 p_2 \cdot p_3) \\ & + (4p_3 \cdot p_4 + 2p_4 \cdot p_5 + 2p_3 \cdot p_5)(p_1 \cdot p_3 p_2 \cdot p_4 + p_1 \cdot p_4 p_2 \cdot p_3) \\ & + m_3 m_4 (-4p_1 \cdot p_5 p_2 \cdot p_5 + p_1 \cdot p_2(2p_3 \cdot p_5 + 2p_4 \cdot p_5 + 4p_3 \cdot p_4 + 2m_A^2)) \\ & \left. + 2m_A^2 p_3 \cdot p_4 p_1 \cdot p_2 \right] . \end{aligned} \quad (\text{C.11})$$

In  $A_1$ ,  $A_2$  and  $A_{12}$  the heavy lepton masses are taken to be  $m_3 = m_4 = m_L$  for  $q\bar{q} \rightarrow L^+L^-A$ ,  $m_3 = m_4 = m_N$  for  $q\bar{q} \rightarrow NNA$  and  $m_3 = m_N, m_4 = m_L$  for  $q\bar{q} \rightarrow NLA$ .

Finally, in Eq. C.8, the values of  $G_L$  and  $G_R$  are given as follows:

$$\begin{array}{lll}
 & G_L & G_R \\
 q\bar{q} \rightarrow L^+L^-A & g_A (g_L^L g_L^q P - q_i e^2 / \hat{s}) & g_A (g_L^L g_R^q P - q_i e^2 / \hat{s}) \\
 q\bar{q} \rightarrow NNA & g_A g_L^N g_L^q P & g_A g_L^N g_R^q P \\
 q\bar{q} \rightarrow NLA \text{ (model 3)} & g_A g^2 / 2(\hat{s} - m_W^2) & 0 \\
 q\bar{q} \rightarrow NLA \text{ (model 4)} & 0 & 0
 \end{array} \tag{C.12}$$

where  $P = (g / \cos \theta_W)^2 / (\hat{s} - m_Z^2)$  and  $g_L^L$  and  $g_L^N$  in model 3 and 4 are given in Eq. C.4 for  $l = L$  and  $N$ .

## Appendix D

### Fortran Programm for Chapter 3

As an example, we give here the Fortran program for the heavy lepton production  $pp \rightarrow LL$  in Chapter 3.

```
*****
Production of heavy lepton in pp collider.
model = 1 : right-handed singlet
model = 2 : right-handed doublet
model = 3 : singlet aspon model
model = 4 : doublet aspon model
qi is the charge of the quark in the unit of e.
*****

implicit real*8(a-h,m,o-z)
dimension ppLL(4)
common/dum/rts,ml,mh,mz,zwidth,hwidth,sinhw2
common/main/nmodel
external fxnq,fxng
data mh,hwidth,mz,zwidth,sinhw2/100.,0.5,91.175,2.48,0.23/
rts=17000.
open(1,file="ppLL.data")
ndim=2
ncall=1000
nitf=10
ndim=2
do 1 i=1,16
ml=50.0*float(i)
nmodel=1
```

```

glufusn=avgi(ndim,fxng,ncall,nitf)
quafusn=avgi(ndim,fxnq,ncall,nitf)
ppLL(1)=glufusn+quafusn

do 2 nn=2,4
  nmodel=nn
2  ppLL(nn)=avgi(ndim,fxnq,ncall,nitf)
  write(1,'(5e15.5)') ml,(ppLL(k),k=1,4)
  write(*,'(5e15.5)') ml,(ppLL(k),k=1,4)
1  continue
  stop
  end
  include "avgi.for"
  include "ehlq.for"

double precision function fxng(ww)
implicit real*8 (a-h,m,o-z)
dimension ww(9)
common/dum/rts,ml,mh,mz,zwidth,hwidth,sinhw2
xm=4.0*ml**2/rts**2
det1=0.95*0.95-xm
tau=xm+det1*ww(1)
det2=0.95-tau
x1=tau+det2*ww(2)
x2=tau/x1
shead=tau*rts**2
nset=1
scale2=shead/4.
call ehlq(nset,x1,scale2,uv,dv,se,st,ch,bo,to,g)
g1=g/x1
call ehlq(nset,x2,scale2,uv,dv,se,st,ch,bo,to,g)
g2=g/x2
gluon=g1*g2/x1
if(g1.lt.0.or.g2.lt.0)write(2,*)x1,x2
fxng=gluon*ggLL(shead)*det1*det2
return
end

double precision function fxnq(ww)
implicit real*8 (a-h,m,o-z)
dimension ww(9)

```

```

common/dum/rts,ml,mh,mz,zwidth,hwidth,sinhw2
xm=4.0*ml**2/rts**2
det1=0.95*0.95-xm
tau=xm+det1*ww(1)
det2=0.95-tau
x1=tau+det2*ww(2)
x2=tau/x1
thead=tau*rts**2
nset=1
scale2=thead/4.
call ehlq(nset,x1,scale2,uv,dv,se,st,ch,bo,to,gl)
u1=(uv+se)/x1
d1=(dv+se)/x1
c1=ch/x1
s1=st/x1
a1=se/x1
ad1=se/x1
call ehlq(nset,x2,scale2,uv,dv,se,st,ch,bo,to,gl)
u2=(uv+se)/x2
d2=(dv+se)/x2
c2=ch/x2
s2=st/x2
a2=se/x2
ad2=se/x2
up=(u1*a2+a1*u2+2.*c1*c2)/x1
down=(d1*ad2+ad1*d2+2.*s1*s2)/x1
if (up .lt. 0. .or. down .lt. 0.) then
write (2,*)x1,x2
endif
fxnq=(up*qqLL(1,thead)+down*qqLL(2,thead))* det1*det2
return
end

```

```

double precision function qqLL(i,s)
implicit real*8 (a-h,m,o-z)
common/dum/rts,ml,mh,mz,zwidth,hwidth,sinhw2
common/main/nmodel
pie=3.1415926
costhw2=1.-sinhw2
if (i .eq. 1) then
qi=2.0/3.0

```

```

ti=1.0
endif
if (i .eq. 2) then
qi=-1.0/3.0
ti=-1.0
endif
scale2=s/4.
qcd2=0.2**2
aem=1.0/128.
as=alphas(scale2,qcd2)
beta=Sqrt(1-4*ml**2/s)
B=3.0-beta**2
if (nmodel .eq. 1) then
gel=-1.0+2.*sinhw2
ger=2.*sinhw2
endif
if (nmodel .eq. 2 .or. nmodel .eq. 4) then
gel=-1.0+2.*sinhw2
ger=gel
endif
if (nmodel .eq. 3) then
gel=0.
ger=0.
endif
gql=ti-2.0*qi*sinhw2
gqr=-2.0*qi*sinhw2
zpro=(s-mz**2)/((s-mz**2)**2+zwidth**2*mz**2)
sig1=qi*s*zpro*(gql+gqr)*(gel+ger)/8.0/sinhw2/costhw2
sig2=beta*s**2
K=(B*(gql+gqr)**2+2.*beta**2*(gql-gqr)**2)
sig2=sig2*(gel**2+ger**2)*K
sig2=sig2/256./sinhw2**2/costhw2**2*zpro/(s-mz**2)
qqLL=(4.*pie*aem**2/9.0/s)*(0.5*beta*B*(qi**2-sig1)+sig2)
qqLL=qqLL*0.389d6
return
end

```

```

double precision function ggLL(s)
implicit real*8 (a-h,m,o-z)
common/dum/rts,ml,mh,mz,zwidth,hwidth,sinhw2
complex*16 ah,az

```

```

pie=3.1415926
mw=mz*sqrt(1.0-sinhw2)
scale2=s/4.
qcd2=0.2**2
aem=1.0/128.
as=alphas(scale2,qcd2)
beta=sqrt(1-4*ml**2/s)
hpro=s**2/((s-mh**2)**2+hwidth**2*mh**2)
ahr=real(ah(s))
ahi=dimag(ah(s))
AI=9.0*(ahr**2+ahi**2)
azr=real(az(s))
azi=dimag(az(s))
AJ=4.0*(azr**2+azi**2)
sigz=beta*(aem*as*ml)**2*AJ/(2048.*pie*sinhw2**2*mw**4)
V=(4608.*pie*sinhw2**2*mw**4)
sigh=beta**3*(aem*as*ml)**2*AI*hpro/V
ggLL=(sigz+sigh)*0.389d6
return
end

```

```

double precision function alphas(scale2,qcd2)
implicit real*8 (a-h,m,o-z)
pie=3.1415926
mb2=4.8**2
mt2=100.0**2
d=25.0*dlog(scale2/qcd2)
if (scale2 .lt. mb2) go to 1
d=d-2.0*dlog(scale2/4.0/mb2)
if (scale2 .gt. mt2) d=d-2.0*dlog(scale2/4.0/mt2)
1 alphas=12.0*pie/d
return
end

```

```

complex*16 function Ah(s)
implicit real*8 (a-h,m,o-z)
dimension x(2)
complex*16 rml,phi(2)
rml=(0,1.0d0)
pie=3.1415926
mb2=4.8**2

```

```

mt2=100.0**2
x(1)=4.0*mb2/s
x(2)=4.0*mt2/s
do 2 i=1,2
if (x(i) .gt. 1.0) then
phi(i)=- (asin(1.0/sqrt(x(i))))**2
else
y1=1.0-sqrt(1.0-x(i))
y2=1.0+sqrt(1.0-x(i))
phi(i)=0.25*(dlog(y2/y1)-rml*pie)**2
endif
2 continue
U=x(2)*(1.0+(x(2)-1.)*phi(2))
ah=0.5*(x(1)*(1.+(x(1)-1.)*phi(1))+U
return
end

complex*16 function Az(s)
implicit real*8 (a-h,m,o-z)
dimension x(2)
complex*16 rml,phi(2)
rml=(0,1.0d0)
pie=3.1415926
mb2=4.8**2
mt2=100.0**2
x(1)=4.0*mb2/s
x(2)=4.0*mt2/s
do 2 i=1,2
if (x(i) .gt. 1.0) then
phi(i)=- (asin(1.0/sqrt(x(i))))**2
else
y1=1.0-sqrt(1.0-x(i))
y2=1.0+sqrt(1.0-x(i))
phi(i)=0.25*(dlog(y2/y1)-rml*pie)**2
endif
2 continue
az=0.5*(1.+x(1)*phi(1))+0.5*(1.0+x(2)*phi(2))
return
end

```

## Appendix E

### Approximating the Renormalization-Group Equations of Minimal Supersymmetry

The minimal supersymmetric model has remarkable predictive power. One inputs, at the grand unification scale, five parameters:[35] the gaugino mass parameter  $M$ , the top-quark Yukawa coupling  $h_t$ , the scalar mass-squared parameter  $m_0$ , the Higgs mixing parameter  $m_4$ , and the  $A$  parameter. The renormalization-group equations (RGE's) are then used to evolve down to the electroweak scale. One can then extract the masses of the top quark,  $W$  and  $Z$  bosons, the gluinos, the two charginos, the four neutralinos, the twelve scalar quarks, the nine scalar leptons, the three physical neutral Higgs scalars, the charged Higgs scalar, as well as all of the couplings, mixing angles, etc.

As a result of this predictive power, a flurry of papers appears whenever new experimental data become available. The four-dimensional parameter space (the weak scale determines the fifth parameter) must be scanned, and the RGE's solved for each point in the parameter space. Since this involves a large amount of computer time, approximation schemes for the solution of the RGE's

can be quite useful.

One such scheme was proposed by Kounnas et al.[36]. They found an approximation which gave analytic formulas for the low-energy parameters in terms of the parameters which were input at the unification scale. This approximation has since been used by many authors[37]. At the time of their work, it was widely believed that the top quark had been discovered with a mass of about 40 GeV, and they stated explicitly that their approximation was valid for masses in that range. It is now known that the top quark is much heavier[38]. We examine the validity of their approximation for heavier top-quark masses.

Consider the RGE's for two of the parameters of the minimal supersymmetric model, the difference between the mass squared of the scalar top and that of the scalar up,  $\Delta \equiv m_{Q_3}^2 - m_Q^2$ , and the top-quark Yukawa coupling:

$$\begin{aligned} \frac{d\Delta}{dt} &= \frac{h_t^2}{2\pi^2} F_M, \\ \frac{dh_t}{dt} &= \frac{h_t}{16\pi^2} F_h, \end{aligned} \quad (\text{E.1})$$

where  $t = \ln(\mu/M_W)$  and

$$\begin{aligned} F_h &= -\frac{16}{3}g_3^2 - 3g_2^2 - \frac{13}{15}g_1^2 + 6h_t^2, \\ F_M &= m_{Q_3}^2 + m_{U_3}^2 + m_{H_2}^2 + A_U^2 m_0^2. \end{aligned} \quad (\text{E.2})$$

Here, we use the notation of Ref. [35] for the scalar mass-squared parameters.

These equations can be trivially integrated to give

$$\begin{aligned} h_t(M_X) - h_t(M_W) &= \int_0^{\ln(M_X/M_W)} \frac{h_t^2(t)}{16\pi^2} F_h(t) dt, \\ \Delta(M_W) &= -2 \int_0^{\ln(M_X/M_W)} \frac{h_t^2(t)}{4\pi^2} F_M(t) dt. \end{aligned} \quad (\text{E.3})$$

Note that  $\Delta(M_X) = 0$ .

The approximation of Ref. [36] consists of using the approximation

$$\int_0^{\ln(M_X/M_W)} h_t^2(t) \phi(t) dt = \phi(0) \int_0^{\ln(M_X/M_W)} h_t^2(t) dt \quad (\text{E.4})$$

in Eq. E.3. This means that the only integration to be performed is the integration of  $h_t^2$  from  $M_W$  to  $M_X$ ; this integral will then give all of the relevant mass-squared parameters, *as well as  $h_t$  itself*. Solving iteratively, the integral can then be determined from the Yukawa coupling. As a result, no integrals need be evaluated numerically (see Ref. [35] for expressions).

The rationale for using the approximation of Eq. E.4 is that the Yukawa coupling is a very rapidly decreasing function of  $t$ , and thus most of the contribution of the integral on the left-hand side of Eq. E.4 comes from small  $t$ , and thus if  $\phi(t)$  is not too rapidly changing, the approximation should be valid. It was argued in Ref. [36] that the approximation is valid for top-quark masses below 50-100 GeV. Many of the detailed numerical results of Refs. [35]-[37] depend on this approximation (although most of the qualitative features do not).

To examine the validity of this approximation, we will consider three cases: (1) the calculation of the Yukawa coupling at  $M_W$ , (2) the calculation of the difference between the low-energy mass-squared parameters of the third generation and those of the first (or second) generation, and (3) the calculation of the ratio of the vacuum expectation values of the Higgs fields (which leads to all the scalar masses, top-quark mass, etc.).

We first examine the result of the Yukawa coupling. Here, there are no free parameters—given  $h_t$  at  $M_X$ , one can determine  $h_t$  at  $M_W$ . We have calculated

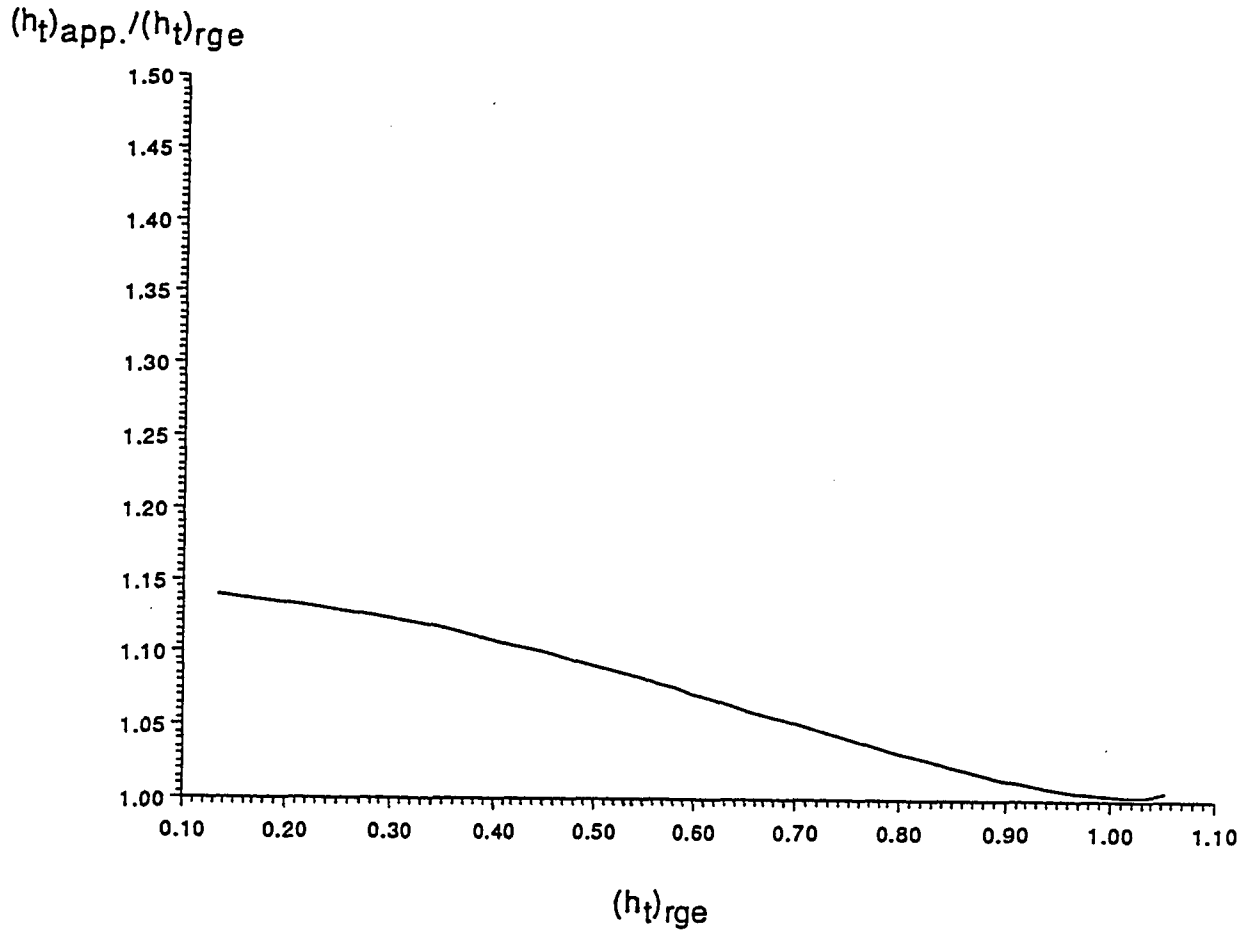


Figure E.1: Given the Yukawa coupling at  $M_X$ , the Yukawa coupling at  $M_W$  can be found in two ways: (1) using the renormalization-group equations and (2) using the approximation. The ratio of the results of the second method to the results of the first is plotted as a function of the Yukawa coupling at  $M_W$ .

$h_t(M_W)$  in terms of  $h_t(M_X)$  in two ways: (1) solving the RGE numerically, and (2) using the formulas given in Refs. [35] and [36]. In Fig. E.1, we have plotted the ratio of the results of the two methods as a function of  $h_t(M_W)$ . Keeping in mind that the top-quark mass probably never be measured to much better than 10%, we see that the analytic formula gives good results for all reasonable values of the Yukawa coupling.

However, the formula is not, in general, useful unless one can also extract the mass-squared parameters. We now examine the RGE for the difference between the first- and third-generation mass-squared parameters  $\Delta \equiv m_{Q_3}^2 - m_{Q_1}^2$ . We have chosen this quantity since  $m_{Q_1}^2$  can be found analytically (in terms of integrals over gauge couplings which can be explicitly solved); the difference  $\Delta$  is independent of the gauge couplings. Here, the calculation does depend on several of the input parameters; we will give a few representative samples. In Fig. E.2, we have plotted the ratio of the result for  $\Delta$  calculated using the above approximation to that calculated numerically from the RGE's. We see that the approximation is not, in general, very accurate. However, it does not have to be. The value of  $\Delta$  in most models ranges from 20 to 60 GeV. Experimentally, it will be difficult to measure scalar quark masses (or splitting) to an accuracy much better than about 20 GeV (recall that the cross section for scalar production just above threshold rises very slowly). As a result, 30% accuracy will always be sufficient, and in many cases, even accuracy of a factor of 2 in  $\Delta$  would suffice. The approximation typically does give results which are accurate to within a factor of 2, and also typically over estimates the splitting. We conclude that the approximation will give a reasonable qualitative estimate of the size of the splitting, but that a precise quantitative estimate, which

approaches the resolution of a typical experiment, will not be possible without solving the RGE's numerically.

Finally, we turn to the accuracy of the approximation for calculating the ratio of the vacuum expectation values of the two Higgs bosons:  $\tan \beta \equiv v_2/v_1$ . This ratio is essential in finding the top-quark mass, given the Yukawa coupling, the scalar quark masses, the various Higgs-boson masses, the chargino and neutralino masses, etc. Here, we cannot show how the approximation behaves as a function of  $h_t$  since only a small range of  $h_t$  gives (for a given set of the other parameters) acceptable masses; rather we give results for a few representative values. One might expect the approximation to be most suspect in this calculation. The reason is that the value  $\beta$  is extracted from the quadratic mass-squared parameters in the potential:  $\sin 2\beta = 2m_3^2/(m_1^2 + m_2^2)$ , and the value of  $m_3^2$  is very sensitive to the contribution of  $h_t$  to its RGE's, and a small change in  $m_3^2$  can give a large change to  $\sin 2\beta$ . Even more importantly, the  $W$ -boson mass is very sensitive to the value of  $m_1^2$  and  $m_2^2$  and thus the overall scale of the masses will be sensitive to changes in  $m_2^2$ . The results, for several representative values of the parameters, are shown in Table E. The top-quark mass is calculated from the relation  $m_{top}^2/M_W^2 = (2h_t^2/g^2) \sin^2 \beta$ . We see that although the calculation of  $\tan \beta$  using the approximation is very inaccurate, the prediction of the top-quark mass is fairly close (since it is proportional to  $\sin \beta$  not  $\tan \beta$ ), especially for fairly light top quarks. As the top-quark mass increases, however, the prediction value begins to deviate significantly. As a result, the range of Yukawa couplings which give acceptable electroweak symmetry breaking can be determined accurately using the approximation, but the acceptable range of top-quark masses cannot be determined with any sig-

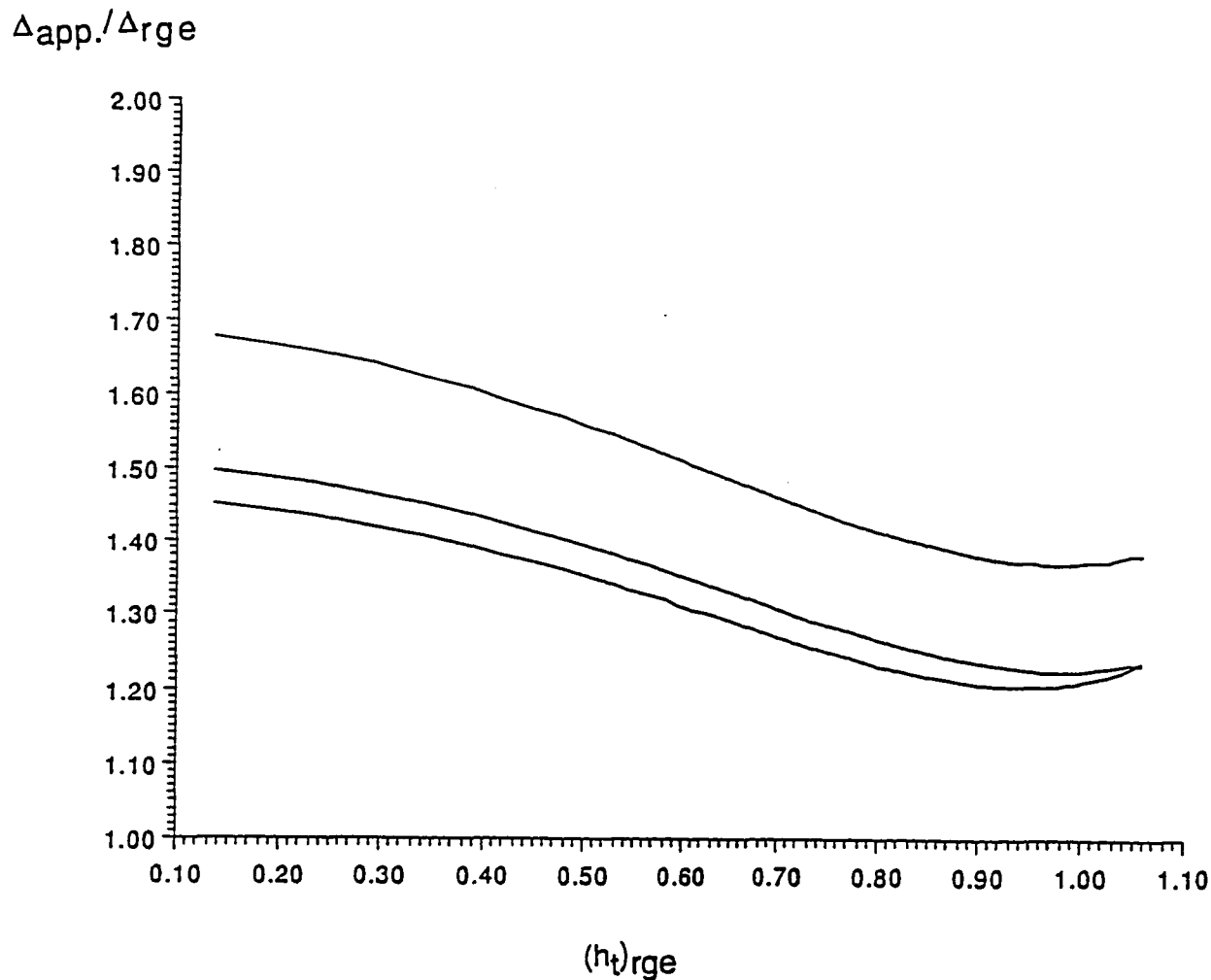


Figure E.2: The splitting between the third-generation scalar quark mass and that of the other two is calculated in two ways: (1) using the renormalization-group equations and (2) using the approximation. The ratio of the results of the second method to the results of the first is plotted as a function of the Yukawa coupling at  $M_W$ . Several choices of input parameters are used: for the upper line,  $\xi = 2.5$ ,  $A = 0.5$ , and  $m_4/m_0 = 1.4$ ; for the middle line,  $\xi \equiv M/m_0 = 1.0$ ,  $A = 0.5$ , and  $m_4/m_0 = 0.5$ ; for the lower line,  $\xi = 1.0$ ,  $A = 1.0$ , and  $m_4/m_0 = 1.4$ .

nificant accuracy. A much more serious discrepancy occurs in the calculation of scalar quark masses. This is due to the sensitivity of these masses to the overall scale, which, as noted above, is very sensitive to the precise value of  $m_2^2$ . Here, we see that the approximation gives very inaccurate results.

What would happen in more complicated models? One can easily add extra gauge bosons to the analysis, since their contributions can be determined analytically. If one were to add singlets, additional terms can be added coupling those singlets to the Higgs doublets. The  $\beta$  functions for these couplings depend on the gauge couplings and the Yukawa coupling. Again, the approximation will work well *given* the Yukawa coupling, but will not if one is given the top-quark mass. In addition, if these couplings are large, the approximation is suspect. Note also that in string models, the Yukawa couplings are of the same order as the gauge couplings, and thus the approximation will be likely to have similar difficulties in these models.

In finding the phenomenological implication of the minimal supersymmetric model, it is necessary to integrate many coupled renormalization-group equations from the grand unified theory or Planck scale down to the weak scale. In many papers, an approximation has been used in order to avoid having to numerically integrate the equations for many points in a multiple dimensional parameter space<sup>1</sup>. In this chapter, we have looked at the validity of this approximation, in light of the fact that top quark is much heavier than was believed when the approximation was first proposed. It has been shown that the calculation of the weak-scale Yukawa coupling is quite reliable, that the

---

<sup>1</sup>Of course, in a serious attempt to extract the predictions of any model, one would need to do an exact one-loop treatment (if not a two-loop); but one could hope to use the approximation to get a rough idea of the region of parameter space in which to explore.

Table E.1: For five representative values of the parameters.  $M$ ,  $A$ ,  $m_4$ , and  $h_t$ , we calculate the ratio of vacuum expectation values  $\tan \beta = v_2/v_1$ , the top-quark mass, and the scalar quark mass using both the renormalization-group equations and the approximation. All masses are given in GeV.

	1	2	3	4	5
$M/m_0(M_X)$	2.5	2.5	1.0	1.0	1.0
$A(M_X)$	0.5	0.5	0.5	0.5	1.0
$m_4/m_0(M_X)$	0.5	1.4	0.5	1.4	1.4
$h_t(M_W)$	0.41	0.54	0.63	0.86	0.92
$(\tan \beta)_{RGE}$	11.4	13.5	7.4	3.5	4.1
$(\tan \beta)_{app}$	3.1	20.1	2.4	1.7	1.6
$(m_{top})_{RGE}$	72	94	108	144	155
$(m_{top})_{app}$	69	94	100	130	135
$(m_Q)_{RGE}$	560	430	270	385	170
$(m_Q)_{app}$	190	170	130	100	75

calculation of scalar quark mass splitting is qualitatively reliable but quantitatively suspect (depending on the precision needed), and that the calculation of the weak scale, top-quark mass, Higgs-boson masses, etc., are very inaccurate. Thus, to extract the low-energy predictions of the minimal supersymmetric model, there appears to be no substitute for a full numerical analysis.

## Bibliography

- [1] S. Glashow, *Rev. Mod. Phys.* **52**, 539(1980).  
A. Salam, *Rev. Mod. Phys.* **52**, 525(1980).  
S. Weinberg, *Rev. Mod. Phys.* **52**, 515(1980).
- [2] O. Shanker, *Nucl. Phys.* **B206**, 253(1982).
- [3] B. McWilliams and L. F. Li, *Nucl. Phys.* **B179**, 62(1981).
- [4] T. P. Cheng and M. Sher, *Phys. Rev.* **D35**, 3490(1987).
- [5] J. Ellis and M. K. Gaillard, *Phys. Lett.* **88B**, 315(1979).
- [6] See, for example, B. McWilliams and L. F. Li, *Nucl. Phys.* **B179**, 62(1981);  
I. I. Bigi et al. [*Phys. Lett.* **166B**, 238(1986)] do discuss the bounds on  $B$   
and  $\tau$  decays, but in terms of a single universal coupling.
- [7] P. Frampton, *Gauge Field Theories* (Benjamin/Cummings, New York,  
1987), p.529.
- [8] Particle Data Group, J. J. Hernández et al., *Phys. Lett.* **239B**, 1(1990).
- [9] D. Chang, *Proc. 1992 Div. of Particles and Fields, Fermilab.* ed. C. Al-  
bright et al., World Scientific (1993) VolII, p1250.

- [10] J. D. Bjorken and s. Weinberg, *Phys. Rev. Lett.* **38**, 622(1977).
- [11] W. J. Marciano and A. I. Sanda, *Phys. Rev. Lett.* **38**, 1512(1977).
- [12] L. B. Okun, *Leptons and Quarks* (North-Holland, Amsterdam, 1982), p.29.
- [13] N. Isgur and D. Scora, *Phys. Rev.* **D39**, 799(1988).
- [14] CLEO Collaboration, A. Bean et al., *Phys. Rev.* **D35**, 3533(1987).
- [15] UA1 Collaboration, M. Mohammadi, in *High Energy Hadronic Interactions*, Proc. XXVth Rencontre de Moriond, Les Arcs, France, 1990, ed. J. Tran Thanh Van (Editions Frontieres, Gif-sur-Yvette, 1990), p.433.
- [16] V. V. Ammosov et al., *Phys. Lett.* **93B**, 210(1980).  
U. P. Sukhatme, K. E. Lassila, and R. Orava, *Phys. Rev.* **D25**, 2975(1982).
- [17] B. McWilliams and O. Shanker, *Phys. Rev.* **D22**, 2853(1980).
- [18] R. M. Barnett et. al., Proc. Summer Study on High Energy Physics in the 1990s, ed. S. Jensen, (World Scientific, Singapore, 1989), p.159.  
A. Datta and A. Pilaftsis, *Phys. Lett.* **278B**, 162(1992).  
D. Dicus and P. Roy, *Phys Rev.* **D44** 1593(1991).  
D. Dicus, D. Karatas and P. Roy, *Phys. Rev.* **D44** 2033(1991).
- [19] E.W. Kolb and M.S. Turner, *The Early Universe*, (Addison-Wesley, Reading, MA, 1990).
- [20] K. Enqvist, K. Kainulainen and J. Maalampi,  
*Nucl. Phys.* **B317**, 647(1989).
- [21] K. Griest and M. Kamionkowski, *Phys. Rev. Lett.* **64**, 615(1990).

- [22] S. Dimopoulos, D. Eichler, R. Esmailzadeh and G.D. Starkman, *Phys. Rev. D* **41**, 2388(1990).
- [23] P. F. Smith, *Comtemp. Phys.* **29**, 159(1988).
- [24] C. Burigana, G. De Zotti and L. Danese, *Astrophys. J.* **379** , 1(1991).
- [25] J. R. Carter, in Joint Lepton-Photon Symposium and Europhysics conference on High Energy Physics, ed. S. Hegarty, K. Potter and E. Quercigh, World Scientific(1992) Vol II, p3.
- [26] P. H. Frampton and T. W. Kephart, *Phys. Rev. Lett.* **66**, 1666(1991).  
P. H. Frampton and D. Ng, *Phys. Rev. D* **43**, 3034(1991).  
P. H. Frampton, T. W. Kephart, D. Ng and T. J. Weiler, *Phys. Rev. Lett.* **68**, 2129(1992).
- [27] J. N. Bahcall et. al., *Rev. Mod. Phys.* **54**, 767(1982).
- [28] V. A. Gavrin, in Joint Lepton-Photon Symposium and Europhysics Conference on High Energy Physics, *op.cit.* Vol I, p638.
- [29] E. Bellotti, in Joint Lepton-Photon Symposium and Europhysics Conference on High Energy Physics, *op.cit.* Vol I, p635.
- [30] R. Davis, Jr., in Seventh Workshop on Grand Unification , ed. J. Arafune, World Scientific(1987)237.
- [31] K. S. Hirata et. al., *Phys. Rev. Lett.* **63**, 16(1990); *ibid* **65**, 1297(1990).
- [32] L. Wolfenstein, *Phys. Rev. D* **17**, 2369(1978).  
S. P. Mikheyev and A. Yu. Smirnov, *Sov. J. Nucl. Phys.* **42**, 913(1986).

- [33] D. R. O. Morrison, In Joint Lepton-Photon Symposium and Europhysics Conference on High Energy Physics, *op.cit.* Vol I, p599.
- [34] E. Eichten et. al., Rev. Mod. Phys. 56, 579(1984).
- [35] We use the notation of A. B. Lahanas and D. V. Nanopoulos, Phys. Rev. 145, 1(1987).
- [36] C. Kounnas, A. B. Lahanas, D. V. Nanopoulos, and M. Quiros, Phys. Lett. 132B, 95(1983); Nucl. Phys. B236, 438(1984).
- [37] B. Gato, J. Leon, J. Perez-Mercader, and M. Quiros, Phys. Lett. B141, 191(1984); Nucl. Phys. B260, 203(1985).  
G. F. Guidice and C. Ridolfi, Z. Phys. C41, 447(1988).  
B. Gato, Z. Phys. C35, 77(1987); Nucl. Phys. B278,189(1987).  
In the last two papers, an improvement on the approximation was made, but our comments about the validity of the approximation will not be significantly changed.
- [38] CDF Collaboration, F. Abe et al., Phys Rev. Lett. 62,1825( 1989).

## Vitæ

**Yao Yuan**

Born in Beijing, China, August 7, 1964. Graduated from Tsinghua University, Beijing, China, with B.S. in Electrical Engineering, July, 1987. Received M.S. in Physics at the College of William and Mary, May, 1990. Ph.D candidate, College of William and Mary, 1990-1993, with a concentration on theoretical particle physics.